Chapter 5

Technologies

Prior to explaining the different models (or macros) and their particular technologies, it is necessary to give a small introduction to common elements (TRNSYS types, that, as seen in Table 4.1, are consistently used in various macros to concentrate on the specific types used to represent different technologies. Some of the types described are taken from a dedicated library generated by TESS (Thermal Energy System Specialists), and others have been developed by the TRNSYS team or taken from successful user models. Afterwards, the model for the acquisition of meteorological data will be explained. Then several models of heat generation will be introduced, such as solar thermal and boilers. Cooling models such as absorption and compression chillers will also be presented. Finally, storage models will be described, followed by the model used to represent demand for the simulation.

5.1 General Types

Description of the types will be done in order of appearance on Table 4.1, which appeared in the previous section:

5.1.1 Pipes (TRNSYS Type 709)

This component simulates the thermal behavior of fluid flow in a pipe or duct using variable-size segments. The entry of new fluid causes shifts in the position of existing segments, with each new segment's mass determined by the flow rate and simulation time step. The temperature of each newly added segment matches that of incoming fluid (see Figure 5.1). At the outlet, elements are "pushed" out by the inlet flow to form a collection known as a "plug-flow" model, which does not account for mixing or conduction between adjacent segments. A maximum limit of 25 segments exists within this pipe system. Once this limit is reached, two contiguous segments with temperatures closest to one another are merged into a single segment. Regardless, only one node (segment) will be used for computational time-saving purposes. Unlike Type 31 (which is a standard TRNSYS type used for pipe simulation), Type 709 requires specific inputs regarding physical characteristics such as pipe material properties, fluid properties, and insulation material instead of an overall UA value for both pipe and insulation from the user's perspective (as Type 31 demands) to account for

losses. These values are mainly set through correlations based on the information provided by the user [92].

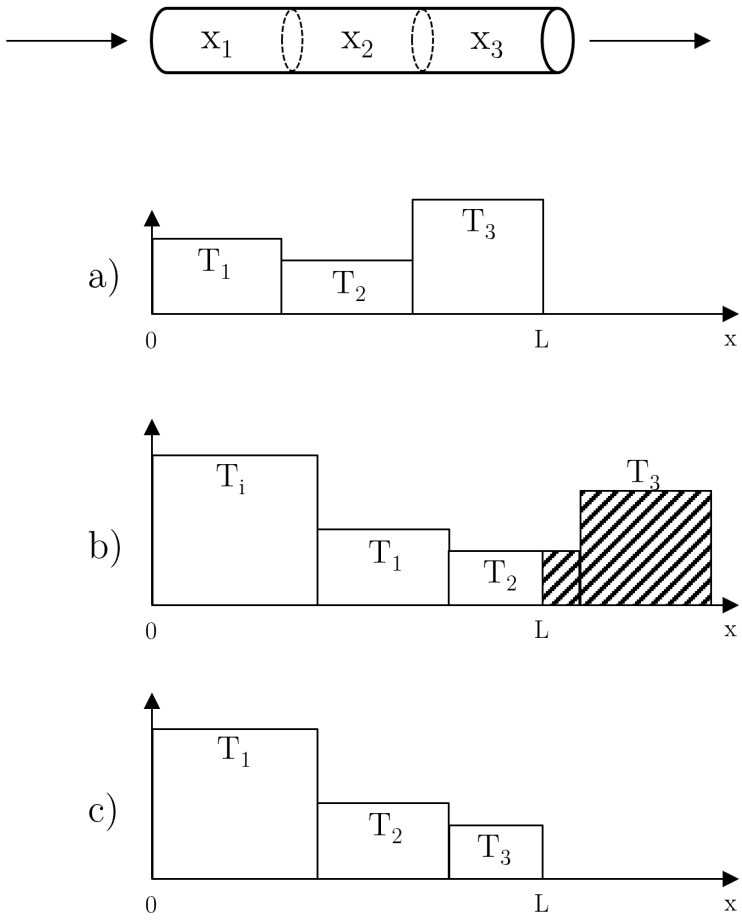

Figure 5.1: TRNSYS pipe scheme

For Figure 5.1, outlet temperature is defined by:

$$T_o = \frac{M_3 T_3 + (\dot{m}\Delta t - M_3) T_2}{\dot{m}\Delta t} \tag{5.1}$$

This definition is derived from a more general equation:

$$T_o = \frac{1}{\dot{m}\Delta t} \sum_{j=1}^{k-1} (M_j T_j + a M_k T_k) \tag{5.2}$$

For Equation 5.2, a and k must satisfy:

$$0 \leq a \leq 1$$

$$\sum_{j=1}^{k-1} (M_j + a M_k) = \dot{m}\Delta t$$

Where,

- M: The total mass of liquid contained in the pipe or if subscripted, contained in a segment [kg].
- $\dot{m}$: The mass flow rate of liquid through the pipe [$\frac{kg}{h}$].
- Δt: Simulation time step [h].
- j,k: Subscripts to denote pipe segments.
- a: Weight coefficient.

An explanation of how the methodology helps to obtain most of this type's parameters around different macros was explained in section 4.1.2. An additional characterization can be provided for most pipes by selecting whether they are to be assumed external, buried, or internal, through the use of the "LOC" parameter, this is possible because the different macros have been supplied with ambient temperature, ground temperature and an average temperature between external and 20°C, which is selected depending on this parameter.

For the pipes used for different technologies two main variables have been calculated:

- Internal diameter [m]: Considering the flow that will be going through the pipe by design, a correlation has been used to size this pipe properly to fulfill minimum diameter requirements, and maximum velocity criteria.
- Thickness [m]: Correlations with the pipe diameter calculated have been followed considering low-pressure systems to arrive at an estimated pipe thickness.
- Outer diameter [m]: With the Internal diameter and the thickness calculated, an outer diameter can be determined.
- Transfer coefficients [$\frac{W}{m^2K}$]: Considering three possible locations (internal, external, or buried), values have been set.
- External temperature [°C]: Considering three possible locations (internal, external, or buried), temperatures are set. As explained in the previous paragraph.

5.1.2 Pumps (TRNSYS Type 110)

Type110 in TRNSYS has the capability to adjust its outlet mass flow rate within a range from zero to a rated value. The control signal setting linearly affects the mass flow rate of the pump. However, when modeling the power draw of the pump, a polynomial equation is used instead. Also, pressure-oriented power consumption is assumed in the different macros, generating correlations that consider the pump size to be used depending on the system being supplied. It should be noted that Type110 does not model characteristics related to starting and stopping of pumps nor does it consider pressure drop effects. Similar to other pumps and fans in TRNSYS, Type110 takes input for mass flow rate but only uses it for performing mass balance checks without considering its actual value. Instead, based on its

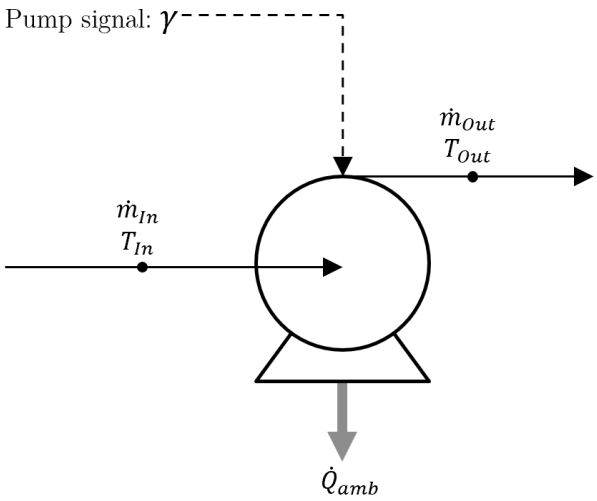

Figure 5.2: TRNSYS variable speed pump

rated flow rate parameter and current control signal input value (Equation 5.9), Type110 determines and sets the downstream flow rate accordingly [92].

$$P = P_{rated}(a_0 + a_1\gamma + a_2\gamma^2 + \ldots) \tag{5.3}$$

$$\eta_{pumping} = \frac{\eta_{overal}}{\eta_{motor}} \tag{5.4}$$

$$P_{shaft} = P\eta_{motor} \tag{5.5}$$

$$Q_{fluid} = P_{shaft}(1 - \eta_{pumping}) + (P - P_{shaft})f_{mortorloss} \tag{5.6}$$

$$Q_{amb} = (P - P_{shaft})(1 - f_{motorloss}) \tag{5.7}$$

$$T_{Out} = T_{In} + \frac{Q_{fluid}}{\dot{m}_{out}} \tag{5.8}$$

$$\dot{m}_{out} = \dot{m}_{Rated} \cdot \gamma \tag{5.9}$$

For the pumps used for different technologies four main variables have been calculated:

- Rated mass flow rate ($\dot{m}_{Rated}$): considering the capacity needed for that pump (usually related to the capacity of the equipment associated).
- Rated volumetric flowrate: from the mass flowrate previously calculated, considering density as the relation between these two variables volumetric flowrate is calculated. This value is intermediate for the calculation of the rated power.
- Pressure drop: from inputs from different sites and considering that design values for circuits prevent having excessive losses, a correlation is calculated for the different pumps depending on their service.
- Rated Power (P_{rated}): from the calculated pressure drop for the system and the volumetric flow rate, a rated power arises. Considering hydraulic power to be the pressure

drop times the volumetric flow rate, and the electrical power, this hydraulic power divided by the efficiency of the pump (also an input in the models).

Macro	Pump Code	Use	ΔP Correlation [Pa]	Observations
M1200	M1200_PU01	Primary Circuit	MIN(GT(M1300_PU01_V,0.2)*((9.49779473*10**-6)*M1300_PU01_V**3-0.00350971*M1300_PU01_V**2	Uses the density of the primary circuit in case the two circuits differ.
M1300			+0.4427464**2*M1300_PU01_V+5.876420 27)+LE(M1300_PU01_V,0.2)*25*M1300_PU01_V,30)*M1300_RoPri*gravity	
	M1200_PU02	Secondary Circuit	MIN(GT(M1200_PU02_V,0.2)*((9.49779473*10**-6)*M1200_PU02_V**3-0.00350971*M1200_PU02_V**2	Could be reduced. Is taken as equal
			+0.4427464**2*M1200_PU02_V+5.876420 27)+LE(M1200_PU02_V,0.2)*25*M1200_PU02_V,30)*M1200_RoSec*gravity	to be conservative.
M3100	M3100_PU01	Pump Circuit	58.06*M3100_PU01_V+1287.8+101325	Minimum value of one bar fixed.
	M4100_PU01	Generator	MAX(MIN(52332+50000,-259.32*M4100_PU01_V+52332+50000),50000+20000)	Minimum value of 102332 Pa fixed considering control valve in 50000 Pa (0.5 bar, typical value)
M4100	M4100_PU02	Evaporator	MAX(MIN(200000,292.39*M4100_PU02_V+50741+50000),50000)	Minimum value of 100741 Pa fixed considering control valve in 50000 Pa (0.5 bar, typical value)
	M4100_PU03	Condenser	MAX(MIN(155802,-306.85*M4100_PU03_V+105802+500000),50000)	Minimum value of 1055802 Pa fixed considering control valve in 50000 Pa (0.5 bar, typical value)
	M4100_PU04	Absorber	MAX(MIN(155802,-306.85*M4100_PU03_V+105802+500000),50000)	Absorber and condenser considered with similar losses.
	M4200_PU01	Generator	MAX(MIN(52332+50000,-259.32*M4200_PU01_V+52332+50000),50000+20000)	Minimum value of 102332 Pa fixed considering control valve in 50000 Pa (0.5 bar, typical value)
M4200	M4200_PU02	Evaporator	MAX(MIN(200000,292.39*M4200_PU02_V+50741+50000),50000)	Minimum value of 100741 Pa fixed considering control valve in 50000 Pa (0.5 bar, typical value)
	M4200_PU03	Condenser/ Absorber	MAX(MIN(155802,-306.85*M4200_PU03_V+105802+500000),50000)	Minimum value of 1055802 Pa fixed considering control valve in 50000 Pa (0.5 bar, typical value)
M4600	M4600_PU03	Geothermal BHX	2.05*M4600_PU03_BHXDepth*1000	Considered a typical loss per distance of 1000 Pa/m for the borehole and that the route is twice the depth plus a 5% overdesign.
M7200 M7300	M7300_PU01	Distribution	MAX(250000;MIN(600000;450*(M7300_PI01_L+200)))	Considered a typical loss per distance of 500 Pa/m for the network and a minimum pressure drop for the network of 6 bar.

Table 5.1: Pressure drop for different pumps in different macros.

5.1.3 Heat exchanger (TRNSYS Type 5b)

Type 5 utilizes a modeling approach that considers the minimum capacitance in order to determine its effectiveness. In this method, users are required to input the heat exchanger's UA value and inlet conditions. Based on these inputs, the model determines whether the cold side (load) or hot side (source) has minimum capacitance and calculates effectiveness accordingly, taking into account the specified flow configuration and UA value. Finally, it computes the outlet conditions of the heat exchanger.

It is called Type 5 "b" because of the counterflow setting parametrized.

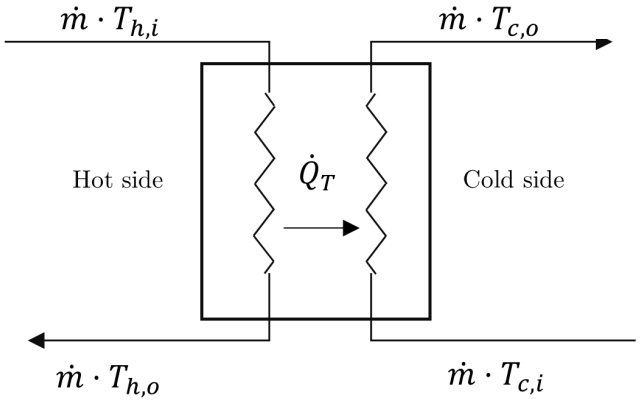

Figure 5.3: TRNSYS heat exchanger scheme

Equations:

$$C_c = \dot{m}_c \cdot Cp_c \tag{5.10}$$

$$C_h = \dot{m}_h \cdot Cp_h \tag{5.11}$$

$$C_{\max} = max(C_c, C_h) \tag{5.12}$$

$$C_{\min} = min(C_c, C_h) \tag{5.13}$$

$$\varepsilon = \frac{1 - exp\left[-\frac{UA}{C_{\min}}\left(1 - \frac{C_{\min}}{C_{\max}}\right)\right]}{1 - \left(\frac{C_{\min}}{C_{\max}}\right)\exp\left[-\frac{UA}{C_{\min}}\left(1 - \frac{C_{\min}}{C_{\max}}\right)\right]} \tag{5.14}$$

$$T_{h,o} = T_{h,i} - \varepsilon\left(\frac{C_{\min}}{C_h}\right)(T_{h,i} - T_{c,i}) \tag{5.15}$$

$$Q_T = \varepsilon C_{\min}(T_{h,i} - T_{c,i}) \tag{5.16}$$

5.1.4 Control with hysteresis (TRNSYS Type 2)

This controller generates a control function (γ_o) that can have a value of 0 or 1, depending on the temperature difference between upper and lower temperatures compared to two deadband

temperature differences (ΔTH and ΔTL). The new value of γ_o is determined by whether the input control signal is on or off ($\gamma_i = 0$ or 1). Typically, this controller is used with the output control signal (γ_o) connected to the inlet control signal (γ_i), creating a hysteresis effect. It also includes a high-limit cut-out feature. Regardless of the dead band conditions, if the high limit condition is exceeded, the control function will be set to zero. Please note that while temperature notation is used throughout this section, this controller can be applied to other applications beyond temperature sensing [92].

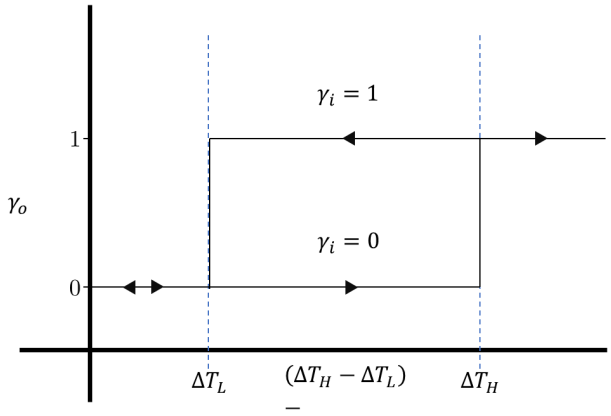

Figure 5.4: Control function

If the controller was previously ON ($\gamma_I = 1$):

$$\gamma_o = \begin{cases} 1, & if\ \Delta T_L \leq (T_H - T_L) \\ 0, & if\ \Delta T_L > (T_H - T_L) \end{cases} \tag{5.17}$$

If the controller was previously OFF ($\gamma_I = 0$):

$$\gamma_o = \begin{cases} 1, & if\ \Delta T_H \leq (T_H - T_L) \\ 0, & if\ \Delta T_H > (T_H - T_L) \end{cases} \tag{5.18}$$

5.2 Meteo

As it will be shown in section 5.2.1, meteorological TMY files are obtained from publicly available information.

For the use of this information, Type 15-6 is available in TRNSYS. This component has the function of extracting data at consistent time intervals from an external weather data file. It then uses interpolation techniques to estimate the values of variables such as solar radiation for tilted surfaces at intervals smaller than one hour. The interpolated data is made accessible to other components in TRNSYS. Additionally, this model computes various important terms including the temperature of mains water and effective sky temperature.

For this macro, Type 77 is also used, to obtain ground values. In this subroutine, the vertical temperature distribution of the ground is simulated based on several input parameters. These include the mean ground surface temperature for the year, the amplitude of the ground surface temperature for the year, the time difference between the beginning of the calendar year and when the minimum surface temperature occurs, and thermal diffusivity of soil. Relevant information regarding these values can be found in various sources such as ASHRAE Handbooks (specifically in reference to soil temperature).

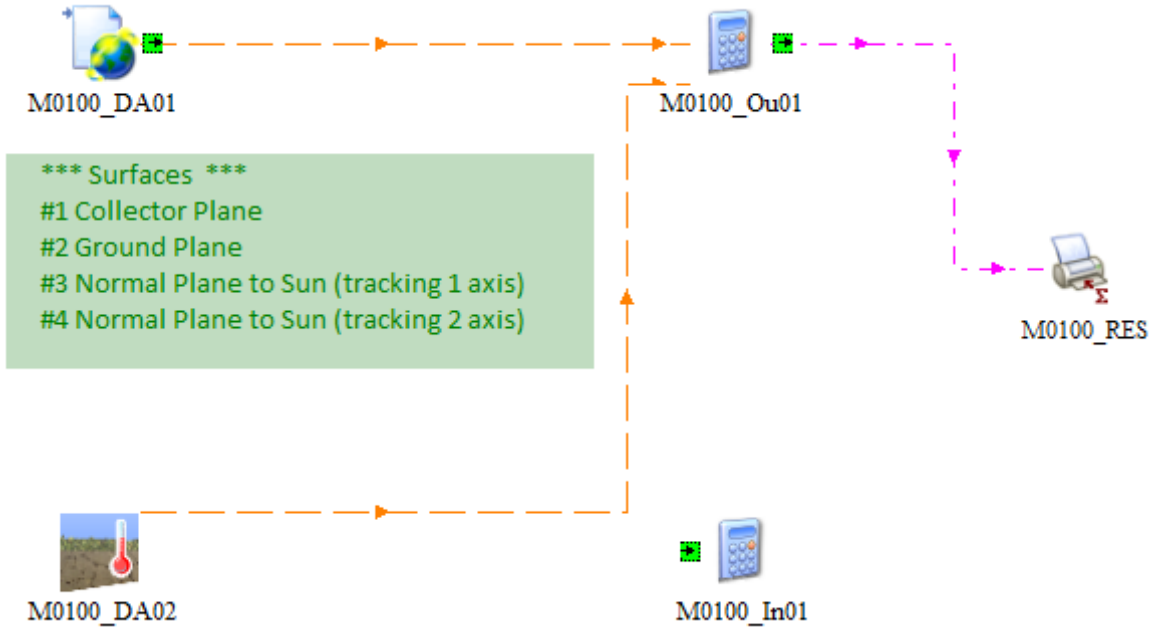

Figure 5.5: TRNSYS meteorological macro

Code	Type	Use	Description	External File
M0100_DA01	15-6	Weather Data	Able of reading different formats: TMY, TMY2, Energy+, IWEC, CWEC, Metoenorm, TMY3, German TRY 2004 German TRY 2010	Yes. User-supplied.
M0100_DA02	77	Ground Data	Calculated from parameters	No.

Table 5.2: Types used in M0100.

5.2.1 Meteorological files generation

Weather data is of utmost importance when simulating heating and cooling systems, this has led to the generation of various methods of gathering this information. The most used one

being the Typical Meteorological Year (TMY) which was first introduced by Sandia National Laboratories [93].

TMY datasets are created by selecting one year of climatic data from a larger set spanning multiple years. This selection process ensures that the chosen data for each month represents the most typical conditions among all available years in the long-term dataset. The method outlined in International Standard ISO15927-4 provides guidelines on how to construct TMY datasets [94]. If a particular year was chosen, values could lead to an under or over-sizing of the installation.

Information gathering

For the different locations the Photovoltaic Geographical Information System (PVGIS) database was used, which allows to select any location in Europe with ease [95]. Through the use of this system, TMY information can be accessed and downloaded in EnergyPlus format which can also be read by TRNSYS meteorological type (Type 15-6). A specific parameter has been set in "PAR_MDW" to select the format of the weather file provided ("Type_Meteofile"), by changing this parameter, the user can select between TMY format, TMY2 format, EnergyPlus format, International Weather for Energy Calculation (IWEC) format, Canadian Weather Year for Energy Calculation (CWEC) format, Metoenorm for TRNSYS format, TMY3 format, German Test Reference Year (TRY) 2004 format and German TRY 2010 format.

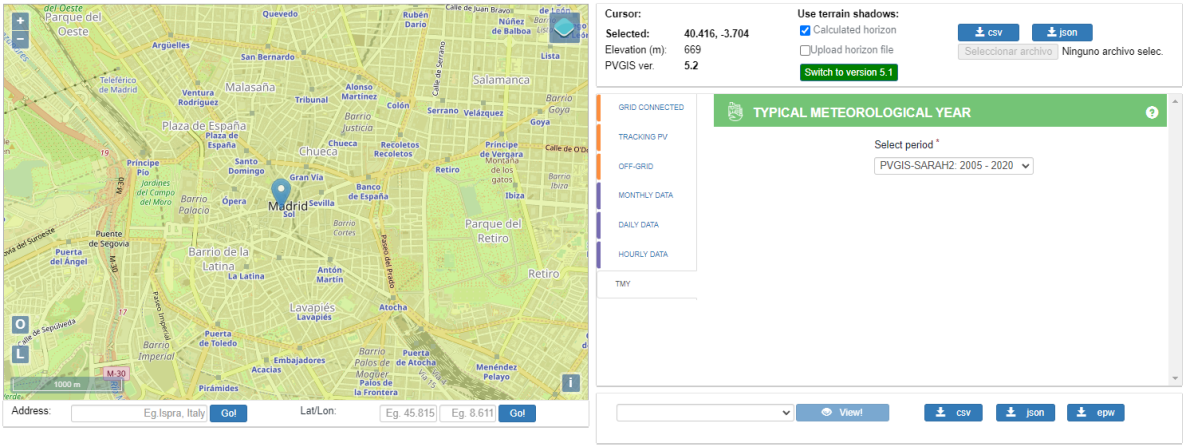

Figure 5.6: Screen capture of PVGIS online interface [96]

5.3 Solar Thermal

This model has been designed to replicate the behavior of concentrating solar collectors (PTC and Fresnel). It takes irradiation data from meteorological files, filters it taking into account shading and calculates the amount delivered to HTF. It considers input from both a secondary thermal fluid circuit and a primary thermal fluid circuit, with the possibility of assuming only one circuit by disregarding the heat exchanger's contribution and assigning it an artificially high overall heat transfer coefficient.

5.3.1 Hypotheses

A series of hypotheses were taken when producing this model:

- No safety dissipation method was considered in the models (air heat exchanger) used normally in this kind of networks to avoid damage due to overheating. The model itself simulates a flow control able to deal with over temperatures and calculates possible dumped energy.
- Design of the heat exchanger is done by considering a fixed logarithmic mean temperature difference which is set to a common value of 4°C, and along with the design capacity of the installation, calculate a value for the overall heat transfer coefficient (UA) of the exchanger to have it parametrized.

5.3.2 Heat and Mass Balance

A first simplified scheme of the macro is presented for clarification in Figure 5.7. This figure also shows a draft of what will be the energy and mass balance.

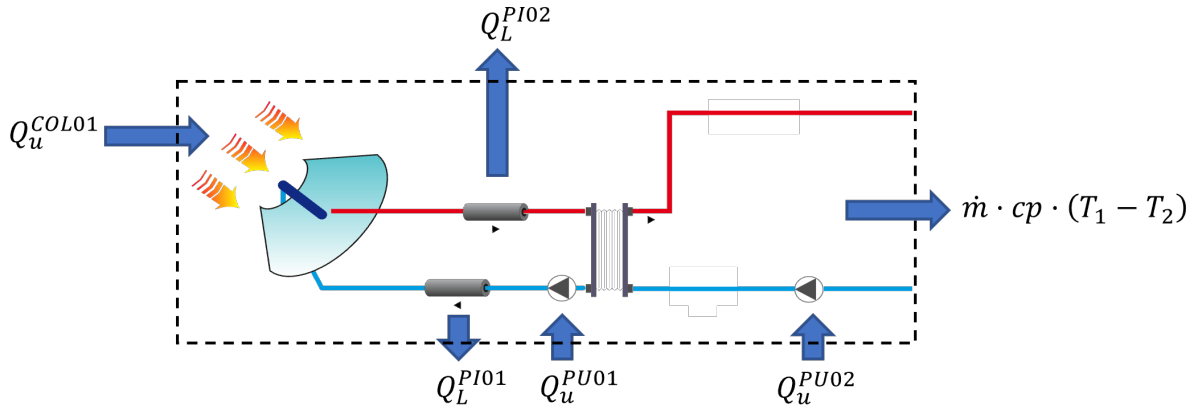

Figure 5.7: Macro M1200 scheme and energy and mass balance

Where,

- Q_u^{COL01}: is the rate at which energy is transmitted by the collector into the HTF [kW].
- $\dot{m} \cdot cp \cdot (T_2 - T_1)$: is the rate at which energy is transmitted by macro into the HTF [kW].
- $Q_L^{PI01/PI02}$: is the rate at which energy is lost by the pipes into the environment [kW].
- $Q_u^{PU01/PU02}$: is the rate at which energy is transmitted by the pumps into the HTF due to inefficiencies [kW].

Using this scheme, a TRNSYS macro has been developed which is shown in Figure 5.8.

From the macro generated in TRNSYS different types used and what is the role they play in the macro is described in Table 5.3.

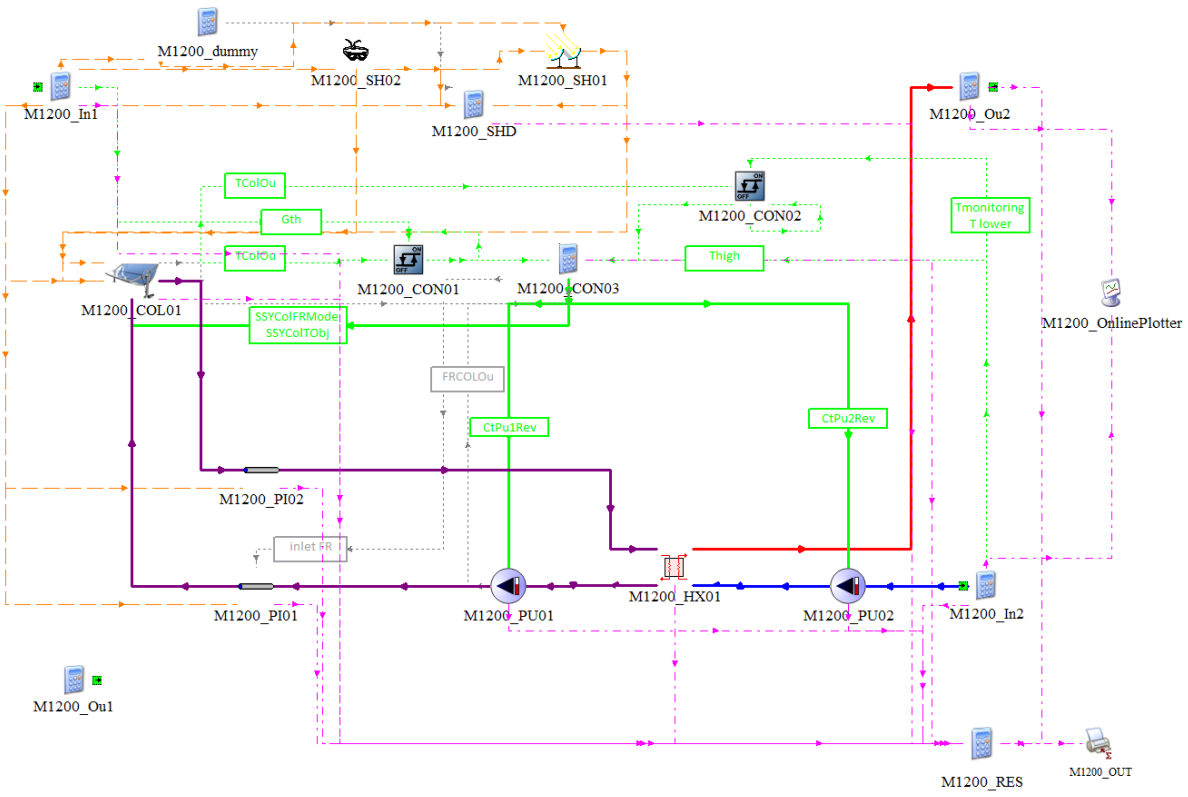

Figure 5.8: Macro M1200 in TRNSYS simulation studio

5.3.3 Parametrization

Using the minimum number of variables to parametrize the macro, the array area and the inlet and outlet temperatures are needed as explained in section 4.1.2.

5.3.4 Control

Taking a closer look at Figure 5.8, various dashed green lines representing signals being transmitted can be observed. This macro employs two main type 2 controls. The first control is used to detect the presence of radiation in order to prevent both the secondary and primary circuits from operating when there is no radiation available for harnessing. The second control determines the district's energy demand and assesses whether the solar collector can heat the tank by comparing the temperature coming out of the collector with M1200_HX01 logarithmic mean temperature difference (LMTD) as a threshold. If the tank is full, achieving this will not be feasible, and thus, it will halt the operation of the secondary circuit.

Flows are internally regulated by the type of collector, with control being dependent on a parameter that determines how flow is calculated by the model, offering three options:

- M1200_COL01_Control=0: run at specified inlet flow and calculate the outlet temperature.

Code	Type	Use	Description	External File
M1200_COL01	1245	Solar PTC Collector	Considering efficiency coefficients. Controls output temperature. IAMs from file.	Yes. From supplier's information.
M1200_SH02	67	Shading Mask	Considers obstructions to the collectors' surface from surrounding sources.	Yes. Must be developed from site information. Should be set to cero as default.
M1200_SH01	1262	Shading Mask	Considers Shading from different rows in the collector array.	No.
M1200_CON02	2b	Differential controller	Ensures that there is a positive difference between tank top and bottom to turn on the pump.	No.
M1200_CON01	2d	Differential controller	Controls whether there is solar radiation to operate the collectors or not.	No.
M1200_HX01	5b	Counter-flow heat exchanger	Used to connect primary and secondary circuit.	No.
M1200_PU0X	110	Variable speed pump	Used to set the flow of the different circuits.	No.
M1200_PI0X	709	Circular pipe	Calculates heat losses from pipes.	No.

Table 5.3: Types used in M1200

- M1200_COL01_Control=1: modulate flowrate to maintain outlet temperature but turn off if the setpoint can't be maintained (setpoint in this mode is the desired temperature at the top of the tank plus the LMTD of the heat exchanger to obtain such temperature in the secondary circuit).
- M1200_COL01_Control=2: modulate flowrate and keep the outlet as close to the setpoint as possible if the collector is gaining energy but turn off the collector if the collector is losing energy (setpoint in this mode is a parametrized temperature).

All the ON-OFF controls are sent to a main controller (M1200_CON03), which then transmits the corresponding signals to the pumps and sends the established settings to the collector type (M1200_COL01) in order to establish the correct flow.

5.3.5 Results

The macro has as a result the following variables:

- Irradiation on the horizontal and collector's plane. And also these results affected by both horizon shading mask and proximity-based shading from other collectors.
  - Total
  - Beam
  - Sky diffuse
  - Ground diffuse

- Energy gain of the collector (without taking into account energy loss to the surroundings).
- Energy losses (piping). Along with the integrated change in internal energy from the beginning of the simulation.
- Heat transfer (heat exchanger).
- Macro's work (considered from the pumping requirements). These results are provided by individual pumps and as a whole.
- Heat delivered by the macro.
- Energy balance.
- The ratio of auxiliary components to the heat generated.
- The final energy consumption (FEC) for the electricity and the heat provided to the networks.
- The operation time. This is calculated by taking into account the time when the primary circuit pump is operative.

5.4 Conventional Absorption Chiller

This model has been designed to replicate the behavior of a conventional absorption chiller. The thermodynamic cycle of an absorption chiller is simulated by the macro, with all its flows, to remove heat from the chiller's evaporator in order to cool a flow. It considers a heat input for the generator from the heat network, standard cooling towers for the absorber and the condenser, and the evaporator working against a storage tank that serves as a buffer. The layout of the model in TRNSYS simulation Studio can be seen in Figure 5.9.

From the macro generated in TRNSYS different types used and what is the role they play in the macro is described in Table 5.4.

5.4.1 Hypotheses

A series of hypotheses were taken when producing this model:

- Pumps are assumed to be on off for this equipment.
- Partial Load Ratios are taken from a performance map file used by the absorber TRNSYS type.

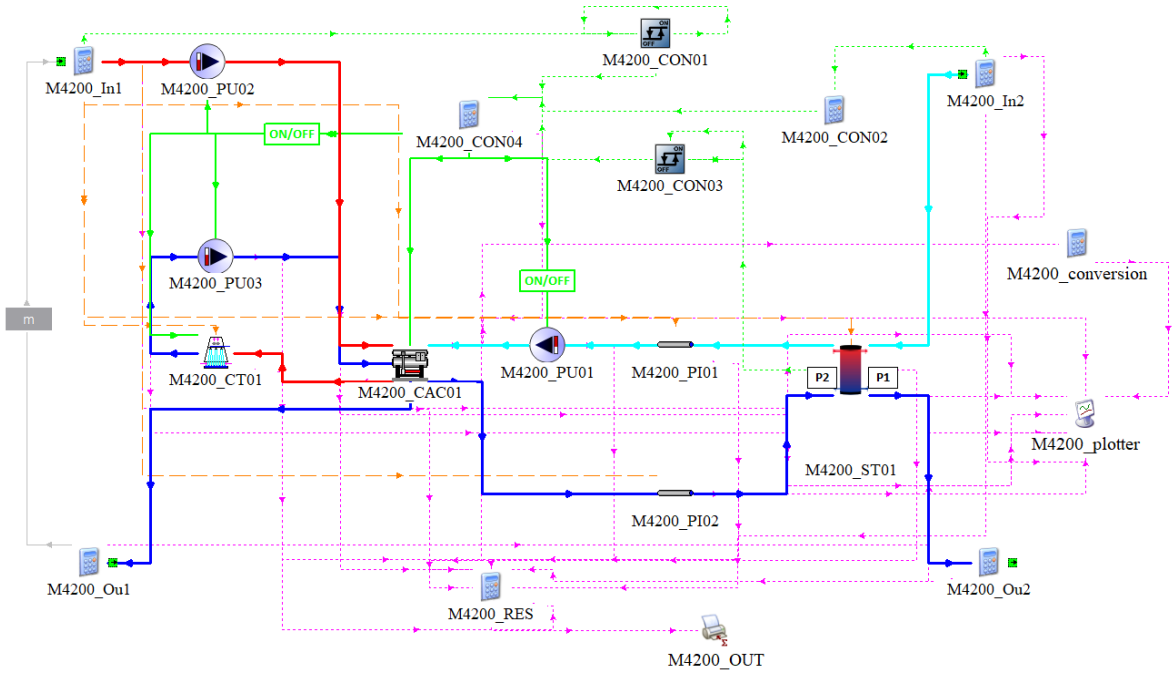

Figure 5.9: Macro M4200 in TRNSYS simulation studio

5.4.2 Heat and Mass Balance

A first simplified scheme of the macro is presented for clarification in Figure 5.10. This figure also shows a draft of what will be the energy and mass balance.

Where,

- Q_{In}^{CAC01}: is the rate at which energy is entering the cycle through the generator [kW].
- $\dot{m}_{Out2} \cdot cp \cdot (T_1 - T_2)$: is the rate at which energy is removed by macro into the HTF [kW].
- $Q_{L}^{PI01/PI02}$: is the rate at which energy is lost by the pipes into the environment [kW].
- Q_{L}^{ST01}: is the rate at which energy is lost by the storage into the environment [kW].
- $Q_{U}^{PU01/PU02/PU03}$: is the rate at which energy is transmitted by the pumps into the fluid due to inefficiencies [kW].
- W_{U}^{CAC01}: is the rate at which work is done by the absorber cycle (mostly cycle pump) [kW].

5.4.3 Parametrization

Using the minimum number of variables to parametrize the macro, the chilled water capacity is asked from the user along with the temperatures in and out of the evaporator side and generator side. Once this is supplied, the correlations calculate the different mass flows

Code	Type	Use	Description	External File
M4200_CAC01	107	Absorption Chiller	Considering all circuits into the chiller. Also performance mapping for Partial Load Ratio.	Yes. From supplier's information
M4200_ST01	534	Storage	As buffer for the evaporator production.	No.
M4200_CT01	128	Cooling Tower	Simple design of a cooling tower from ambient conditions.	No.
M4200_CON01	2d	Differential Controller	Ensures that there is enough difference between the setting and the generators nominal temperature to start.	No.
M4200_CON03	2d	Differential Controller	Checks that the tank is not full comparing its temperature against the setting.	No.
M4200_PU0X	110	Variable Speed Pump	Used to set the flow of the different circuits.	No.
M4200_PI0X	709	Circular Pipe	Calculates heat losses from pipes	No.

Table 5.4: Types used in M4200.

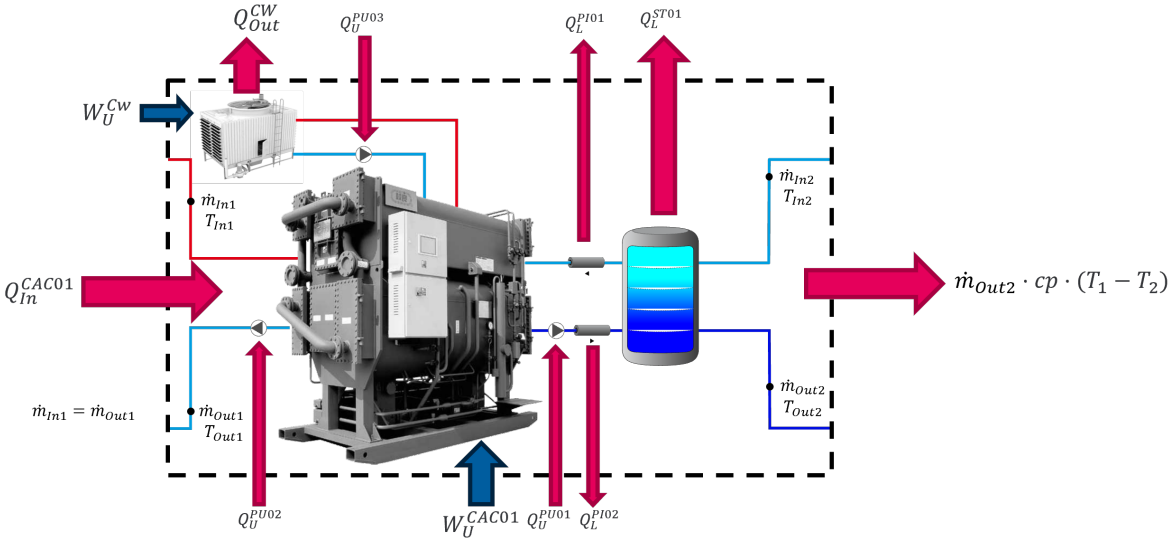

Figure 5.10: Macro M4200 scheme and energy and mass balance

needed considering the nominal COP. Values are also supplied automatically for the Cooling Tower (CT) using standard temperature differences but can also be changed by the user if desired.

5.4.4 Control

The control on this macro is subdivided into three different requirements. The need for energy as a resource in the generator for the absorption chiller to function, the need for demand to be present as a driving force of the operation, and the need for the tank not to be full as to be able to charge it. These three requirements are monitored by the use of two type 2d (ON-OFF controllers with hysteresis) for the temperatures (generator's and tank's), and an equation that checks that the flow entering the system is higher than cero (demand requirement). Once these three conditions are met, the macro proceeds to power on.

5.4.5 Results

The results of this macro could be subdivided into heat and work flows, performance indicators, and operating variables. In the first category,

- Heat flows coming in and out of the system.
- Electrical work.

As performance indicators the following variables can be found,

- COP.
- Operation time.

As operating variables,

- Evaporator temperatures (to determine possible variations in case the COP is not as high as expected due to performance issues).

5.5 Compression Chiller

This model has been designed to replicate the behavior of a compression chiller. The thermodynamic cycle of an compression chiller is simulated by the macro, with all its flows, to remove heat from the chiller's evaporator in order to cool a flow. It considers an air cooled condenser, an electrical compresor, and the evaporator working cooling a working fluid. This macro has similar features as the boiler macro (Section 5.7), so it allows series and parallel operation against a possible storage tank that serves as a buffer outside the macro. The layout of the model in TRNSYS simulation Studio can be seen in Figure 5.11.

From the macro generated in TRNSYS different types used and what is the role they play in the macro is described in Table 5.5.

Code	Type	Use	Description	External File
M4300_ACC01	655	Air compression Chiller	Considering all circuits into the chiller. Also performance mapping for Partial Load Ratio.	From supplier's information.
M4300_MIX01	649	Mixer	To combine flows to change control modes.	No.
M4300_DIV01	647	Diverter	To separate flows to change control modes.	No.
M4300_CON01	2d	Differential Controller	Checks that the tank is not full comparing its temperature against the setting.	No.
M4300_PU01	110	Variable Speed Pump	Used to set the flow for the parallel operation.	No.
M4300_PI01	709	Circular Pipe	Calculates heat losses from pipes	No.

Table 5.5: Types used in M4300.

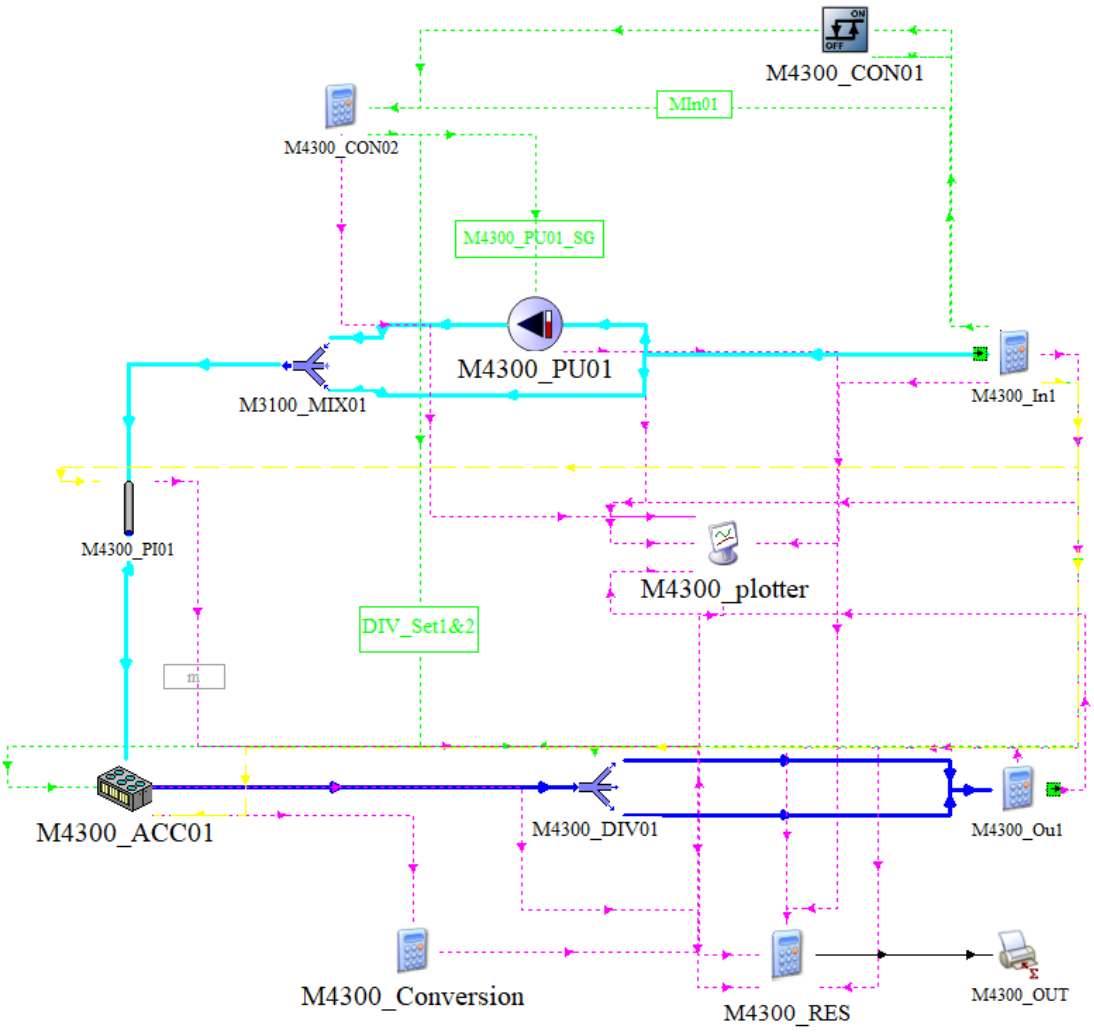

Figure 5.11: Macro M4300 in TRNSYS simulation studio

5.5.1 Hypotheses

A series of hypotheses were taken when producing this model:

- Only one representative pipe circuit is set as loss for the macro.
- Partial Load Ratios are taken from a performance map file used by the chiller type.
- As it is based on an external file, this component can be used to model single and multi-stage chillers.

5.5.2 Heat and Mass Balance

A first simplified scheme of the macro is presented for clarification in Figure 5.12. This figure also shows a draft of what will be the energy and mass balance.

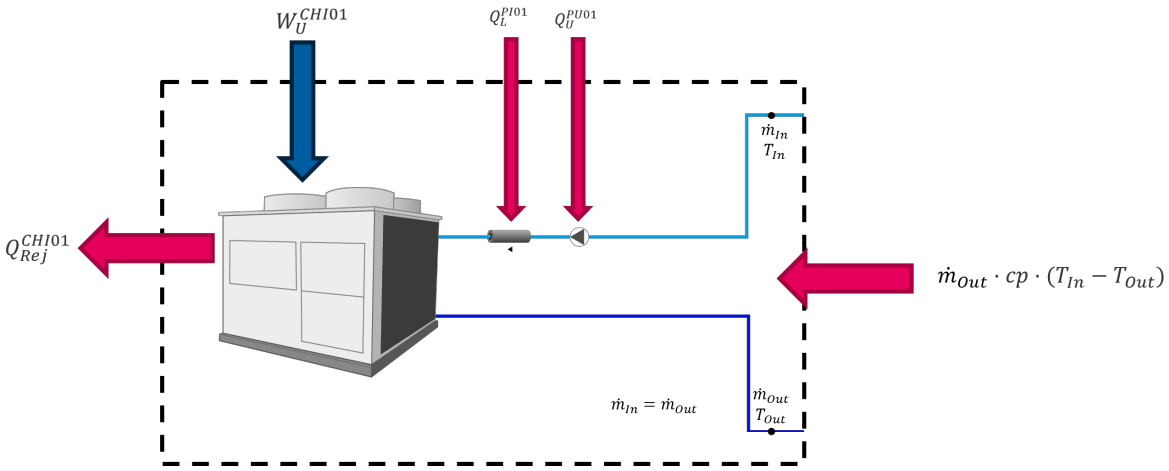

Figure 5.12: Macro M4300 scheme and energy and mass balance

Where,

- Q_{Rej}^{CHI01}: is the rate at which energy is being rejected by the cycle through the condenser [kW].
- $\dot{m}_{Out} \cdot cp \cdot (T_{In} - T_{Out})$: is the rate at which energy is removed by macro into the HTF [kW].
- Q_L^{PI01}: is the rate at which energy is lost by the pipes into the environment [kW].
- Q_U^{PU01}: is the rate at which energy is transmitted by the pumps into the fluid due to inefficiencies [kW].
- W_U^{CAC01}: is the rate at which work is done by the compression chiller cycle (mostly cycle compressor) [kW].

5.5.3 Parametrization

Using the minimum number of variables to parametrize the macro, the chilled water capacity is asked from the user along with the temperatures in and out of the evaporator side. Once this is supplied, the correlations calculate the different mass flows needed considering the nominal COP. Values for the air flow are calculated automatically by the time considering the amount of heat to be rejected using the ambient conditions.

5.5.4 Control

Most of the control done by this macro is handled by the compression chiller type. However, the operation can be controlled externally by an input signal to the macro (defined in the deck which is used). Series or parallel control sets the sense of the flow, to make the circuit go through the pump to be set, or directly take flows from the network in case of series operation. In the case of parallel control, there is a M4300_CON01 which serves as a comparison controller to charge the external tank with an upper and lower deadband that can be set by the user through parameters "M4300_CON01_DTH" and "M4300_CON01_DTL" (See 5.1.4).

5.5.5 Results

The results of this macro could also be subdivided into heat and work flows, performance indicators, and operating variables. In the first category,

- Heat flows coming in and out of the system. Should be noted that heat flow coming in the macro should be mainly the inlet flow by the chilled current.
- Electrical work.

As performance indicators the following variables can be found,

- COP.
- Operation time.

As operating variables,

- Inlet and outlet temperatures.

5.6 Heat Pumps

This model has been designed to replicate the behavior of a heat pump. The thermodynamic cycle of heat pump is simulated by the macro, with all its flows, to remove heat from the heat pump's evaporator in order to cool a flow and the reverse cycle in case the heat pump is in heating mode. It considers a water/brine condenser (depending on fluid parameters), an electrical compressor, and the evaporator working cooling a working fluid. This macro, instead of having the feature seen in the boiler and air compressor macro (Section 5.7 and 5.5), has two different macro codes for the possibility of having the storage tank that serves as a buffer outside the macro. However, in this alternate configuration, tests have only been done for heating-only operation. The layout of the model in TRNSYS simulation Studio can be seen in Figure 5.13 for macro code M4600 (with tanks inside the macro).

The layout of the model for M4610 can be seen in Figure 5.14 (with tanks outside the macro) only with control for the heating operation.

Macro with inside tanks (M4600) will be used for explanation as its control is more complex for having both heating and cooling operations.

The different TRNSYS types used in the generated macro and their respective roles are described in Table 5.6.

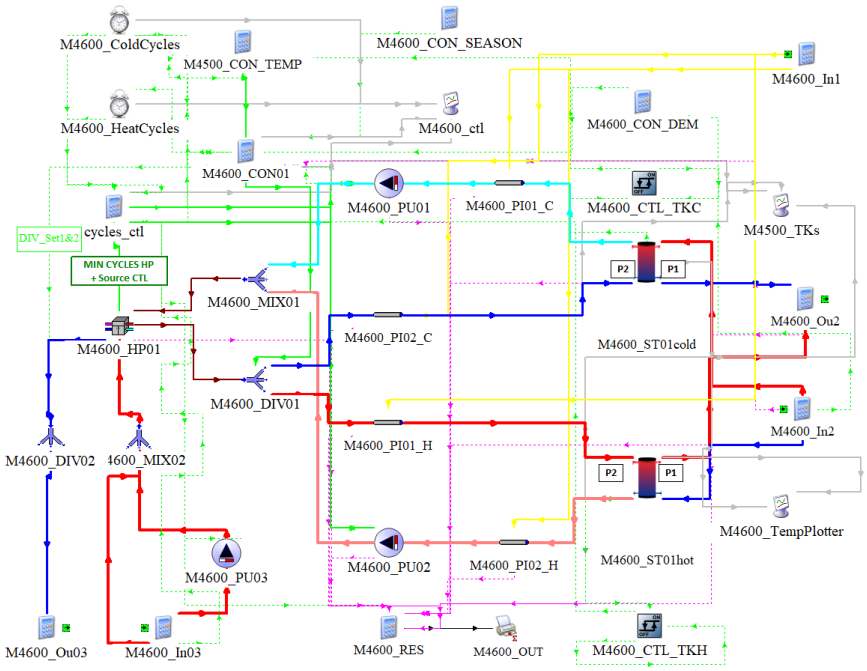

Figure 5.13: Macro M4600 in TRNSYS simulation studio

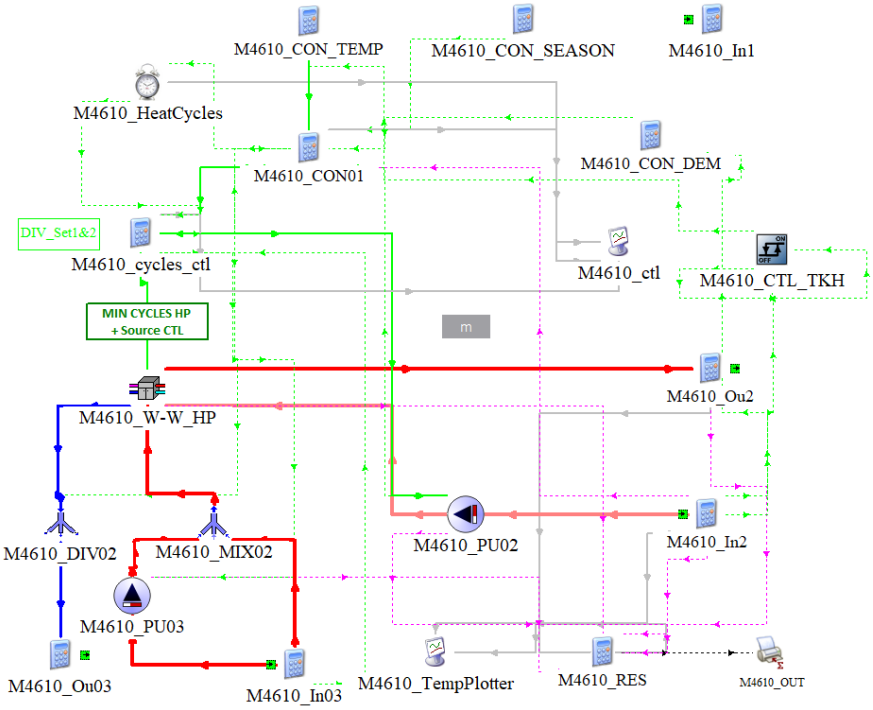

Figure 5.14: Macro M4610 in TRNSYS simulation studio

Code	Type	Use	Description	External File
M4600_HP01	927	Water-Water Heat Pump	Considering all circuits into the Heat pump. Also performance mapping for Partial Load Ratio.	From supplier's information.
M4600_MIX01	649	Mixer	To combine flows to change control modes.	No.
M4600_DIV01	647	Diverter	To separate flows to change control modes.	No.
M4600_CTL_TKC	2d	Differential Controller	Checks that the cold tank is not full comparing its temperature against the setting.	No.
M4600_CTL_TKH	2d	Differential Controller	Checks that the hot tank is not full comparing its temperature against the setting.	No.
M4600_PU01	110	Variable Speed Pump	Used to set the flow for the heating operation mode.	No.
M4600_PU02	110	Variable Speed Pump	Used to set the flow for the cooling operation mode.	No.
M4600_PU03	534	Variable Speed Pump	Used to set the flow for the source operation in both modes.	No.
M4600_ST01Hot	534	Buffer tank	Water storage tank without a heat exchanger for hot circuit.	No.
M4600_ST01Cold	709	Buffer tank	Water storage tank without a heat exchanger for cold circuit.	No.
M4600_ColdCycles	1233	Timer control	Sets a minimum running time for the HP in cooling mode.	No.
M4600_HeatCycles	1233	Timer control	Sets a minimum running time for the HP in heating mode.	No.

Table 5.6: Types used in M4600.

5.6.1 Hypotheses

A series of hypotheses were taken when producing this model:

- Only two representative pipe circuit is set as loss for the macro.
- Partial Load Ratios are taken from a performance map file used by the heat pump type.
- As it is based on an external file, this component can be used to model both water and brine heat pumps.
- Two sets of tank heat pump circuits are needed to simulate both cooling and heating modes.
- This macro represents a two-pipe heat pump arrangement, simultaneous heat pumps are not simulated by this macro.

5.6.2 Heat and Mass Balance

A first simplified scheme of the macro is presented for clarification in Figure 5.15. This figure also shows a draft of what will be the energy and mass balance.

Where,

- Q_{Source}^{HP01}: is the rate at which energy is being rejected or absorbed by the cycle [kW].

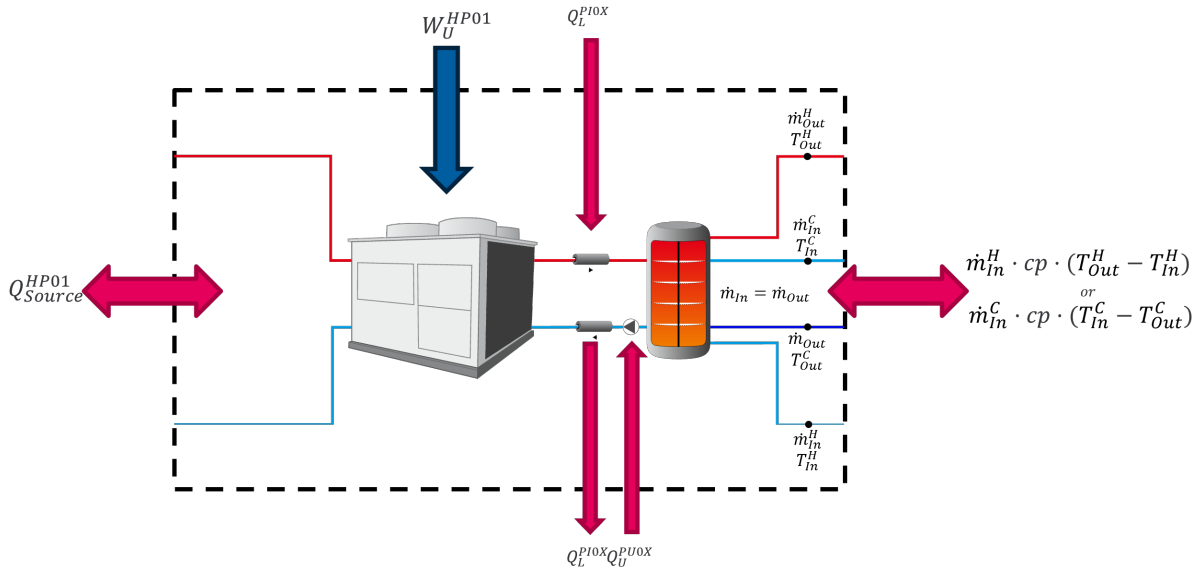

Figure 5.15: Macro M4600 scheme and energy and mass balance

- $\dot{m}_{Out} \cdot cp \cdot (T_{In} - T_{Out})$: is the rate at which energy is removed or set by macro into the HTF [kW].
- Q_L^{PI0X}: is the rate at which energy is lost by the pipes into the environment [kW].
- Q_U^{PU0X}: is the rate at which energy is transmitted by the pumps into the fluid due to inefficiencies [kW].
- W_U^{HP01}: is the rate at which work is done by the heat pump (mostly cycle compressor) [kW].

5.6.3 Parametrization

Using the minimum number of variables to parametrize the macro, the chilled water capacity is asked from the user along with the temperatures in and out of the machine in both modes. Once this is supplied, the correlations calculate the different mass flows needed considering the nominal COP. Values for the source water (or brine) are calculated automatically by the time considering the amount of heat to be rejected or absorbed using the standard source temperature difference expected.

5.6.4 Control

Control done by this macro is handled by different equations, considering a set of conditions. However, the operation can be controlled externally by an input signal to the macro (defined in the deck which is used). Cooling or Heating mode sets the sense of the flow, to make the circuit go through the pump to be set. Different conditions are temperature to arrive at a temperature setting in each of the tanks. Demand coming in from cold and hot networks in the case for comparison (highest demand generates this control). Seasonal control,

Which considers a user-supplied heating and cooling season (taking into account that this heat pump does not work simultaneously). The user has to select which kind of control to prioritize, demand, seasonal, or demand and season. In the case of M4600, there are differential controllers set for both tanks, which serve as a comparison controller to charge the external tank with an upper and lower deadband that can be set by the user through parameters "M4600_CTL_TKH" and "M4600_CTL_TKC" (See 5.1.4).

5.6.5 Results

The results of this macro could also be subdivided into heat and work flows, performance indicators, and operating variables. In the first category,

- Heat flows coming in and out of the system. Should be noted that heat flow coming in the macro should be mainly the inlet flow by the chilled current in the case of cooling operation or the heat absorbed from the source in the case of heating operation.
- Electrical work.

As performance indicators, the following variables can be found,

- COP.
- Operation time.

As operating variables,

- Inlet and outlet temperatures.

5.7 Boiler

The model described in this section has been designed to replicate the behavior of a condensing boiler (considering the higher efficiencies and the temperatures in which DHNs work). It takes a heat input that considers the possibility of different fuels by values of Low Heating Value (LHV) to determine approximate values of fuel consumption. It can also work in series or parallel, considering a parallel operation to be done against a storage tank to keep it at a desired temperature. The layout of the model in TRNSYS simulation Studio can be seen in Figure 5.16.

From the macro generated in TRNSYS different types used and what is the role they play in the macro is described in Table 5.7.

5.7.1 Hypotheses

A series of hypotheses were taken when producing this model:

- No additional heat losses are calculated by pipe circuits inside this macro.
- Partial Load Ratios are taken from a performance map file used by the boiler type.

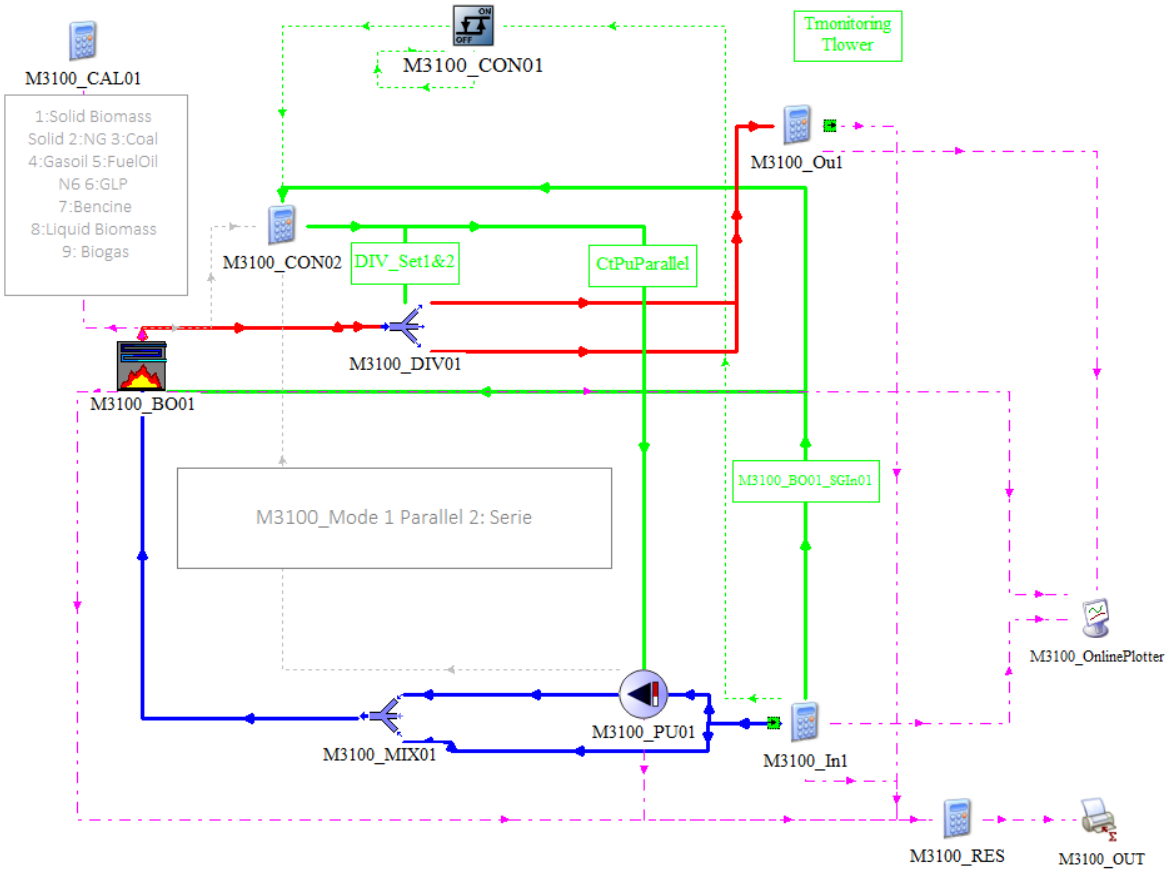

Figure 5.16: Macro M3100 in TRNSYS simulation studio

- Boiler type is related to the performance map provided, this boiler could mathematically represent other types of boilers if the supplied file was representative of these types.
- Fuel calculation is done by parametrization, taking fuel standard LHV, these values can be changed by the user, however, the difference in efficiencies by the change of fuel type is not considered by parametrization, hence, user discretion is advised.
- Boiler electrical consumption is assumed to be null, only pump consumptions are taken into account in parallel mode.

5.7.2 Heat and Mass Balance

A first simplified scheme of the macro is presented for clarification in Figure 5.17. This figure also shows a draft of what will be the energy and mass balance.

Where,

- Q_{Fuel}^{BO01}: is the rate at which energy is entering the boiler through the fuel combustion [kW].

Code	Type	Use	Description	External File
M3100_BO01	751	Boiler	Considering all circuits into the chiller. Also performance mapping for Partial Load Ratio.	From supplier's information.
M3100_MIX01	649	Mixer	To combine flows to change control modes.	No.
M3100_DIV01	647	Diverter	To separate flows to change control modes.	No.
M3100_CON01	2d	Differential Controller	Checks that the tank is not full comparing its temperature against the setting.	No.
M3100_PU01	110	Variable Speed Pump	Used to set the flow for the parallel operation.	No.

Table 5.7: Types used in M3100.

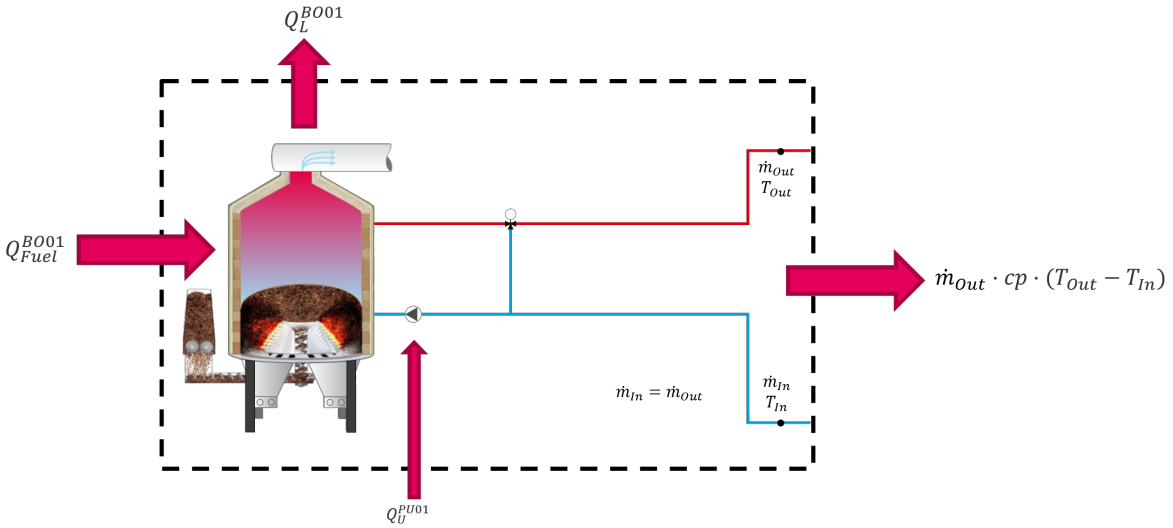

Figure 5.17: Macro M3100 scheme and energy and mass balance

- $\dot{m}_{Out} \cdot cp \cdot (T_{Out} - T_{In})$: is the rate at which energy is being transferred by macro into the HTF [kW].
- Q_L^{BO01}: is the rate at which energy is lost by the boiler to the environment (mostly through the flue gases) [kW].
- Q_U^{PU01}: is the rate at which energy is transmitted by the pumps into the fluid due to inefficiencies [kW].

5.7.3 Parametrization

This macro can be parametrized using few variables. Firstly the user can choose between different fuels, which have a prestablished LHV. These fuels are:

1. Solid Biomass.
2. Natural Gas.
3. Coal.

4. Gasoil.
5. Fueloil.
6. Liquefied Petroleum Gas (LPG).
7. Bencine.
8. Liquid Biomass.
9. Biogas.

This selection offers a first approach to fuel consumption for the user. The user can also choose, through the parameter "M3100_ Mode", the possibility of working in parallel or in series of the network. Parallel operation demands information from a connected tank and heats the contents of the tank until reaching a desired temperature setting, also needed to parameterize this macro. Finally, one of the most important parameters of this macro is the capacity of the boiler, which sets also the pump capacity in the case of parallel operation.

5.7.4 Control

Most of the control done by this macro is handled by the boiler type. However, the operation can be controlled externally by an input signal to the macro (defined in the deck which is used). Series or parallel control sets the sense of the flow, to make the circuit go through the pump to be set, or directly take flows from the network in case of series operation. In the case of parallel control, there is a M3100_CON01 which serves as a comparison controller to charge the external tank with an upper and lower deadband that can be set by the user through parameters "M3100_CON01_DifDelTH" and "M3100_CON01_DifDelTL" (See section 5.1.4).

5.7.5 Results

The results of this macro could also be subdivided into heat and work flows, performance indicators, and operating variables. In the first category,

- Heat flows coming in and out of the system. Should be noted that heat flow coming in the macro will be mainly the fuel consumption. This fuel consumption is assigned to its corresponding FEC number automatically.
- Electrical work (then used for FEC calculations).

As performance indicators the following variables can be found,

- Efficiency.
- Operation time.

As operating variables,

- Inlet and outlet temperatures.
- Preliminary fuel flow calculations.

5.8 Storage

This macro has been designed to represent a vertical water storage tank. The macro serves mostly as an inertial component for the system (to store energy) and also presents the possibility of developing thermocline storage. In the development of this macro several simplifications have been made. Firstly, a more thorough tank had been established but for simulation time purposes changes were made through different versions as it is visible in Figure 5.18 and Figure 5.19.

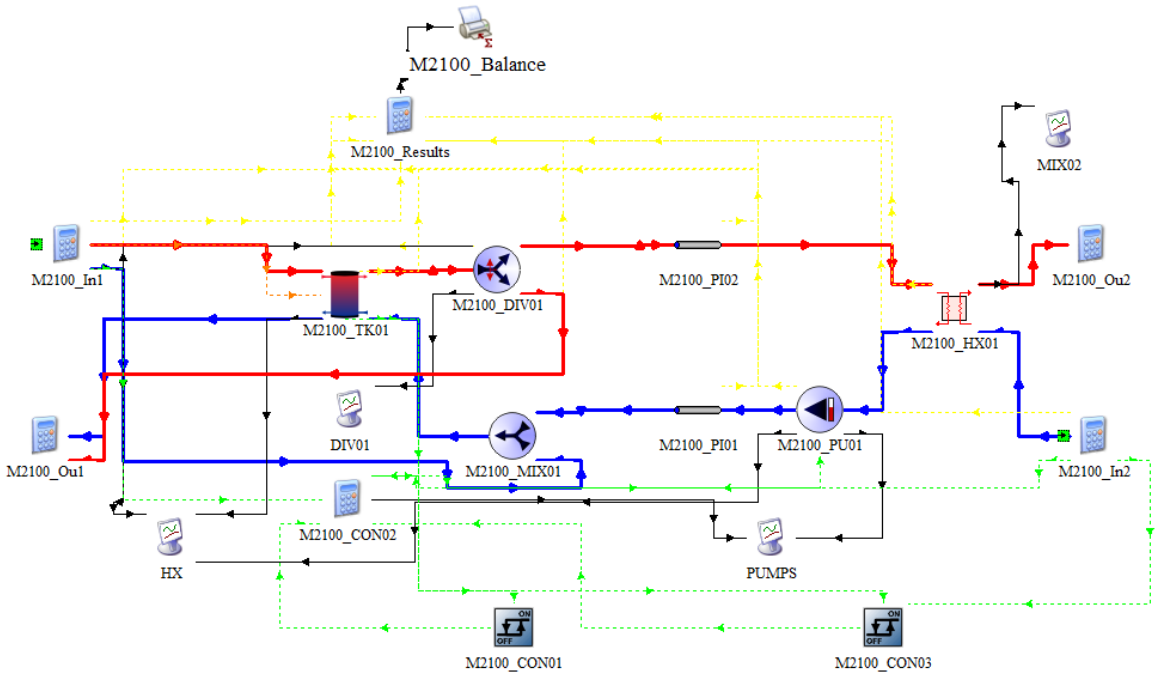

Figure 5.18: First version of M2100 TRNSYS macro

From the macro generated in TRNSYS different types used and what is the role they play in the macro is described in Table 5.8.

Code	Type	Use	Description	External File
M2100_TK01	534	Water Tank	Water storage tank without a heat exchanger.	No.

Table 5.8: Types used in M2100

5.8.1 Hyphotheses

Type 534 is a water storage tank that does not have a heat exchanger. The key outcomes of this component include the temperature and mass flow rate of the working fluid at both main nodes (top and bottom), the amount of thermal energy lost to the surrounding environment

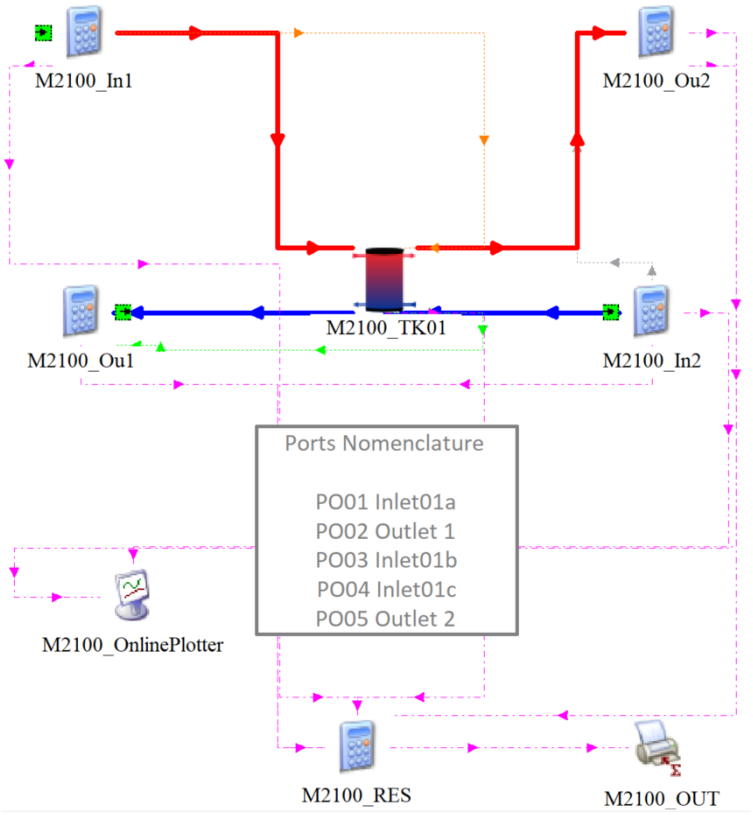

Figure 5.19: Last version of M2100 TRNSYS macro

by the fluid, and the stored energy within its volume. The tank macro does not take into account pipes surrounding the tank as those are considered to be part of the surrounding macros. Heat loss coefficient for the tank was fixed as per reference [97] in 0.16 $W \cdot m^{-2} \cdot K^{-1}$ (0.576 $kJ \cdot m^{-2} \cdot h^{-1} \cdot K^{-1}$).

5.8.2 Heat and Mass Balance

A first simplified scheme of the macro is presented for clarification in Figure 5.20. This figure also shows a draft of what will be the energy and mass balance.

Where,

- $QIn01$: is the rate at which energy is entering the macro through the heating or cooling sources [kW].
- $QOu01$: is the rate at which energy is leaving the macro through the heating or cooling demand [kW].
- Q_L^{ST01}: is the rate at which energy is lost by the storage to the environment [kW].

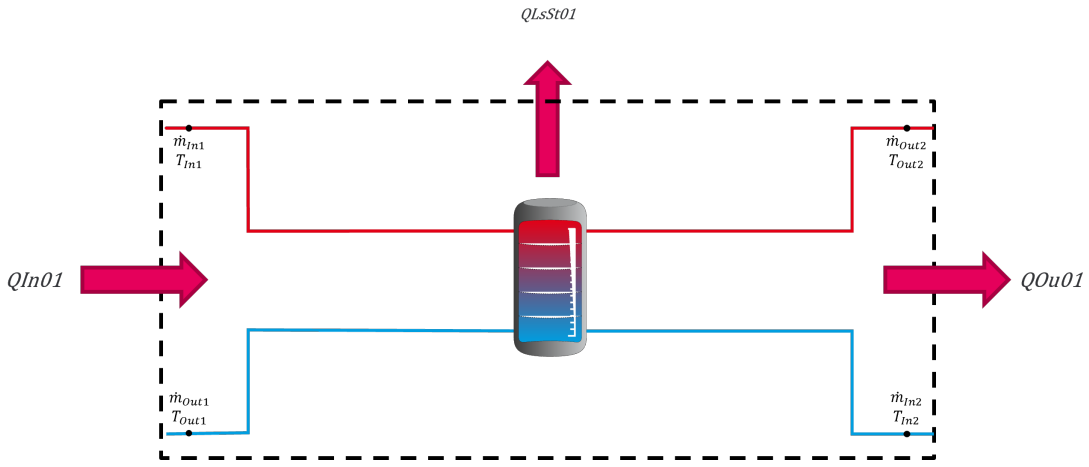

Figure 5.20: Macro M2100 scheme and energy and mass balance.

5.8.3 Parametrization

The inlet parameters of this component are calculated to account for the capacity of the tank, determining its height and diameter based on standard shape coefficients.

5.8.4 Control

This macro does not have control but sends temperature signals to other macros. Three different options for the placement of temperature sensors are available, completely selectable through parameters.

5.8.5 Results

The macro has several results, which include,

- incoming and outgoing energy of the different ports.
- total gain and losses from each port to understand participation of different suppliers and users.
- Tank losses at different points (top, edge, and bottom).
- Energy balance calculations.

5.9 Molten Salts Storage

This macro has been designed to represent a vertical molten salts storage tank. The macro serves as an inertial component for the system (to store energy) and also presents the possibility of developing thermocline storage. This macro also has associated heat exchangers to avoid contact between a primary molten salt circuit and a secondary circuit, to be chosen by the user.

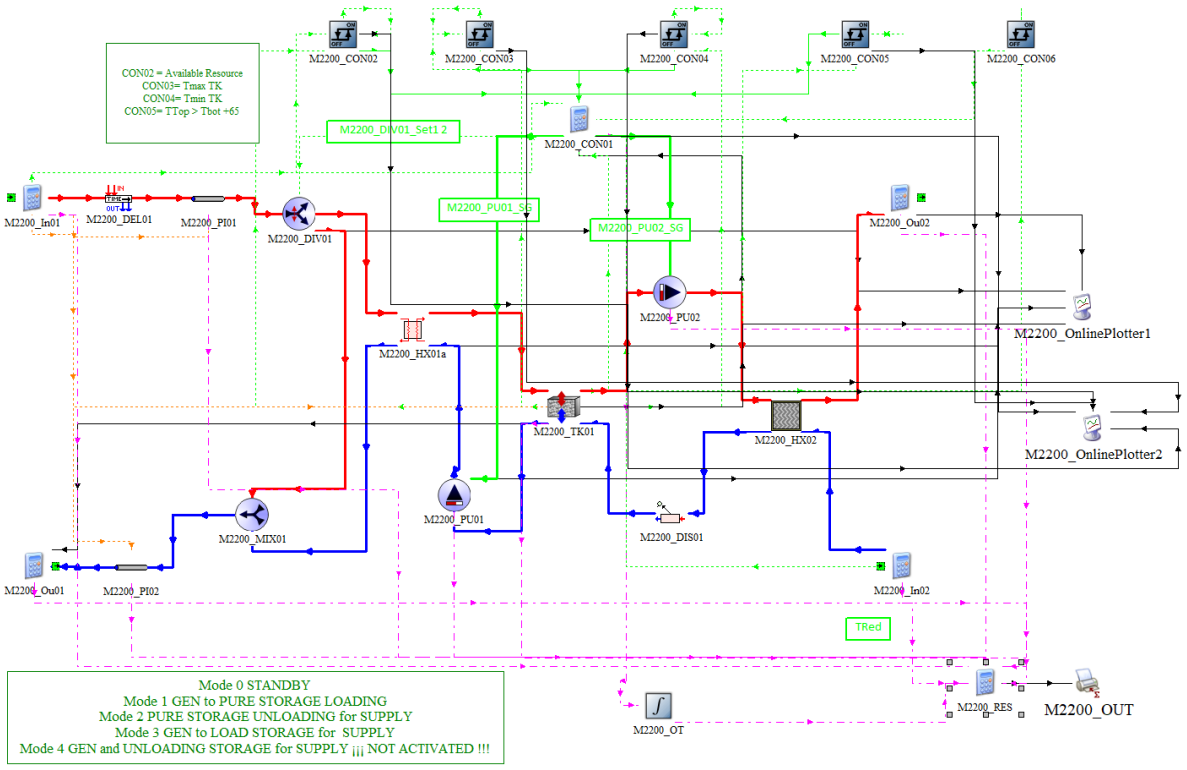

Figure 5.21: M2200 TRNSYS macro

From the macro generated in TRNSYS different types used and what is the role they play in the macro is described in Table 5.9.

5.9.1 Hyphotheses

Type 10 is a packed bed storage tank that does not have a heat exchanger. The key outcomes of this component include the temperature and mass flow rate of the working fluid at both main nodes (top and bottom), the amount of thermal energy lost to the surrounding environment by the fluid, and the stored energy within its volume. Model used for the calculation of the properties of the tank are described in "Proposal of a thermocline molten salt storage tank for district heating and cooling" paper from 2023 [26]. The configuration of a thermocline storage system containing molten salt revolves around a steel tank in a cylindrical shape. This tank includes distributors at the entry and exit points for the salt, as well as a large central area filled with packed bed materials. The stability of the temperature distribution within the tank and its overall capacity is significantly affected by the presence of this packed bed. An Engineering Equation Solver model was developed to evaluate the basic parameters of the thermocline tank vessel, including the mass and energy flow balances. The effective storage volume thermal capacity is estimated by the sum of the molten salt and rock-bed capacities as:

$$\overline{\rho \cdot C_{p_{eff}}} = (\rho \cdot C_p)_{salt} \cdot \varepsilon + (\rho \cdot C_p)_{rock} \cdot (1 - \varepsilon) \tag{5.19}$$

Where, ε: is the porosity of the rock.

Code	Type	Use	Description	External File
M2200_TK01	10	Molten Salts Tank	Packed bed storage tank without a heat exchanger. Uses calculated properties to simulate specific conditions.	No.
M2200_PU0X	110	Variable Speed Pump	Used to set the flow for the modes of operation.	No.
M2200_DEL01	667	Delayed Output Device	Used to set values from previous time steps. To improve convergence.	No.
M2200_DIV01	11f	Diverter	To separate flows to change control modes.	No.
M2200_MIX01	11h	Mixer	To combine flows to change control modes.	No.
M2200_HX01a	5b	Heat Exchanger	Used to connect primary and secondary circuit.	No.
M2200_HX02	650	Heat Exchanger	Constant effectiveness/Cmin HX, able to automatically bypass hot-side to maintain the cold-side outlet setting.	No.
M2200_DIS01	92	Disipator	Reduce fluid energy if necessary to reduce temperature return.	No.
M2200_CON02	2d	Differential controller	Compares temperature from the generators to the bottom of the tank.	No.
M2200_CON03	2d	Differential controller	Compares tank top temperature to maximum setting.	No.
M2200_CON04	2d	Differential controller	Compares tank bottom temperature to minimum setting.	No.
M2200_CON05	2d	Differential controller	Compares tank bottom temperature to tank top temperature, to check if it is possible to charge.	No.
M2200_CON06	2d	Differential controller	Compares tank bottom temperature to setting, to check if it is possible to discharge.	No.

Table 5.9: Types used in M2200

With these values, the total energy accumulated in the effective storage can be calculated as:

$$E = \overline{\rho \cdot C_{p_{eff}}} \cdot V_{eff,st} \cdot \Delta T \tag{5.20}$$

The model is thought for the properties of FERT-1 molten salt, and quartzite rocks for the packed bed. Considering these materials, the user only has to fill the total energy accumulated and charge or discharge capacity for the calculations to take place, along with the temperatures to set the corresponding properties. A first dimensioning was made using EES (Engineering Equation Solver) to check the tank stability.

After the model in EES, a dynamic model was developed in MATLAB to confirm the correspondence of with the one used in TRNSYS (Type 10). In this confirmation, the evolution in charging and discharging of the tank followed the ones simulated in MATLAB without much deviation (Figures figs. 5.22 and 5.23).

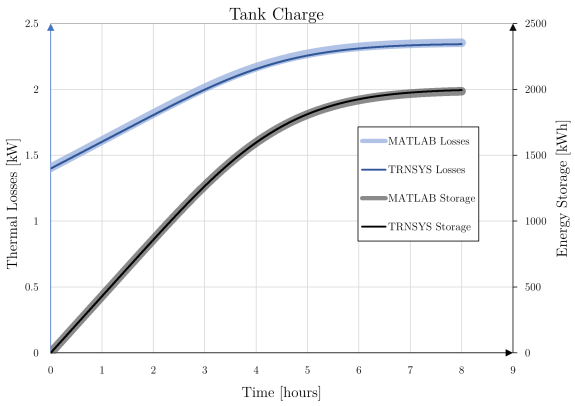

(a) Energy comparison between TRNSYS model and MATLAB model.

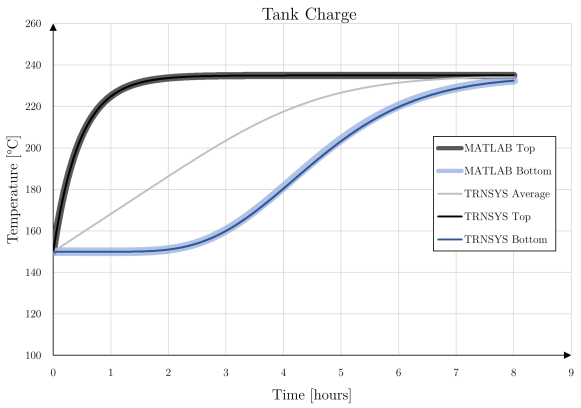

(b) Temperature comparison between TRNSYS model and MATLAB model.

Figure 5.22: Charging operation comparison between TRNSYS model and MATLAB model.

5.9.2 Heat and Mass Balance

A first simplified scheme of the macro is presented for clarification in Figure 5.24. This figure also shows a draft of the energy and mass balance.

Where,

- $\dot{m}'_{Out} \cdot cp \cdot (T_{In} - T_{Out})$: is the rate at which energy is removed by macro into the HTF from the generators [kW].
- $\dot{m}''_{Out} \cdot cp \cdot (T_{Out} - T_{In})$: is the rate at which energy is removed from the macro into the HTF to the system [kW].
- Q_L^{ST01}: is the rate at which energy is lost by the storage to the environment [kW].
- $Q_U^{PU01/PU02}$: is the rate at which energy is transmitted by the pumps into the fluid due to inefficiencies [kW].

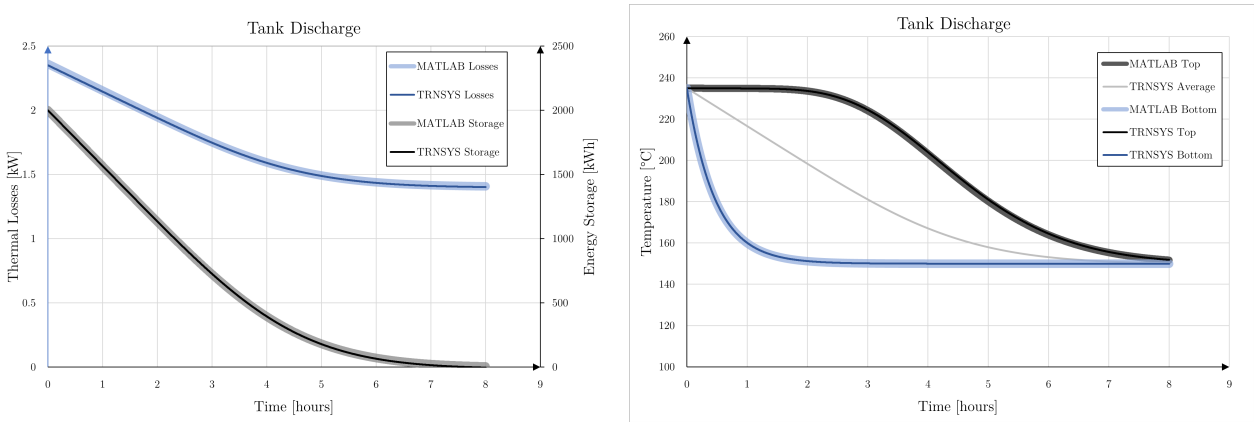

(a) Energy comparison between TRNSYS model and MATLAB model.

(b) Temperature comparison between TRNSYS model and MATLAB model.

Figure 5.23: Discharge operation comparison between TRNSYS model and MATLAB model.

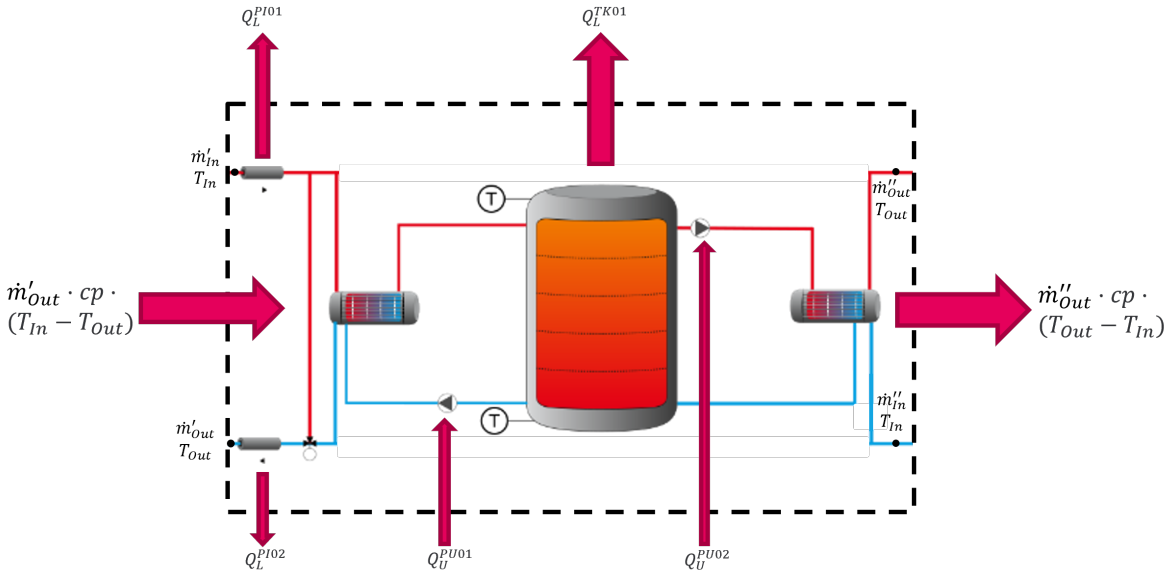

Figure 5.24: Macro M2200 scheme and energy and mass balance.

- $Q_L^{PI01/PI02}$: is the rate at which energy is lost by the pipes into the environment [kW].

5.9.3 Parametrization

The inlet parameters of this component are calculated to account for the capacity of the tank, determining its height and diameter based on standard shape coefficients. Maximum and minimum temperatures are required for the tank to calculate the properties for both the salt and the packed bed to fill the apparent properties of the tank as a whole.

5.9.4 Control

M2200_CON01 will receive inputs from different differential controllers: one that verifies the loading condition of the tank, one that will ensure that the temperature entering the macro is sufficient to supply either the tank or the demand, one that will ensure that the temperature entering the macro is sufficient to supply at least the demand in a low-temperature condition, and one which verifies the unloading condition of the tank. Inside M2200_CON01 a comparison of the amount of energy provided by the source and the demanded by the supplied circuit will be made, which will result in various operation modes.

Mode	Description	Crit 1	Crit 2	Crit 3	Crit 4
1	Pure loading	Qgen>0	Qdem=0		
2	Pure unloading	Qgen=0	Qdem>0		
3	Direct service	Qgen>0	Qdem>0	Qgen=Qdem	
4	Generation excess	Qgen>0	Qdem>0	Qgen>Qdem	
5	Demand excess	Qgen>0	Qdem>0	Qgen<Qdem	Qtank=(N/A)
6	Demand supply + load	Qgen>0	Qdem>0	Qgen>Qdem	Qsto>0
7	Demand supply + unload	Qgen>0	Qdem>0	Qgen<Qdem	Qtank>0

Table 5.10: Operation Modes M2200

In these different modes, valves (diverters in simulation) will be aligned to serve the correct purpose.

5.9.5 Results

The macro has several results, which include,

- Incoming and outgoing energy to and from the tank.
- Energy difference in the tank and pipes to account for storage.
- Tank losses.
- Pipe losses.
- Energy balance calculations.
- Work done by pumps (also for electricity FEC).

5.10 Demand

The model described in this section has been designed to replicate the behavior of the demand side of the network. It takes an external demand file which is established in an hourly time step. It serves both heating and cooling demands, but these macros have been given different codes due to their constant repetition. The macro also has the possibility of considering user-supplied constant temperature for the desired demand or taking these

values from the file. The macro main purpose is to set a circulation flow according to the temperature difference set, either constant or by the file's supplied values, and the demand. The layout of the model in TRNSYS simulation Studio can be seen in Figure 5.25.

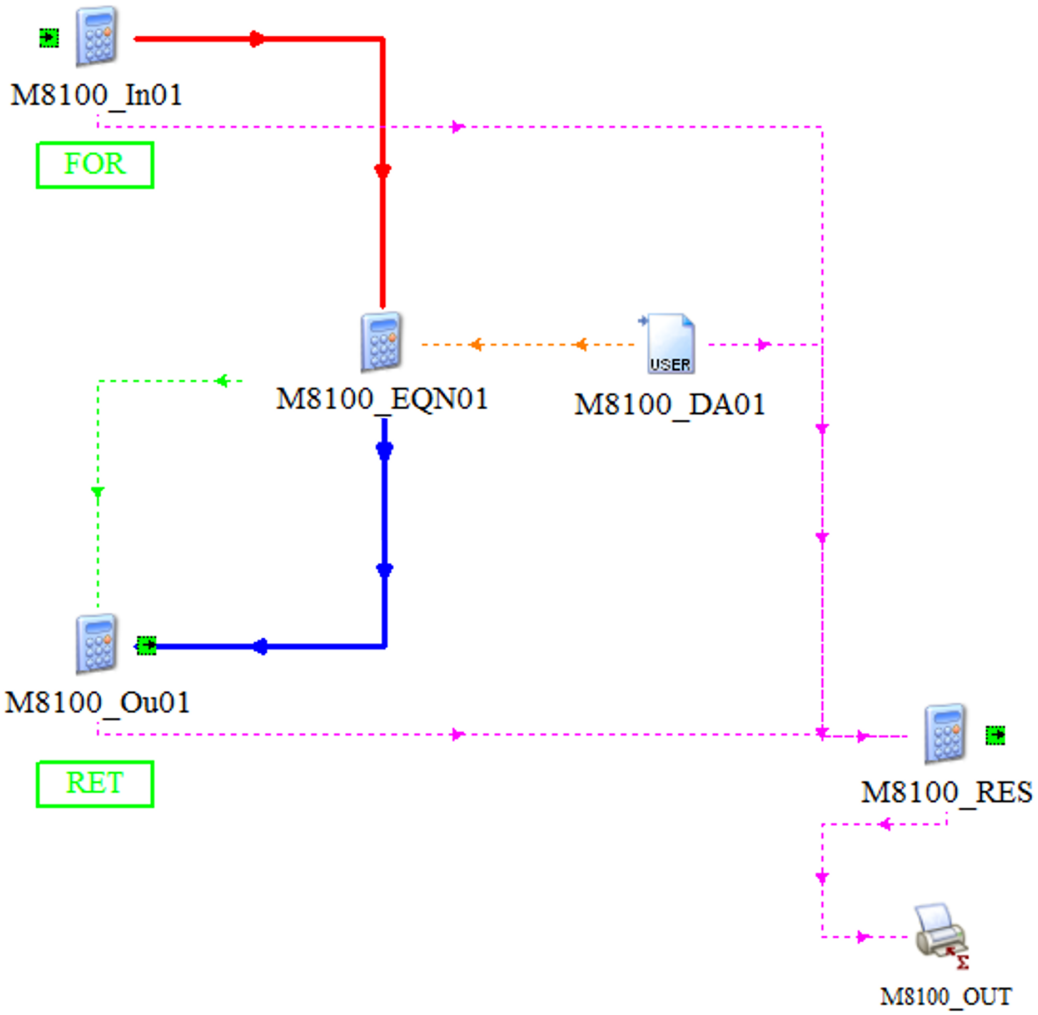

Figure 5.25: Macro M8100 in TRNSYS simulation studio

From the macro generated in TRNSYS different types used and what is the role they play in the macro is described in Table 5.11.

Code	Type	Use	Description	External File
M8100_DA01	9c	Demand Data	Hourly data. Format: Qdem, Tret, Tfor	Yes. User-supplied.

Table 5.11: Types used in M8100.

5.10.1 Hypotheses

A series of hypotheses were taken when producing this model:

- No additional heat losses are calculated by pipe circuits inside this macro.
- Demand values are set hourly by the user, in kW.
- cp values are taken as constant regardless of the temperature change.
- Network circulation pumps work is calculated in network macro (M7200/M7300).

5.10.2 Heat and Mass Balance

A first simplified scheme of the macro is presented for clarification in Figure 5.26. This figure also shows a draft of what will be the energy and mass balance. As this macro is the one in charge of modifying mass flow in the network, mass balance for this macro is not fulfilled, as mass entering and exiting the macro may not be equal.

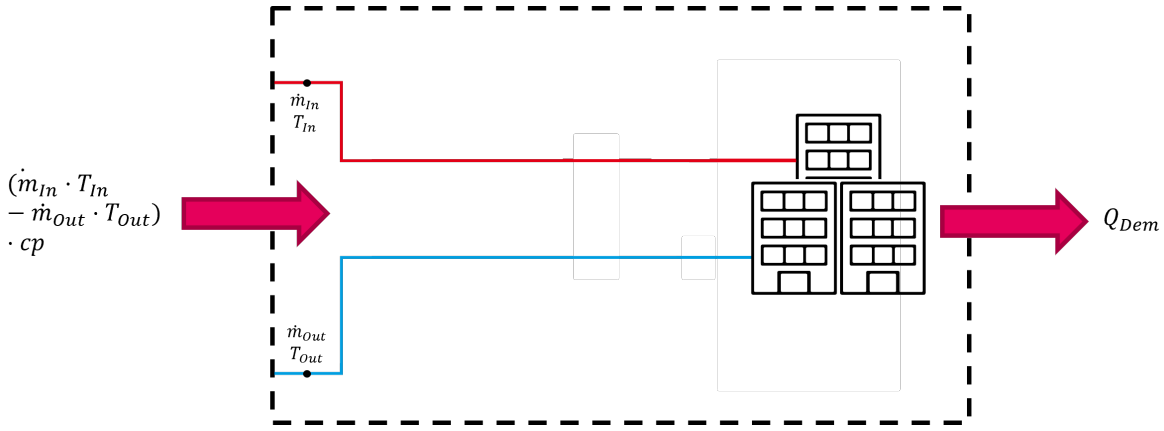

Figure 5.26: Macro M8100 scheme and energy and mass balance

Where,

- Q_{Dem}: is the demand rate at which which the user is requesting from the network [kW].
- $(\dot{m}_{In} \cdot T_{In} - \dot{m}_{Out} \cdot T_{Out}) \cdot cp$: is the actual rate at which energy is being transferred by the system into the network [kW].

5.10.3 Parametrization

This macro can be parametrized using a few variables. The user can select between having fixed temperatures or taking them from the supplied file. The macro also offers the possibility to scale this demand with a single parameter ("M8100_ScaleDem") without changing the temperature preference already set.

Fluid properties can also be set, but the macro uses water as default.

5.10.4 Control

The macro only interprets demand values and translates them into flow values through calculation. A flow rate signal is calculated, considering a nominal demand value, in case there is a need to supply equipment with a signal that depends on the load ratio being used by the network.

5.10.5 Results

The results of this macro could be subdivided into balances, operating variables, and performance indicators. In the first category, heat and mass balances are being taken as an output. As operating variables, the values of demand supplied and demand input by the file are shown. With these values, performance indicators are calculated, checking how much of the actual demand is being covered by the network.

5.10.6 Demand files generation

To ensure precise simulation and minimize uncertainty, it is necessary to gather demand information on an hourly basis for the annual simulation, following a similar frequency as the meteorological files.

The generation of his demand files is based on the need of two fundamental pillars of information:

- Total demand (kWh) assumed for the involved location.
- Hourly distribution of this demand.

Total demand is assumed considering Hotmaps project from European Union (EU) [98].

This generation of demand data is based on STRATEGO project from the Intelligent Energy Europe Programme (IEEP) of the EU [51], in which the Degree Days (DD) methodology is used as a basis to obtain an hourly demand profile. Degree days have been used for a long time in demand analysis [99], and their calculation is fairly simple [100]. It is mainly the comparison of outside temperature against a temperature setting of our choosing, which usually responds to comfort needs.

It is feasible to create a TRNSYS file that compares the hourly outside temperature information from the files generated in step 5.2.1 and generates an output file with these values.

In this file, the following equations will be used for Heating Degree Days (HDD) and Cooling Degree Days (CDD):

$$HDD = \begin{cases} T_{HDDset} - T_{amb}, & if\ T_{HDDset} > T_{amb} \\ 0, & if\ T_{HDDset} \leq T_{amb} \end{cases} \tag{5.21}$$

$$CDD = \begin{cases} T_{amb} - T_{CDDset}, & if\ T_{amb} > T_{CDDset} \\ 0, & if\ T_{amb} \leq T_{CDDset} \end{cases} \tag{5.22}$$

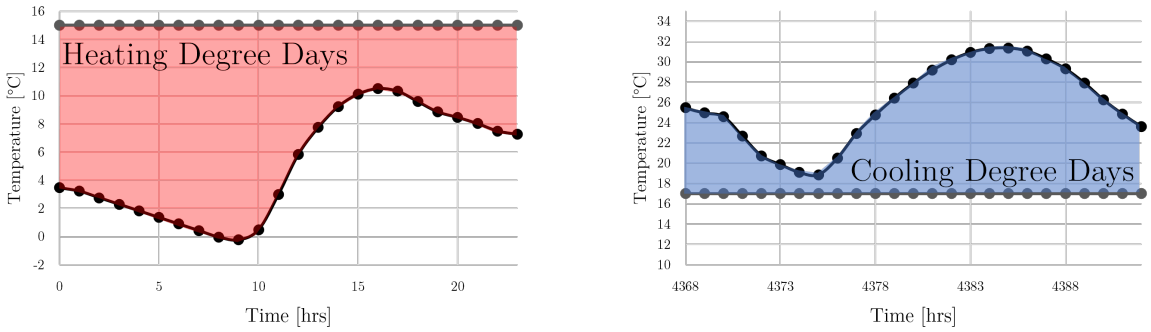

(a) HDD graphical calculation example for T_{set}=15°C.

(b) CDD graphical calculation example for T_{set}=17°C.

Figure 5.27: HDD and CDD calculations examples.

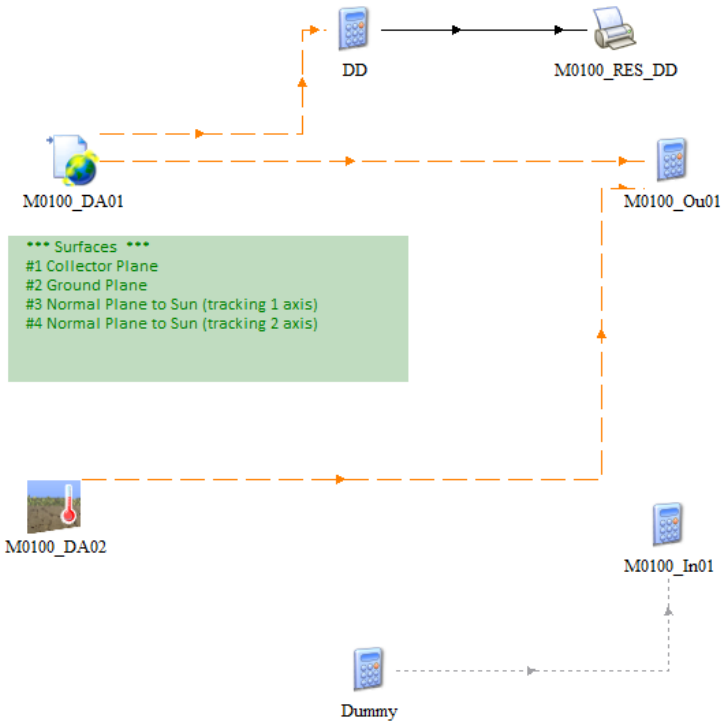

Figure 5.28: TRNSYS DD generation file

From this file, a new output is obtained which has an hourly distribution of HDD and CDD, from which through the use of Microsoft Excel we generate a profile based on the distribution of HDD and CDD obtained. From this point two alternative paths arise, one in which the HDD and CDD values are divided by the maximum HDD/CDD yearly value, in which case the distribution will be considering this maximum value as the maximum heating/cooling capacity of the network. Another, in which daily HDD/CDD values can be calculated, and from which the amount of daily demand can be considered as the total yearly HDD divided by the ones corresponding to that day. Once this value is obtained, and assuming a normalized daily profile for each day (Figure 5.29), a new normalized hourly

profile is generated. This profile will depend on the yearly demand value instead of the maximum capacity for the site. This was the methodology used for Wedistrict demand generation to generate reference demand profiles to adjust to the users'request.

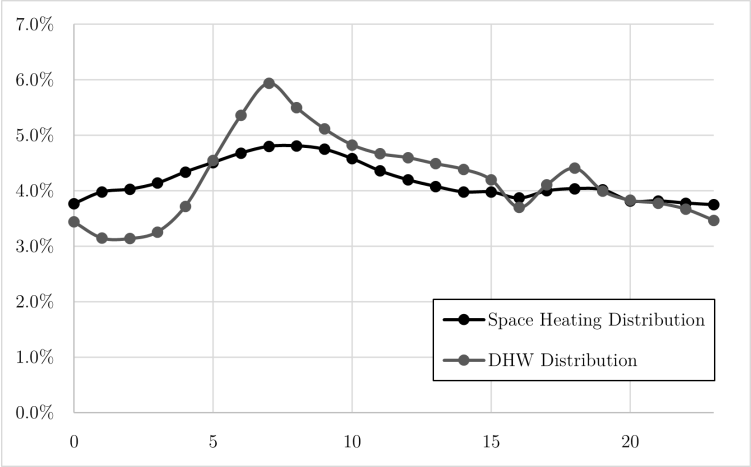

Figure 5.29: Daily distribution for space heating and DHW.

In the case of HDD an additional percentage is considered due to DHW which is considered constant throughout the year based on Eurostat information as shown in Table 5.12 for 2021 [101]. For network losses a fixed percentage was considered using European standard values (18% for Wedistrict) [102]. For DHW the demand is considered part of the value fed to the calculation, in the case of network losses, those are added to this value considering that the demand supplied does not consider an installed network, so the network losses will be additional.

5.10.7 Tool

Locations

Databases needed to develop the tool have first been done for five different established locations. These locations were selected by the project considering a broad HDD distribution around Europe (Table 5.13).

Cooling ratios To make the Tool database generation possible, for district heating and cooling cases, a limiting definition had to be made. If all heating demands are possible, and all cooling demands are possible at the same time, infinite simulations would be possible, and results wouldn't be achievable. For this purpose, a range for the cooling ratio was established for all locations. This range is defined between two values, the minimum being the ratio obtained from the "advanced DC" from Stratego [103] and the maximum heating density from Hotmaps, and the maximum ratio, defined as the value of the relationship between heating and cooling density from Hotmaps. Considering this hypothesis, Table 5.14 shows the values considered for the different locations.

	Space Heating	Space Cooling	Water Heating	Cooking	Lightning	other
EU	64.39%	0.45%	14.47%	5.95%	13.63%	1.11%
Belgium	74.43%	0.09%	10.87%	1.59%	12.31%	0.70%
Bulgaria	53.17%	0.47%	17.37%	8.45%	20.53%	0.00%
Czechia	69.43%	0.08%	15.20%	6.55%	6.85%	1.89%
Denmark	60.11%	0.00%	21.87%	1.75%	15.80%	0.46%
Germany	65.95%	0.20%	16.70%	6.40%	9.64%	1.12%
Estonia	71.05%	0.00%	11.59%	4.90%	12.45%	0.00%
Ireland	60.25%	0.00%	19.78%	2.24%	16.82%	0.91%
Greece	53.22%	4.08%	14.01%	9.03%	19.66%	0.00%
Spain	39.61%	1.00%	19.49%	7.79%	31.38%	0.73%
France	68.75%	0.57%	10.25%	4.84%	15.59%	0.00%
Croatia	68.78%	1.94%	9.71%	6.31%	13.27%	0.00%
Italy	66.93%	0.78%	11.42%	6.44%	13.19%	1.24%
Cyprus	34.93%	10.57%	23.51%	8.11%	21.14%	1.74%
Latvia	64.49%	0.00%	19.20%	7.05%	8.70%	0.56%
Lithuania	67.90%	0.00%	11.73%	6.01%	14.36%	0.00%
Luxembourg	80.33%	0.49%	8.19%	3.40%	7.59%	0.00%
Hungary	72.76%	0.31%	11.88%	4.84%	10.21%	0.00%
Malta	22.50%	16.99%	22.70%	11.26%	25.83%	0.72%
Netherlands	65.85%	0.27%	16.09%	1.94%	15.79%	0.06%
Austria	69.55%	0.01%	14.79%	2.60%	10.04%	3.01%
Poland	65.40%	0.00%	17.08%	8.29%	9.23%	0.00%
Portugal	30.78%	0.89%	16.86%	31.27%	20.19%	0.00%
Romania	62.35%	0.32%	14.14%	9.85%	13.33%	0.00%
Slovenia	64.18%	0.89%	14.89%	4.61%	15.42%	0.00%
Slovakia	74.59%	0.11%	11.70%	4.44%	9.15%	0.02%
Finland	66.76%	0.21%	14.62%	1.23%	12.05%	5.13%
Sweden	53.88%	0.00%	13.82%	1.62%	18.94%	11.74%
Norway	67.03%	0.09%	12.73%	1.51%	17.84%	0.79%
Bosniaand Herzegovina	72.66%	0.61%	9.73%	5.13%	11.87%	0.00%
Moldova	66.98%	0.06%	10.06%	14.02%	8.88%	0.00%
North Macedonia	69.87%	2.47%	9.49%	7.47%	10.70%	0.00%
Albania	32.51%	7.95%	23.54%	31.43%	4.57%	0.00%
Serbia	66.11%	0.40%	11.88%	7.19%	14.42%	0.00%
Kosovo	64.54%	4.69%	8.45%	9.39%	11.57%	1.35%
Georgia	55.78%	0.24%	15.86%	20.70%	7.42%	0.00%

Table 5.12: Eurostat. Disaggregated final energy consumption in households in percentage year 2021

City	**Koppen Geiger Climate**	**Heating degree days**	**Cooling degree days**
Rome	Csa	808	380
Madrid	Bsk	1647	484
Paris	Cfb	1938	96
Bucharest	Cfa	2219	331
Stockholm	Dfb	3319	18

Table 5.13: Locations selected for Wedistrict Tool.

City	Ratio cool/heat										
	Min	Max	Range	Values							
Rome	0.07	0.36	0.30	0.05	0.1	0.15	0.2	0.25	0.3	0.35	
Madrid	0.11	0.79	0.68	0.10	0.2	0.3	0.4	0.5	0.6	0.7	0.8
Paris	0.03	0.14	0.11	0.04	0.09	0.14					
Bucharest	0.09	0.19	0.10	0.09	0.14	0.19					
Stockholm	0.04	0.14	0.11	0.04	0.09	0.14					

Table 5.14: Cooling ratios obtained.

Chapter 6

Results

With the methodology explained in chapter 4 a series of studies were performed inside and outside the Wedistrict project. Each one of these tasks allowed to prove different positive aspects that resulted from its application. These studies were:

- Demonstration sites, which were used to test technologies developed by the project, as well as the methodology. These results were shared in project Deliverable 5.7 [104].
- Demonstration Followers, which were used to test virtually the calculations developed in existing and future DHC networks to compare different technology combinations [105].
- Parametric analyses that were performed to find optimal solutions for particular studies, as was the case presented in the paper "Comprehensive analysis of hot water tank sizing for a hybrid solar-biomass district heating and cooling" [27].

Additionally, the methodology was then used to generate a web tool. The implementation of this web tool is also explained in Project Deliverable 8.6 which is yet to be released.

6.1 Demonstration Sites

For work package 5 (WP5) in the Wedistrict project, three demonstration sites were planned from which three were finally built. Each demo-site intended to provide validation for Wedistrict technologies (see Figure 6.1).

For example, Luleå was intended to test the use of Fuel Cells coordinated with heat pumps, to generate electricity and low-level heat on one hand, and on the other, use that energy to operate a heat pump to improve the quality of this residual energy into a more exploitable form (in this case for the heating of the site).

Bucharest, alternatively, was used to test the implementation of geothermal energy along with heat pumps, also trying to generate the energy used by the heat pumps by renewable means, through the installation of solar panels.

Alcalá was also intended to test a variety of technologies. However, the molten salts tank was tested but ultimately not included in the final scheme. This simulation was conducted by me at UPM and will be discussed in more detail in Section 6.1.3.

These first simulated sites also proved the methodology's ability to provide results for new networks in the design stage.

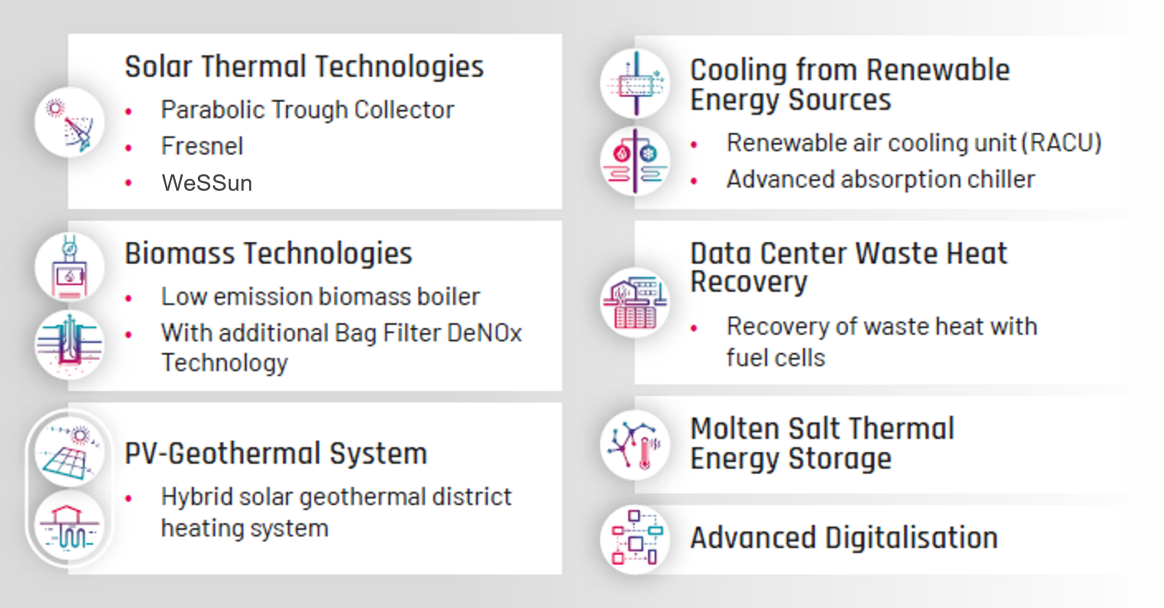

Figure 6.1: Wedistrict Technologies

6.1.1 Luleå

The design of a small-scale data center setup for deploying 22kW peak power digital systems was planned for the Luleå demo-site. The approach involves total liquid cooling of all digital components and powering the data center with biogas-driven fuel cell stacks. These serve as combined heat and power sources to produce waste heat at a sufficient grade. This waste heat functions as a zero-energy overhead heat pump, aiming to demonstrate the possibility of enhancement of data center heating using thermal energy from power generation at lower levels and transferring it to be rejected at the required temperature into the supply side of the local district heating system (see Figure 6.2).

6.1.2 Bucharest

The Bucharest demo-site is designed with a hybrid system that will generate both thermal and electrical energy from renewable sources. The hybrid system consists of a thermal subsystem, which uses geothermal heat pumps to produce thermal energy, and an electrical subsystem, which uses PV panels to generate electrical energy (see Figure 6.3). The integration of these two subsystems facilitates the functioning of the proposed hybrid system within the project. The primary goals of the Bucharest demonstrator include producing electricity, heat, and cold from a combination of renewable energy sources (geothermal and solar). The objective is to ensure that the generated electricity meets or exceeds the consumption of the unit responsible for producing thermal energy on an annual basis. Another aim is to fulfill all heating and cooling requirements for the target building using 100% renewable thermal

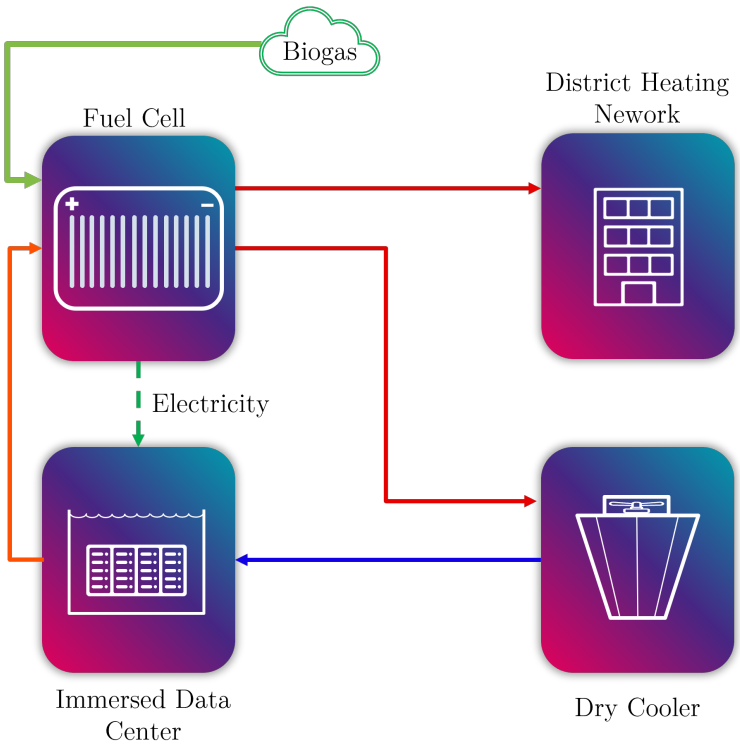

Figure 6.2: Proposed solution for Luleå.

energy. Additionally, excess heat will be reintegrated by injecting it into the POLITEHNICA Bucharest's heat distribution network. Lastly, there is a focus on creating a modular concept to facilitate replication and scaling processes.

6.1.3 Alcalá de Henares

For the demonstration of various technologies in the Wedistirct project, the simulation of a complex network was established in Alcalá de Henares city in Spain. Firstly the system was proposed to test the following technologies:

- Fresnel collectors.
- Parabolic Trough collectors.
- Low concentration flat collectors (WeSSun technology).
- Molten salt storage tanks, to take advantage of high temperatures of concentrating collectors.
- Low emission biomass boiler, paired with bag filters DeNOx technology.
- Advanced absorption chiller.
- Renewable air cooling unit (RACU).

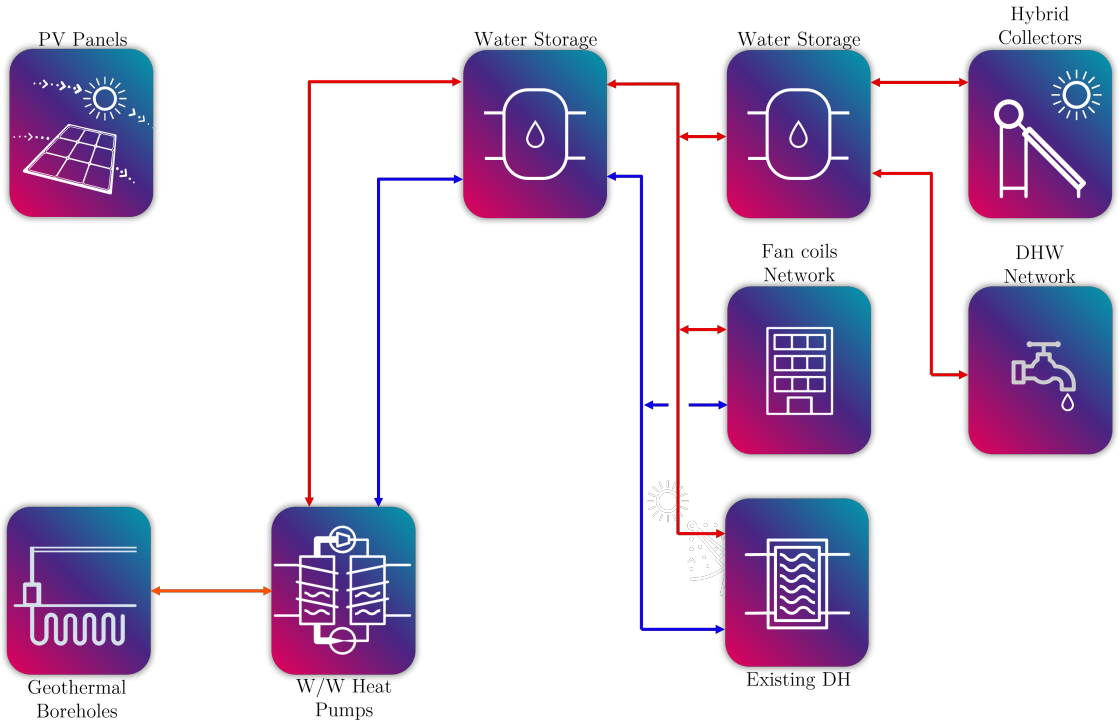

Figure 6.3: Proposed network POLITEHNICA Bucharest.

Some technologies were not well received by the authorities, so the molten salt tank was changed to a bigger water tank for all technologies to allow the construction of the network.

These technologies were thought to cater to an existent building, so demand profiles were established as seen in Figure 6.4.

In the end, the system was simulated, but the construction changed its location to Universidad de Córdoba (UCO), where it is expected to finish in the second half of 2024.

Proposed Scheme

As previously discussed, the initial version of the network aimed to incorporate a broader range of technologies (see Figure 6.5). However, the final version in Figure 6.6 shows that the molten salt storage technology was ultimately discarded due to bureaucratic issues, so technologies were rearranged for the final configuration. It is visible that temperatures were also raised to improve absorption chillers' operation (as higher generator temperatures improve COP as mentioned in Section 3.2.2).

The working principle of the configuration shown in Figure 6.6 is to give priority to the solar systems. If required temperatures and flows are achieved through these systems, the biomass boiler is to be bypassed. Heat generation is also provided for the absorption chillers' generators (conventional and advanced), which will increase its demand during the summer months. An observed problem with the absorption chillers operation has been the low temperature difference between the inlet and outlet of the generator. While temperatures above 95°C are needed for the cycle to work, the ΔT is usually around 5-10°C, which hinders solar design.

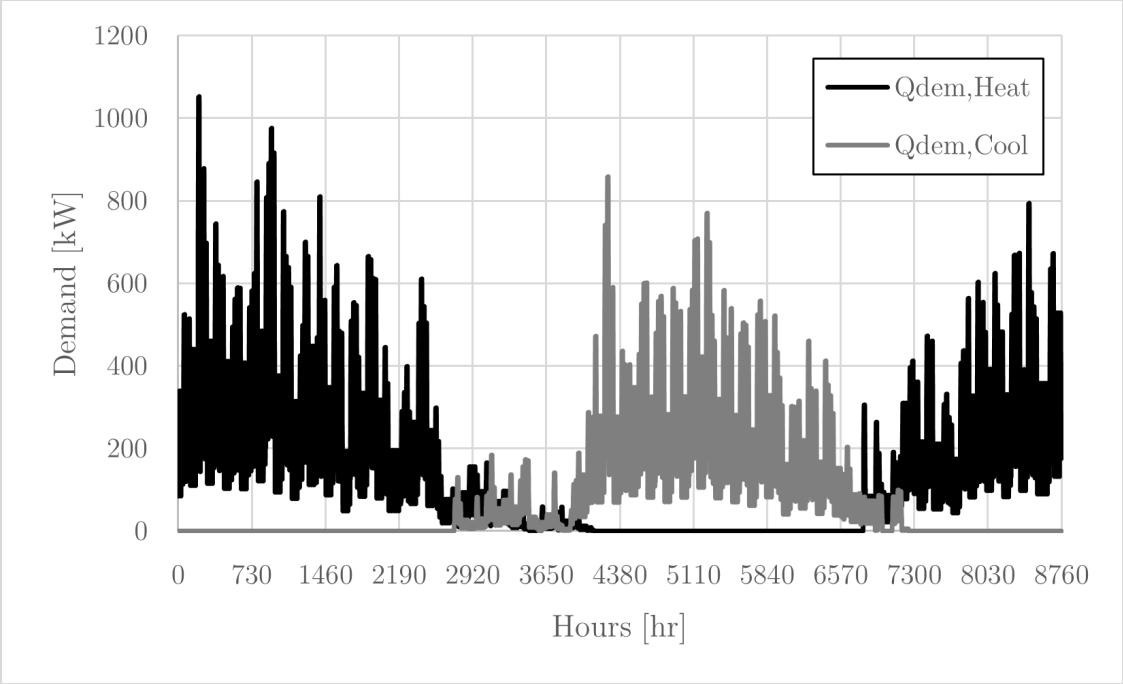

Figure 6.4: Demand profile in Alcalá de Henares.

Final sizes for the solar systems considering efficiencies are 445.5 m^2 for The Linear Fresnel Reflector, 328 m^2 for the parabolic Trough Collector, and 193.43 m^2 WeSSun considering mirrors. The water storage tank gathering all the collectors' production has 50 m^3, as visible in Figure 6.6. In the end, biomass boiler capacity will be covered by two 498 kW capacity boilers. Absorption chillers will be simulated according to their considered model. Conventional absorption chiller (730 kW) is assumed to be a YHAU CL255EXE model made by Hitachi, while advanced absorption chiller (100 kW) will be simulated as a prototype done by Enginyeria Mecànica, CREVER Universitat Rovira i Virgili.

While it is not visible in the figure, RACU technology was simulated but as it is not directly connected to the network, its impact on the heating demand (for regeneration), and cooling demand (by the reduction of the connected area), were taken into account. Note that the RACU capacity is around 10 kW, so the insertion in the simulation directly affected computational times but did not give a clear advantage against the proposed method that involved adding the heat needs to the actual heating demand and subtracting the cooling generation from the cooling demand.

Simulation

After using the values proposed by the engineering it was possible to determine that the scheme proposed was able to cater to the foreseen demand (Figures 6.7 and 6.8). It should be mentioned that the excess heat generation seen in Figure 6.7, responds to the heating requirements of the absorption chillers (advanced and conventional). It can be seen in Figure 6.7, that while capacities of heat generation through solar are considerable, these decrease significantly during winter months (due lower amount of sun hours and incidence angle),

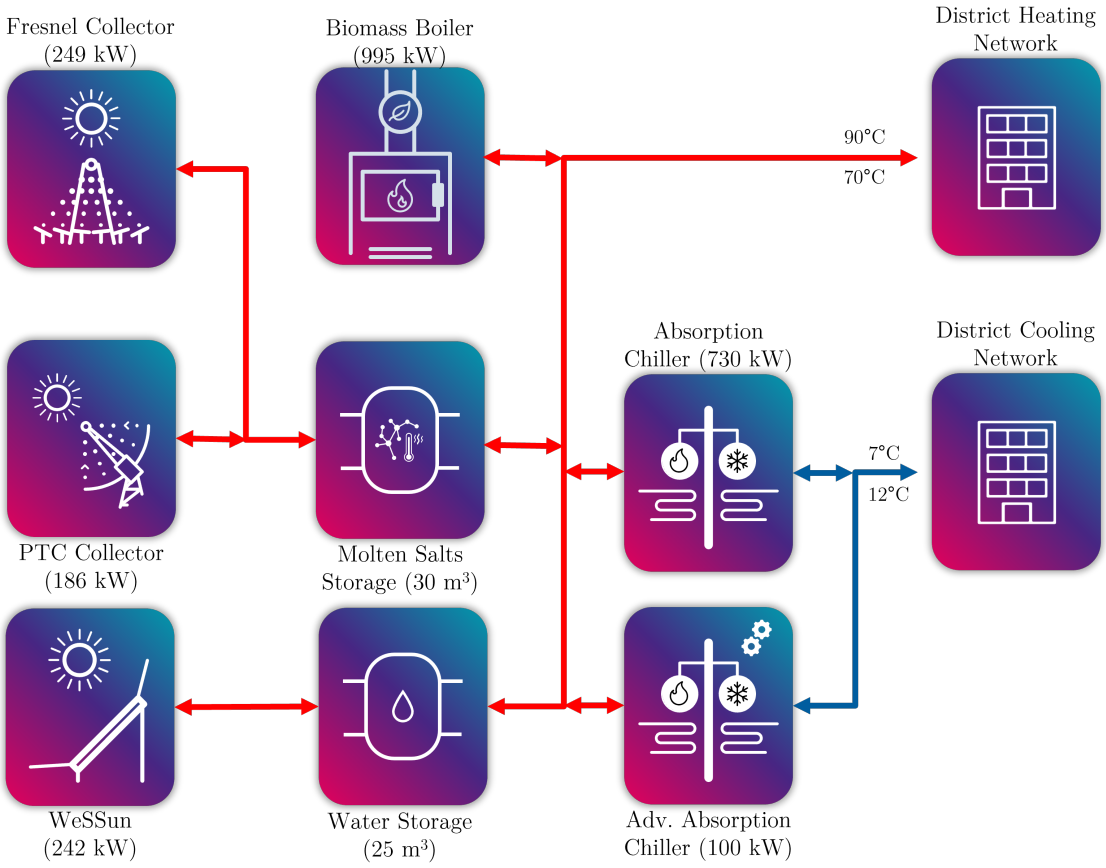

Figure 6.5: First proposed network for Alcalá de Henares.

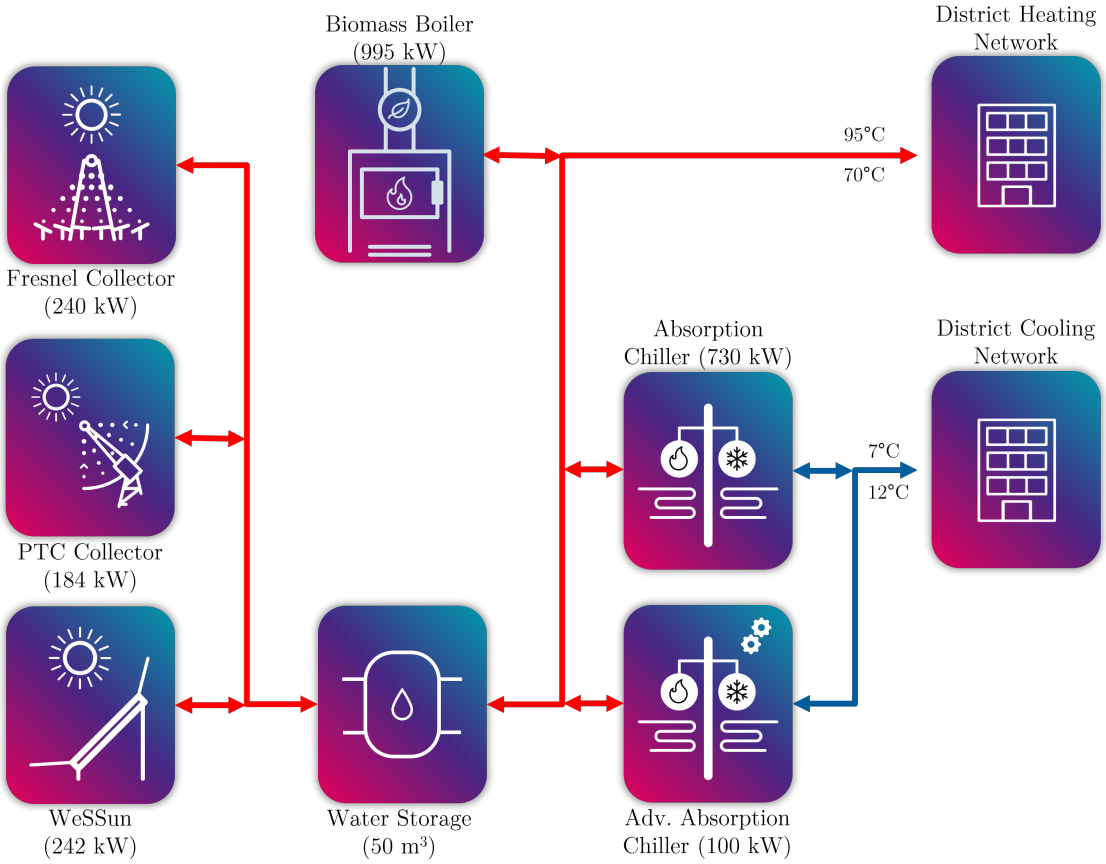

Figure 6.6: Final proposed network for Alcalá de Henares.

generating a high stress on the biomass boiler during winter. This stress is also increased during July and August due to the intense use of absorption chillers during these months for cold production. It must be observed that considering a COP of 0.75 for this type of equipment, 1.33 kW of heat must be generated for each kW of cold generation, impacting the heat demand during these months. This can be seen comparing the cooling demand covered seen in 6.8 and considering the relationship described previously. Other KPIs were also calculated as shown in Table 6.1.

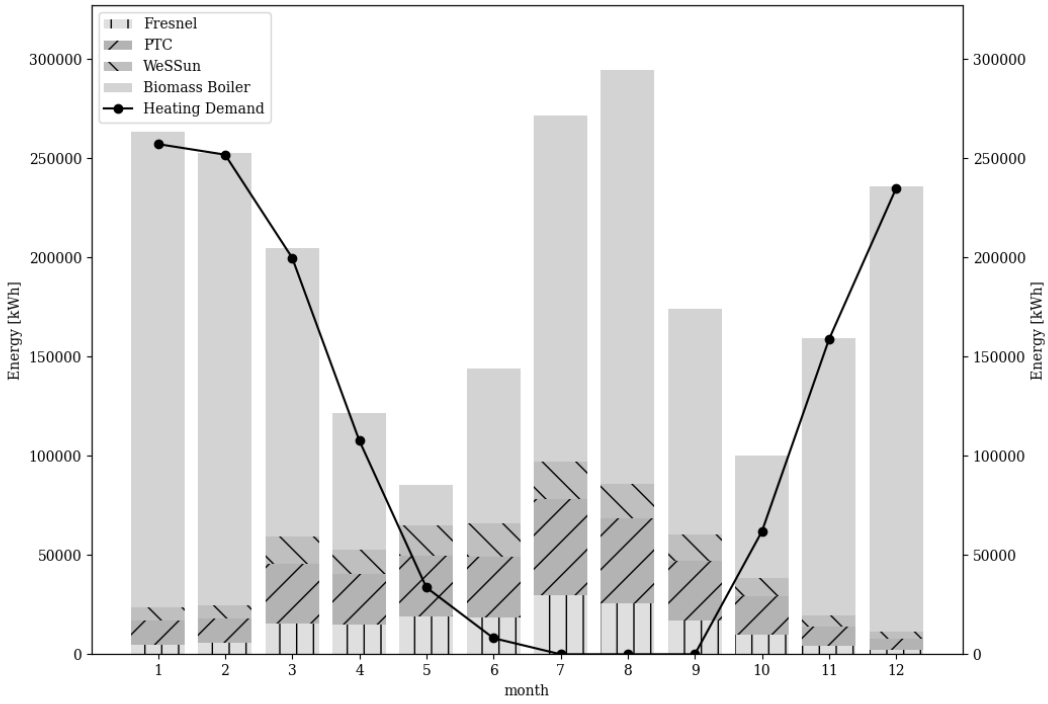

Figure 6.7: Heating demand results in Alcalá.

LCOE	100.46	€/MWh	Heating service equivalent CO_2 em. coef.	34.59	kg/MWh
CO_2 emission coefficient	38.42	kg/MWh	Cooling service equivalent CO_2 em. coef.	45.4	kg/MWh
Heating renewable energy ratio [-]	0.87		LCOE Heating	81.46	€/MWh
Cooling renewable energy ratio [-]	0.87		LCOE Cooling	135.12	€/MWh
Heating Non-renewable primary energy factor [-]	0.17		Payback Heating	0.76	years
Cooling Non-renewable primary energy factor[-]	0.23		Payback Cooling	2.23	years

Table 6.1: Resulting KPIs for proposed system in Alcalá de Henares.

6.2 Demonstration Followers

On the framework of the Wedistric project, additional virtual demonstrators were set. These were called Demo-followers. The primary goal of this activity was to assist the existing

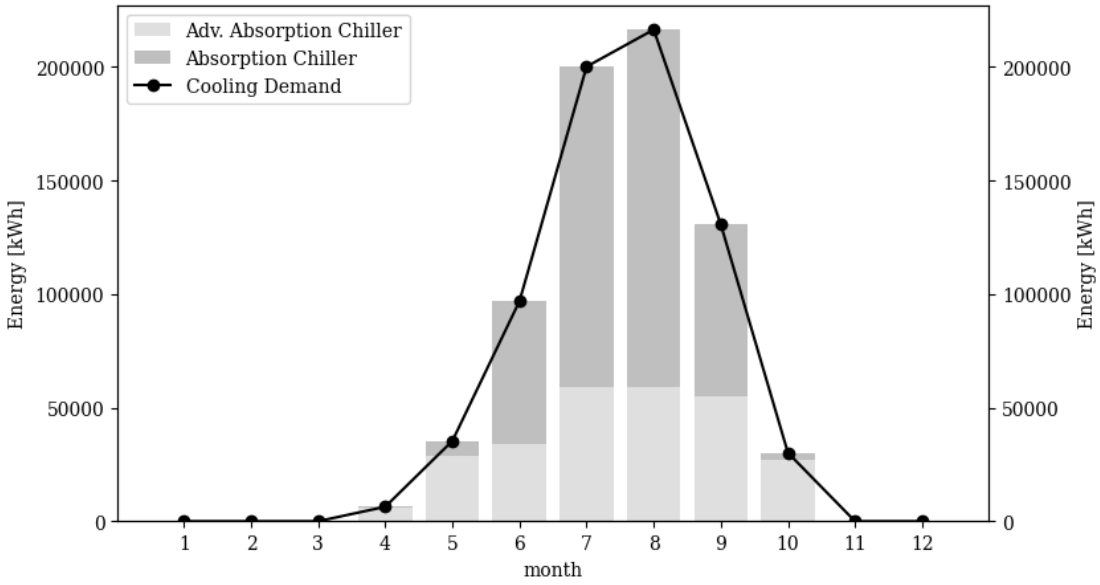

Figure 6.8: Cooling demand results in Alcalá.

system in retrofitting situations or propose a new plan for future development in areas without previous infrastructure. This would showcase the potential for replicating Wedistrict by creating more examples of DHC systems based on renewable energies. Two different situations were approached. The first case, where there was no existent DHC system, and the second scenario, where an existent DHC pursued an improvement on its design. The first set of cases was comprised of 5 locations. While the set of cases that analyze existing networks is 6. These demonstration cases were simulated but were done before the results script was produced, so what was analyzed was the size of the equipment for each solution, and if this equipment was able to cope with the demand supplied or generated. Results and information are gathered from Wedistrict Deliverable 5.8 [105]. While giving assistance to almost all of the cases simulated, Focşani and Mrągowo's cases were performed entirely in-house, for that reason, special attention will be paid to these cases.

6.2.1 SeiMilano

The first scenario of a completely new network is SeiMilano, which is a future network defined by two big residential areas (R1 and R2), an area called tertiary (T), which will have office buildings, and a commercial sector.

It has been concluded for this demo-follower, that both “S2” and “S3” prove to be economically non-viable solutions. Also, in the case of “S2”, RACU technology is not ideal for Milan's humid weather. The required size of the fuel cell to cover the heating demand in “S3” would have been so large that it could generate enough power for the entire city of Milan, making the solution prohibitively expensive. Consequently, it was decided that this outcome was not feasible.

Figure 6.9: SeiMilano network.

Solutions proposed after preliminary assessment			
Technology	S1	S2	S3
Advanced Absorption Chiller	x		
PV/PVT	x	x	
Geothermal system	x	x	
Heat pump (air-to-water)	x	x	x
RACU		x	
Data Center - Fuel Cel - Waste Heat Recovery			x

Table 6.2: Solutions proposed for SeiMilano Demo-follower.

These results make "S1" the only solution worth considering.

6.2.2 Montegancedo

Montegancedo Campus is part of Universidad Politécnica de Madrid, located in Pozuelo de Alarcón. It is currently being supplied by individual gas boilers and compression chillers. The concept behind this project is to generate a network to gather different buildings on the campus to generate a broader network. The campus is composed of six different buildings spread over the 480000 m^2 that the whole campus comprises. Two of these buildings are of

utmost importance due to their high energy consumption. On the one hand, the Center of Biotechnology and Genomics for Plants (CBGP) with its greenhouses. On the other, the super computation and visualization center of Madrid (CESVIMA), with its data centers (Figure 6.10).

Figure 6.10: Montegancedo demo-follower site.

Solutions proposed after preliminary assessment			
Wedistrict Technology	S1	S2	S3
PTC	x	x	x
Fresnel	x	x	x
WeSSun	x	x	x
Biomass	x	x	x
Advanced Absorption Chiller		x	
Data Center - Heat Pump - Waste Heat Recovery			x
Hot water storage	x	x	x

Table 6.3: Solutions proposed for Montegancedo Demo-follower.

For this network, it is especially interesting, due to the presence of the data center together with the greenhouses, to consider the waste heat recovery alternatives.

At the end of this study, "S1" proved to be the most promising solution. The use of solar collector panels holds great potential for reducing CO2 emissions without sacrificing economic viability. The estimation of the solar collector area took into account the availability of land, ensuring a realistic design that would not impact the woodland on campus.

6.2.3 Playa del Inglés

In the southern part of Gran Canaria Island, to the eastern shore, there is a set of touristic towns among which Playa del Inglés is located.

Gran Canaria has a desert climate, according to Köppen climate classification, due to its extremely low precipitation. The island experiences warm temperatures in spring, summer and fall, as well as mild winters. Known for its diverse microclimates, Gran Canaria sees daytime highs ranging from 20 °C in winter to 26 °C in summer on average. Cool nights occur during winter months but temperatures rarely drop below 10 °C near the coast. Inland areas have milder climates while mountainous regions may occasionally experience frost or snowfall. Cloud cover and sunshine levels vary significantly during cooler months with some cloudy days in winter; however, summers are generally sunny, especially on this part of the island. For Playa del Inglés only one solution was proposed due to the advancement in this project in which the selection phase already has been performed.

Solutions proposed after preliminary assessment	
Wedistrict Technology	S1
WeSSun	x
Advanced Absorption Chiller	x
Compression Chiller	x

Table 6.4: Solution proposed for Playa del Inglés Demo-follower.

6.2.4 Tecnoalcalá

The concept behind Tecnoalcalá demo-follower was to increase the proposed solution for Alcalá de Henares demosite to the whole technological park, creating a bigger district heating and cooling network. The park has 370705 m^2, inside the Universidad de Alcalá campus. Most of this area is already occupied by 40 companies, which cover 92% of the available area (see Figure 6.11).

The solution studied in scenario 2 (S2) is not relevant for this type of DHC as it has a low impact on energy efficiency and CO2 emission reduction. It may be more suitable for low-heating applications. From an economic standpoint, it is also irrelevant: the CAPEX would be 200 million euros in "S2".

The best approach for the combination mentioned in S1 would involve optimizing both the CO2 emission coefficient and LCOE. At present, new projects prioritize maximizing the reduction of CO2 emissions due to political mandates. As a result, this optimized S1 may not be pursued in the future; instead, a 100% biomass solution would be more favorable.

6.2.5 Independencia and Recoleta

The Independencia and Recoleta demo-follower includes a newly implemented District Heating and Cooling system, utilizing advanced absorption chiller technology as the primary method of generation.

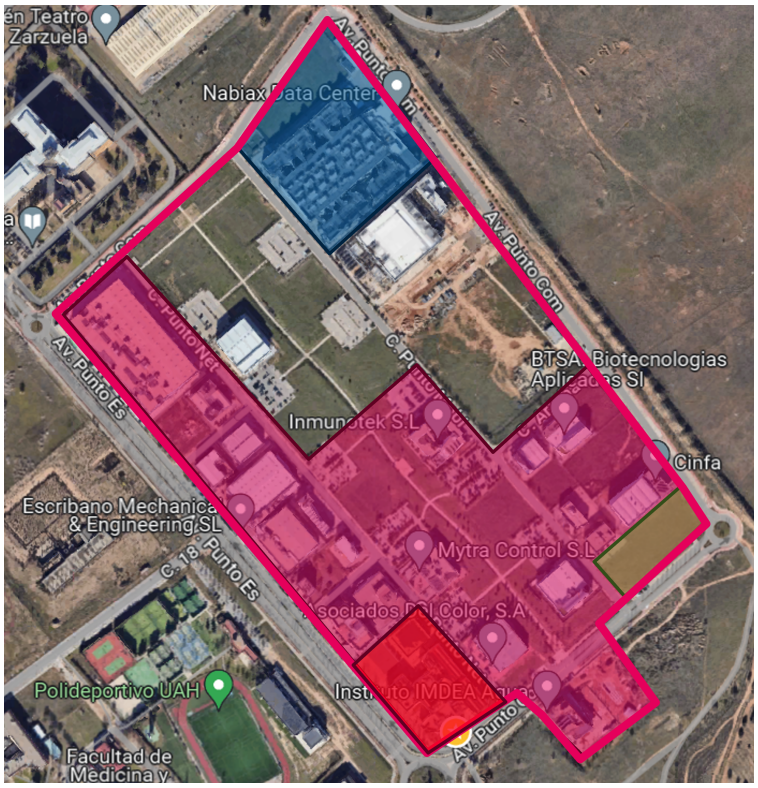

Figure 6.11: Tecnoalcalá demo-follower site. In red, where the original demo-site building was located, and in green, where the construction of the plant was proposed. In blue, the park's datacenter.

Solutions proposed after preliminary assessment			
Technology	S1	S2	S3
PTC	x		
Fresnel	x		
WeSSun		x	
Biomass	x	x	
Molten Salts	x		
PV	(x)	(x)	x
Geothermal			x
Advanced Absorption Chiller	x	x	
RACU	x	x	x
Fuel Cel - Waste Heat Recovery	x	x	x
Hot water storage		x	x

Table 6.5: Solutions proposed for Tecnoalcalá Demo-follower.

Selected for technical support in identifying and pursue district energy projects, the boroughs of Independencia and Recoleta in Santiago have shown promising initial results for densely populated areas and essential infrastructure. This includes addressing heating and cooling needs for healthcare and educational facilities. Additionally, there has been previous collaboration between the Municipalities to streamline administrative and legal processes.

The project examined the findings of an initial assessment that revealed promising results in certain areas of Independencia and Recoleta in Santiago de Chile. The map below indicates the locations of these areas.

A survey was conducted in the area to asses possible clients for the networks.

Client	Sector	Area [m^2]	Existing generation systems
Universidad de Chile Clinical Hospital	Health	65,214	NG boiler, diesel boiler, individual systems
Dental Clinic	Health	4,068	GN boiler, disused diesel boiler, chiller, individual hot and cold systems.
Dental Clinic – Administrative	Administrative	5,308	NG boiler, disused diesel boiler Chiller, individual hot and cold systems
Dental Clinic – Laboratory	Education	4,046	NG boiler, Disused diesel boiler, Chiller, individual systems
Public Library	Administrative	1,320	Does not have
Municipality	Administrative	6,800	Heat pump, LPG boiler and individual hot and cold systems
School of Medicine	Education	73,518	Information Not Available
Roberto del Rio Hospital	Health	23,520	GN and LPG boiler, chiller, individual systems
San Jose Hospital	Health	36,350	Information Not Available
National Cancer Institute	Health	13,057	GN boiler, chiller, heat pump, individual systems
Faculty of Chemistry and Pharmacy	Education	7,592	Diesel boiler, Heat pump, individual systems
Psychiatric Clinic	Health	5,154	Information Not Available
José Horwitz Psychiatric Institute	Health	21,852	GN condensing boilers, solar thermal collectors, steam boiler, chiller

Table 6.6: Survey on the possible main consumers.

Using Design Builder the demand in the different client buildings was calculated. These results are shown in Table 6.7.

A parametric study was performed on the system, generating an optimum system. The KPIs generated for this optimum system are shown in Table 6.8.

6.2.6 Parc de l'Alba

Parc de l'Alba (also referred to as the Directional Centre) is a recent urban project located in Cerdanyola del Vallès, a municipality with 57,000 residents near Barcelona. The park seeks to illustrate sustainable development and has already incorporated a partially operational energy-efficient system that produces electricity, heat, and cooling via a DHC network.

Currently, there are two data centers and three office buildings connected with the expectation of additional services and industrial structures, as well as a planned residential

Building	Heating [MWh/year]	DHW [MWh/year]	Cooling [MWh/year]
Universidad de Chile Clinical Hospital	2,533	3,427	3,600
Dental Clinic	156	214	220
Dental Clinic — Administrative	92	-	205
Dental Clinic — Laboratory	129	-	372
Public Library	25	-	63
Municipality	159	-	63
School of Medicine	2,590	-	819
Roberto del Rio Hospital	1,409	1,236	2,246
San Jose Hospital	2,435	1910	3,867
National Cancer Institute	981	686	1,389
Faculty of Chemistry and Pharmacy	268	-	189
Psychiatric Clinic	505	-	333
José Horwitz Psychiatric Institute	1,018	1,148	1,170
TOTAL	**12,300**	**8,621**	**14,536**

Table 6.7: Demand Calculation

Parameter	Unit	Value	Parameter	Unit	Value
AHPHR Capacity	kW	1	System Renewable factor		46%
Wessun Area	m^2	4.285,7	COPe system		2,34
Solar Multiple	-	3,00	EERe system		3,86
Net Specific Solar Yield (after storage)	kWh/m^2	521,52	SPFe system		2,86
Concept Extended COPe		8,14	IRR concept		17,3%
Concept Extended EERe		2,14	IRR system		14,3%
Concept Extended SHPe		10,27	System CO_2 emissions	$tonCO_2eq$	4.907
Heating Fraction Concept		24%	CO_2 emissions reduction	$tonCO_2eq$	106
Cooling Fraction Concept		12%	System CO_2 emissions	$tonCO_2eq/MWh$	0,13
System solar factor		15%	CO_2 emissions reduction		2,12%

Table 6.8: KPIs and capacity of system

development. One significant aspect of the development is the existence of the Alba Synchrotron, which has specific energy consumption requirements. These structures exhibit notably high demands for cooling and electricity, making Parc de l'Alba primarily reliant on cooling. At its current stage of implementation, Parc de l'Alba operates using a single-generation plant that provides heating and cooling predominantly through combined heat and power engines, backup gas boilers, absorption chillers, and compression chillers. The plant has the capability to expand its capacity in response to growing energy demands by utilizing available space within its facility. Additionally, two more production plants are scheduled for implementation based on urban development progress.

A demand profile was generated developing simulations in TRNSYS for the data centers and offices. Knowledge of the operation of the Synchrotron, was provided from previous projects. This approach, known as "4+1", takes into account that the facility operates continuously for four weeks with a stable 3.3 MW cooling consumption, followed by one week of no cooling consumption. Additionally, it considers a consistent heating consumption

of 245 kW.

Three different scenarios were considered. Two were done following a similar combination ("S1" and "S3"), shown in Table 6.9, but considering different demands (one considering a future shopping mall and the other one without considering it) and in the case of S3 adding Fresnel collectors to the solution. "S2" as visible in the Table, intends to cover the demand as "S3" but without introducing a cooling network, but by covering the cooling demand with RACU technology.

Solutions proposed after preliminary assessment			
Technology	S1	S2	S3
Gas Boiler	x	x	x
Biomass	x	x	x
Conventional Absorption Chiller	x		x
Air Chiller	x		x
Hot water storage	x	x	x
Fresnel Solar Collectors		x	x
RACU			x

Table 6.9: Parc de l'alba

The preliminary feasibility study reveals a particular interest in the RACU technology, which has the potential to provide local cooling without requiring a four-pipe network. However, for this technology to become an attractive solution, it needs to advance into a commercial phase and reduce investment costs. Another finding is that connecting the new 42MW data center to district cooling networks may not be feasible based on the proposed plant layouts within the Wedistrict framework. As an alternative, utilizing local air-cooled chillers along with partial waste heat recovery appears to be the simplest and most convenient solution so far.

6.2.7 University of Cyprus

University of Cyprus (UCY) is a retrofitting DHC demo-follower. The DHC was originally built in 1999, with two expansions completed in 2007 and 2010. A further expansion is planned for 2022. Figure 6.12 displays the most recent aerial photograph of the UCY Campus.

The University of Cyprus requires three different types of energy: cooling for 17 buildings covering a total area of 91,422 m^2 (excluding student residences), heating for 29 buildings with a combined area of 98,520 m^2 (including student residences), and provision of domestic hot water. In the 2022 expansion, UCY plans to install several new technologies: a 5 MWp PV plant with a 2.35 MWh electric battery capacity, as well as various heating and cooling storage systems.

For UCY's case, 4 different solutions were simulated. The first one considers a base case scenario consisting of a gas boiler for DHW and heating, and an air-water Chiller to supply cooling to the system. The other three solutions correspond to possible configurations (Table 6.10).

Figure 6.12: University of Cyprus demo-follower site.

WEDISTRICT Technologies	**S1**	**S2**	**S3**
WeSSun	x	x	x
PV / PVT	x	(x)	(x)
PV-Geothermal Hybrid		x	
Heat pump (A-W or A-A)	x	x	x
RACU		x	(x)
Advanced Absorption Chiller		x	(x)
Biomass			x
OTHER Technologies – to be considered			
Energy storage, in general	x	x	x
Tri-generation (CCHP*), in general	x	x	x
Air-cooled chillers	x		
Oil-fired boilers	x		

Table 6.10: Solutions proposed for UCY after preliminary assessment.

Demand for this reference case was developed from monthly data supplied from 2019.

Based on the studies of the three solutions proposed, "S3" appears to be the most viable. While its LCOE may not be as low as the base case LCOE, and its emissions may be higher than those of scenario 2, it is important to note that the base case is not feasible in the future and that scenario 2 has an unacceptably high LCOE.

It might be feasible to improve the results by eliminating the absorption chiller. Also, integrating solar thermal and PV in a Solar PV-T hybrid solution could present an intriguing prospect. Investigating the potential synergy between solar thermal, TES, and water-to-water heat pumps for optimizing these technologies while decreasing dependence on the boiler would be worthwhile as well.

In future research, adjusting heating and cooling requirements to accommodate possible University expansions could change technology distribution.

6.2.8 Żyrardów

Żyrardów, situated in central Poland, has a population of around 41,400 and possesses a history dating back almost two centuries. The town developed into a prominent center for textile production during the 19th century. In relation to energy goals, Poland has established a target of reaching 21% renewable energy in its final energy consumption by 2030 with the goal of establishing a more sustainable energy industry. Furthermore, it aims to have 70% of all households connected to DH networks by the same year. This strategy is viewed as one of the most effective approaches to increase the utilization of renewable energies within the heat sector.

The installed district heating capacity in Żyrardow is distributed between two heat plants and it covers around 50% of the city. One of the plants consists of coal-fired boilers (63 MW in capacity). And the other one has one 10 MW natural gas boiler, situated 2 km from the main plant.

Figure 6.13: Żyrardów location.

The network is approximately 43 km long and has been updated in the last few years. between 2013 and 2016 almost all remaining sections of traditional pipes with isolation were replaced with pre-insulated ones (currently 99.9% is pre-insulated). With this technology, losses add up to 13-14% of the network production. Hydraulic enhancements have also been made, reducing pumping consumption of the network.

Possible solutions were also established for this demo-follower. These solutions are shown in Table 6.11.

After developing the different solutions proposed, a fourth solution arose considering a mixture of the different solutions. S4, as it may be called, considered the possibility of using pit storage for low-level heating from WeSSun collectors and geothermal HP to achieve higher temperature values. From that pit storage's output, supply a short-term storage, fed primarily by cogeneration, backed up by a gas boiler (described in Figure 6.14).

WEDISTRICT Technologies	S1	S2	S3
PTC		x	
Fresnel		x	
WeSSun		x	
Biomass	x		
Molten Salts			
Hybrid PV-Geothermal			x
CHP			x
Gas boilers	x	x	

Table 6.11: Solutions proposed for Żyrardow after preliminary assessment.

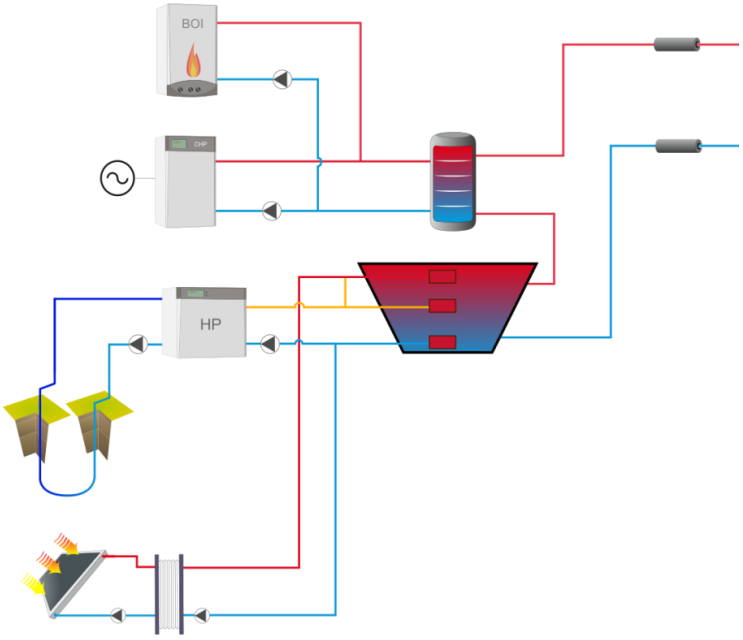

Figure 6.14: Żyrardów S4 solution sketch.

Sizes used for the first calculations are shown in Table 6.12.

Parameter	Unit	Value
Seasonal Storage Volume	m^3	400000
Storage Volume	m^3	1500
Solar Area	m^2	40000
Geothermal Power	MWth	5
CHP Power	MWe	8
Gas Boiler Power	MWth	9

Table 6.12: Żyrardów S4 parameters

After these calculations were made, a parametric analysis was performed which led to the change in some of the sizes first considered.

Based on the results from the TRNSYS simulation a parametric analysis was developed. Different simulation scenarios based on the performance of both the GHP system and the entire generation system were selected. The focus was to explore various configurations of two sensitive parameters affecting system performance and capacity to meet demand: different sizes of both the GHP and solar area of WESSUN collectors were considered. It's worth noting that before this parametric study, an analysis of the base case results identified one issue: an excessively large seasonal storage size. The excessive size meant that for several months, the heat pump was unable to supply the energy needed to meet demand and store enough heat without growing in capacity to inconvenient sizes. Therefore, we are testing smaller storage sizes and aiming to parameterize the size of the heat pump and solar collector area to meet demand.

In the end, the parameters studied ended up being as shown in Table 6.13).

Parameter	Unit	Value
WeSSun Collector Area	m^2	10000
Geothermal HP Capacity	MWth	30

Table 6.13: Żyrardów S4 parameters

6.2.9 Valladolid

Valladolid's demo-follower includes an existing District Heating system based on biomass (100% renewable energy). It was constructed in 2016 and has been operational since 2018.

Valladolid demo-follower actual situation has two biomass boilers of 3.48 MW each, with a peak operational capacity of 6.96 MW. This capacity is only aimed at the connected buildings space heating, in the actual network, DHW is not being supplied.

Construction of this network has been planned in five phases. It is currently in phase 3, serving 8 buildings (4 housing communities, two public administration buildings and two educational buildings).

Solutions proposed for this demo-follower suggest adding cooling to the actual heating network. Two different solutions were proposed, one with absorption and compression chillers for this purpose, and another geothermal solution to supply heat in winter and cooling in summer. No further solutions were proposed, as the actual system already has optimized biomass boilers.

DHC Valladolid employees interviewed believe that LCOE may be a more important criterion than CO2 coefficient emission. Both optimized scenarios have lower CO_2 emissions than the reference DHC, which exceeds 300 kg/MWh. Therefore, the preferred optimized scenario to develop would integrate absorption and compression chiller as in S1, which has an LCOE 44% higher than the reference case, but that also includes the cooling network (which has a higher economic value associated).

6.2.10 Focşani

Focşani is the capital city of Brancea County in Romania. It has around 98000 inhabitants. This city owns its own DH company which supplies heat and DHW to the city. It has

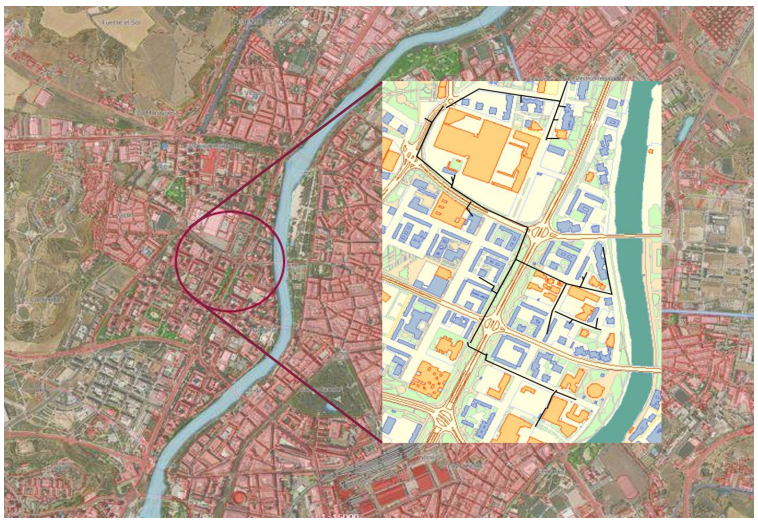

Figure 6.15: Valladolid demo-follower site.

separate networks for both these uses (heating and DHW). Both distribution networks are aound 61 km long while they also travel an additional 23 km from the generation center.

The main issue in this network is the disconnection from the user side, migrating to individual natural gas boilers. Only 55% of the possible users where the network is available are connected, with high disconnection rates (850 flats per year considering the 2005-2018 period). This high disconnection rate is due to the low amount of energy delivered per heating line, which falls below the international benchmark of 2 GWh/km (1.02 GWh/km). This difference may have its cause in the high losses of the network 36.9% in 2018. For this reason, a needed revamp for the network and substations was planned by the municipality. New equipment has also been installed for generation. Two 6.8 MWe gas cogeneration engines and a 50 Gcal/h gas boiler.

Three solutions were proposed for this demo-follower. These solutions are shown in Table 6.14. These solutions propose the addition of a cooling network to the city.

WEDISTRICT Technologies	**S1**	**S2**	**S3**
Fresnel		x	
Biomass boiler	x	x	x
Gas boiler	x	x	
Advanced Absorption Chiller	x	x	
Free cooling			
Thermal storage	x	x	
Hybrid PV-Geothermal-Heat Pump			x
A/W Compression chiller	x	x	

Table 6.14: Solutions proposed for Focşani demo-follower.

Solution one consists of a biomass boiler with a water storage tank to avoid peaks, with a backup gas boiler. All this system has a cooling network associated, with an advanced absorption chiller and a conventional chiller for peaks. This solution schematics is visible in

Figure 6.16.

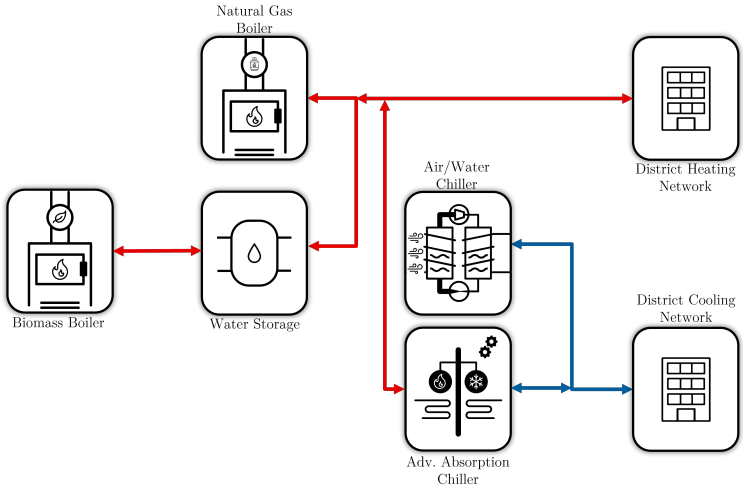

Figure 6.16: Focşani S1 diagram.

S2 has similar considerations as S1, but has an additional Fresnel collector configuration along with a storage tank to provide an additional renewable source. This solution schematics is visible in Figure 6.17.

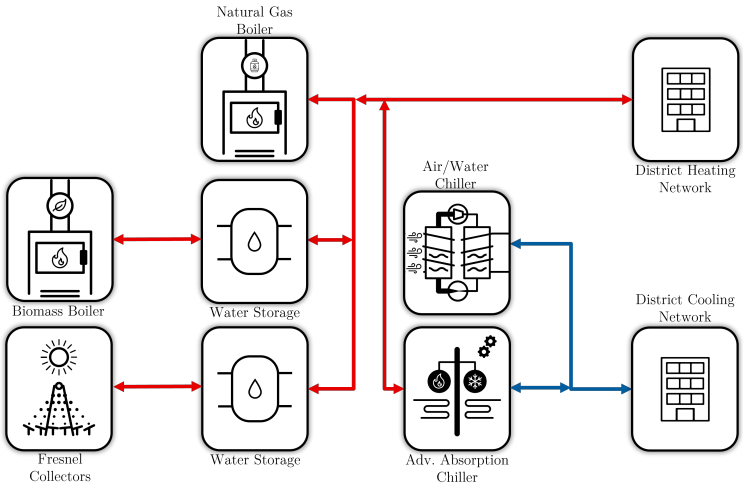

Figure 6.17: Focşani S2 diagram.

S3 takes a different approach altogether. This solution seeks to provide the cooling network by a geothermal heat pump, and cover the rest of the needs of the heating demand by the addition of a biomass boiler. This solution schematics is visible in Figure 6.18.

For the different solutions proposed, parametric analysis were performed, in these, key parameters were varied to select optimum solutions. These variations are shown in Table 6.15. As these calculations were made in-house, further detail will be shown on these calculations.

The first solution results show how absorption chiller's capacity strongly affects KPIs. The situation is in line with the cooling demand profile, making the absorption chiller work

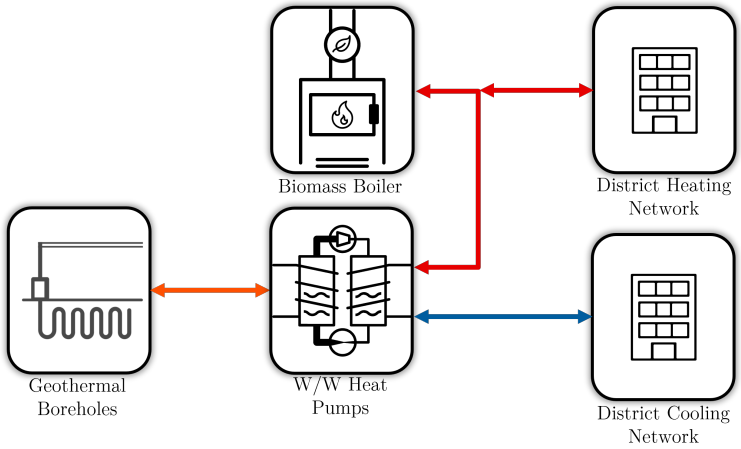

Figure 6.18: Focşani S3 diagram.

Parameter	Unit	S1 values	S2 values	S3 values
Biomass Boiler Capacity	kW	20000-30000	20000-30000	10000-25000
Gas Boiler Power	kW	0-10000	0-10000	-
Biomass Storage Volume	m^3(hours)	(3-12)	1000-3000	-
WeSSun Area	m^2	-	8000-20000	-
Solar Storage Volume	m^3(hours)	-	(3)	-
AAC Capacity	kW	1000-3000	1000	-
Chiller A/W Capacity	kW	6000-8000	8000	-
HP Cooling Capacity	kW	-	-	7000-10000

Table 6.15: Focşani parameters variation. Consider for S3 that HP Heating Capacity= 0.75∗Cooling Capacity.

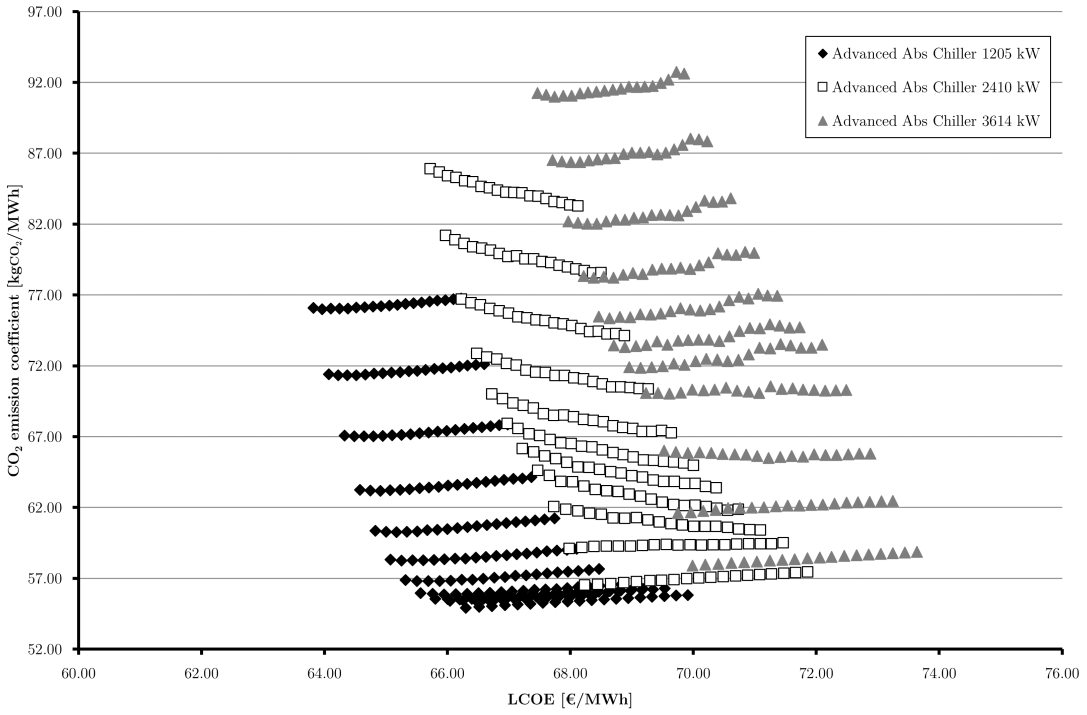

Figure 6.19: Focşani S1 KPIs considering different advance absorption chiller's capacity.

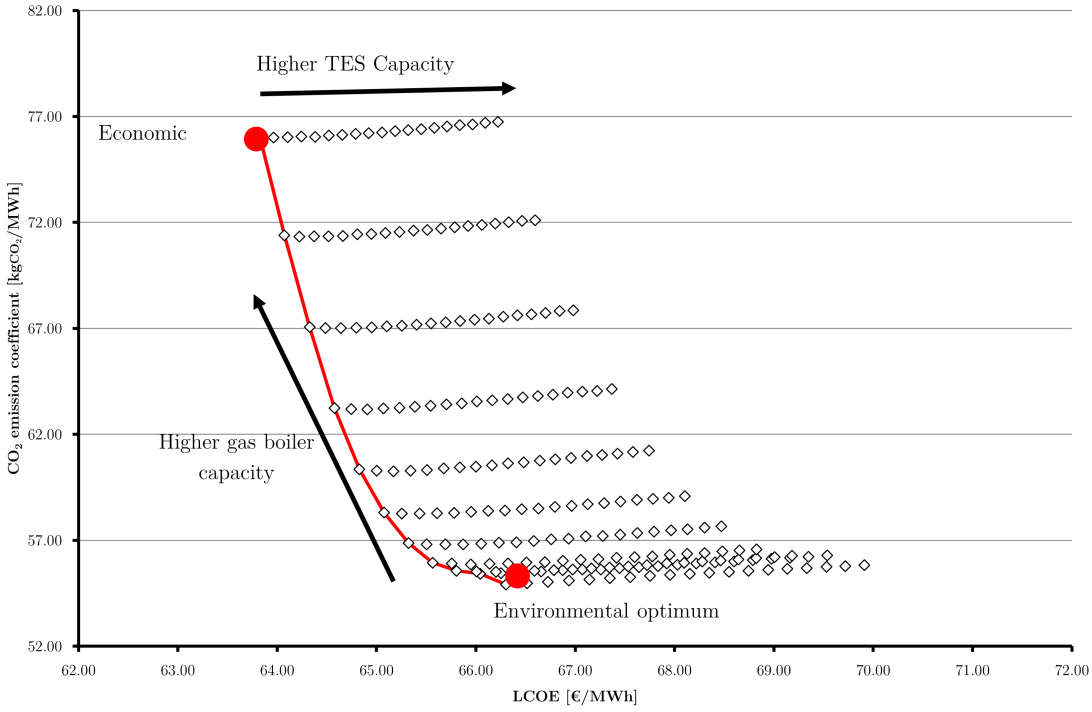

Figure 6.20: Focşani S1 emissions vs LCOE only for the heating network.

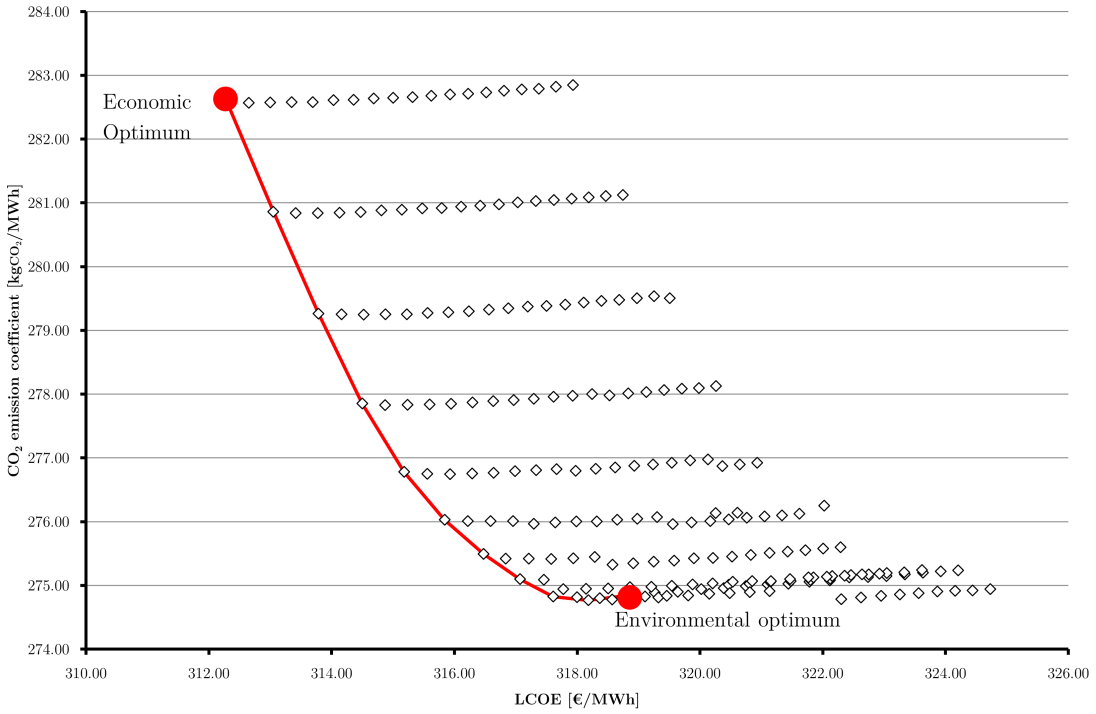

Figure 6.21: Focşani S1 emissions vs LCOE only for the cooling network.

far from its optimum operational point and with very variable demand, a situation that is not preferable for absorption chillers. Also, the increment in absorption chiller's capacity leads to an increment in the boiler size, affecting LCOE from various angles. This led to the selection of the smallest advanced absorption chiller from the parametric study. Figures 6.20 and 6.21 show optimum cases selected from the heating and cooling networks'perspective with this small absorption chiller selected.

Solution	Biomass boiler capacity [kW]	Gas boiler capacity [kW]	TES Volume [h]	Fresnel area [m^2]	AAC capacity [kW]	Chiller capacity [kW]	LCOE [€/MWh]	CO_2 emission coefficient [kg/MWh]
S1-CO_2	30000	-	3	0	1000	8000	66.3	54.91
S1-ECO	20000	10000	3	0	1000	8000	63.82	76.08
S2-CO_2	28000	2000	100*(m^3)	8000	0	0	66.12	53.51
S2-ECO	20000	10000	100*(m^3)	8000	0	0	64.13	73.49

Table 6.16: Focşani Solutions optimized capacities and KPIs.

Case	PV capacity [kW]	Biomass Boiler Capacity [kW]	HP W/W heating [kW]	HP W/W coling [kW]	LCOE [€/MWh]	CO_2 emission coefficient [kg/MWh]
S3	2800	17500	9333	7000	75.81	53.17

Table 6.17: Focşani Solutions optimized capacities and KPIs for S3.

S3 is the selected scenario, where the consumption of fossil fuels is lower compared to other scenarios. This results in a reduced dependency of LCOE on fuel prices. Additionally,

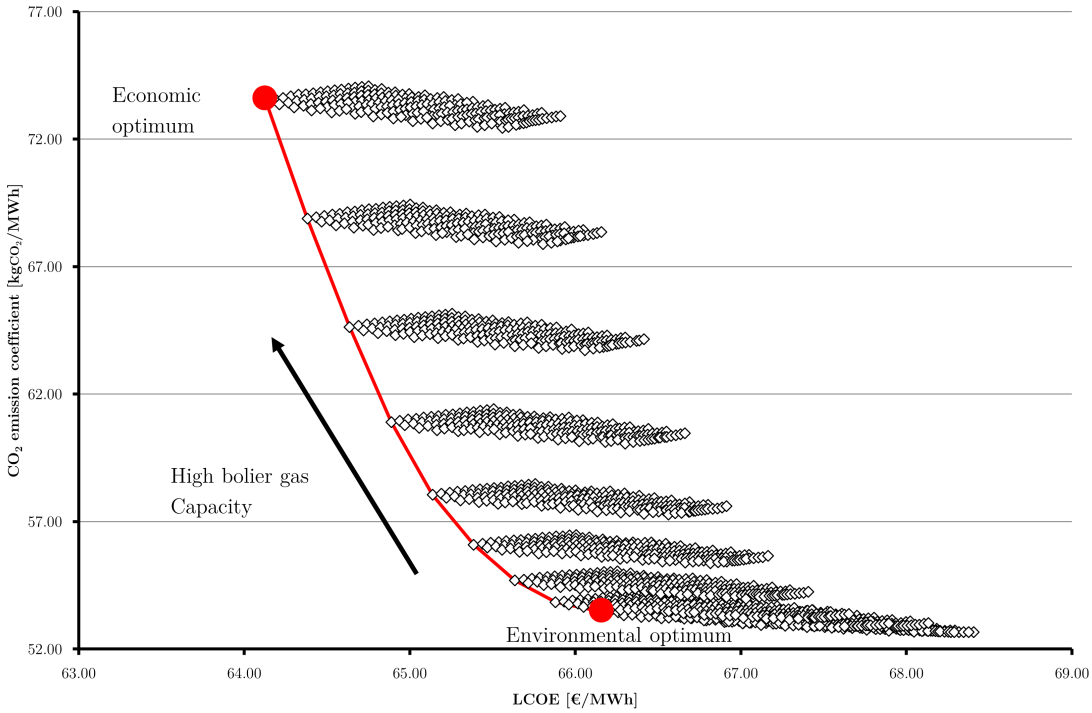

Figure 6.22: Focşani S2 emissions vs LCOE.

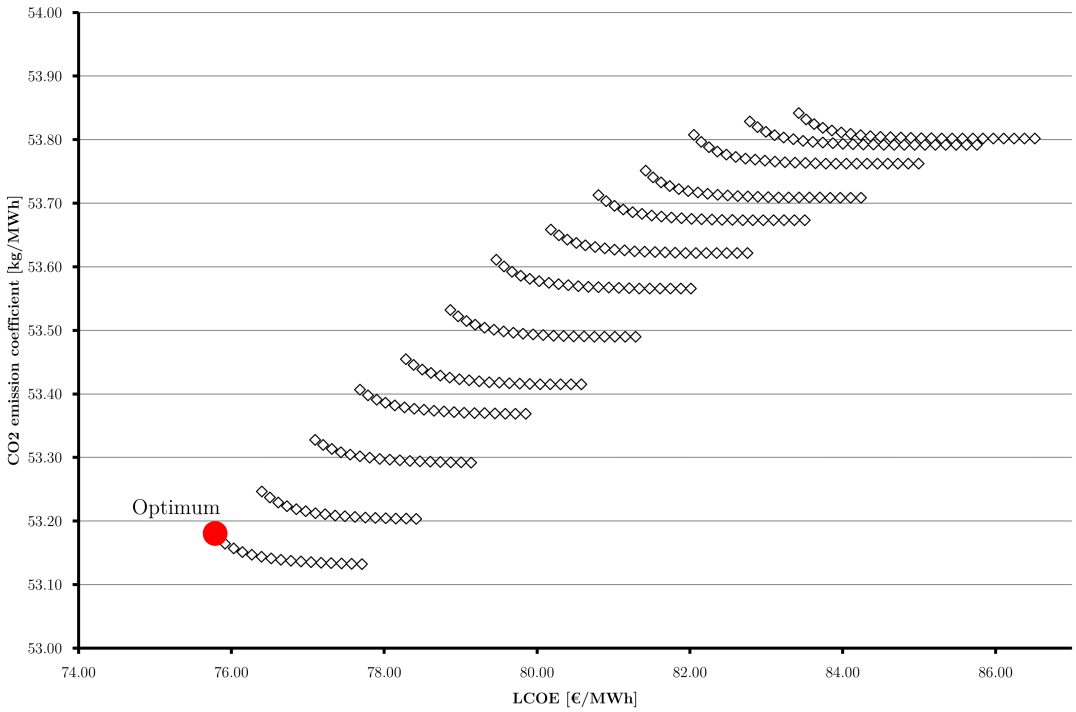

Figure 6.23: Focşani S3 emissions vs LCOE.

there is no gas consumption in this scenario and the photovoltaic system reduces electricity consumption by the heat pump. The cooling demand is met with a low CO_2 emission factor and LCOE. Furthermore, the LCOE for cooling is lower than in other scenarios since the same equipment is used for both heating and cooling purposes.

6.2.11 Mrągowo

Mrągowo is the capital of Mrągowo County, located in the Warmian-Masurian province of northeastern Poland. It has around 22000 inhabitants. Its heating demand is mostly covered by DHN (70%). Most of its generation (40.7 MW) consists of hard coal boilers (three 10 MW boilers, and three 5MW boilers). The network has 247 buildings connected, covering an area of around 416000 m^2. It is planned to substitute the hard coal boilers for biomass boilers in the near future. As this demo-follower's calculation was performed in-house, as with Focşani's case, further detail will be provided than in the rest of the demo-followers. Solutions proposed for Mrąwogo are shown in Table 6.18.

WEDISTRICT Technologies	**S1**	**S2**	**S3**
WeSSun		x	
Biomass boiler	x	x	x
Gas boiler	x	x	x
Thermal storage		x	x

Table 6.18: Solutions proposed for Mrągowo demo-follower.

Solution 1 (S1), responds to a heating-only network which changes the existing coal boilers for a combination of biomass and natural gas boilers. This combination responds to the diagram shown in Figure 6.24.

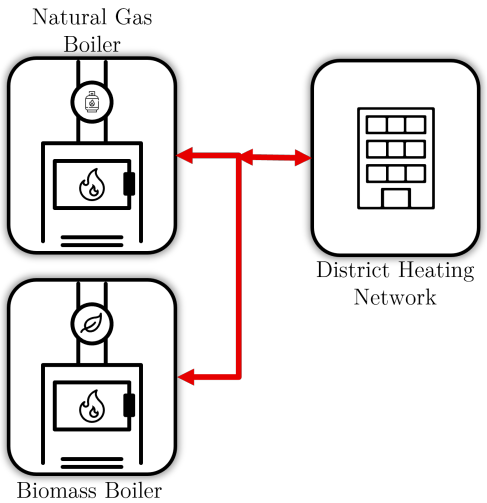

Figure 6.24: Mrąwogo S1 diagram.

Solution 2 (S2), differs slightly from S1, adding WeSSun technology solar panels along with thermal storage. This combination responds to the diagram shown in Figure 6.25.

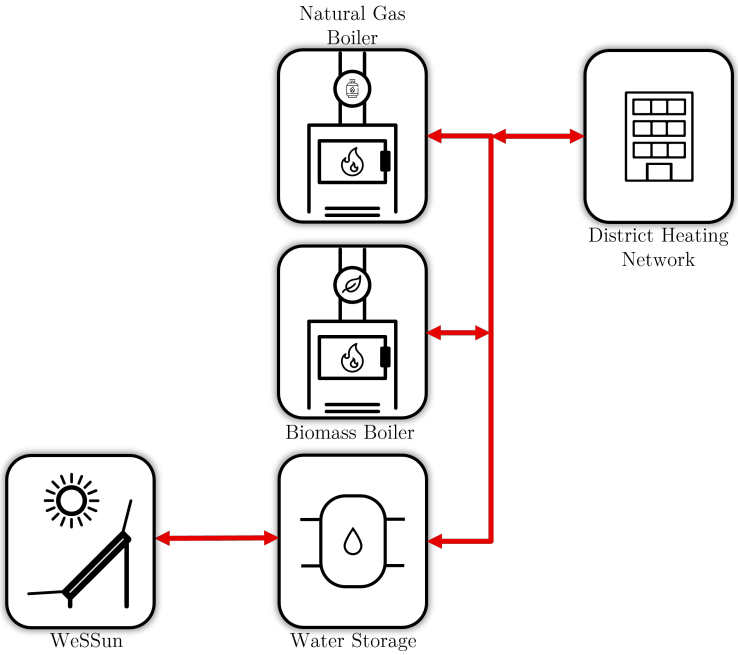

Figure 6.25: Mrągogo S2 diagram.

Finally, Solution 3 (S3), is an improvement from S1, trying to reduce the on-off cycles of the biomass boiler by adding a thermal storage. This combination responds to the diagram shown in Figure 6.26.

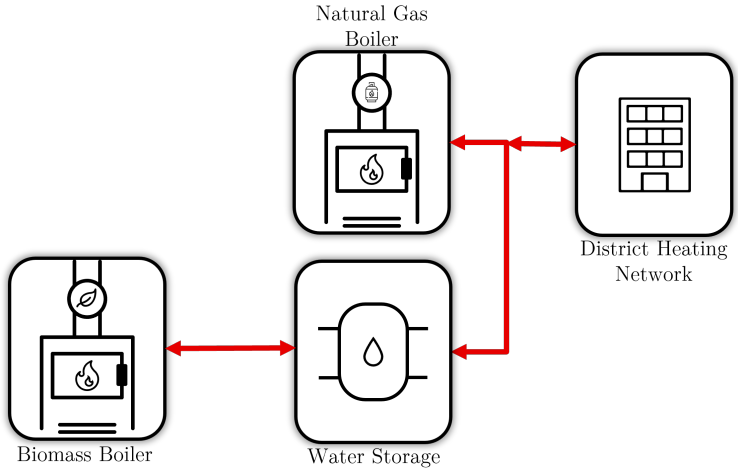

Figure 6.26: Mrągogo S3 diagram.

From these solutions, parametric studies have been performed for the different capacities of the technologies involved giving as a result the following KPIs shown in Figures figs. 6.27 to 6.29.

These studies were carried out by varying different parameters, Table 6.19 shows different parameters varied in each solution.

Parameter	Unit	S1 values	S2 values	S3 values
Biomass Boiler Capacity	kW	7000-13500	8500-13500	6000-11750
Gas Boiler Power	kW	3500-6500	3500	0-5750
Storage Volume	m^3	-	100-1000	-
WeSSun Area	m^2	-	4000-14000	-
Storage Volume	hours	-	-	4-12

Table 6.19: Mrągwogo parameters variation

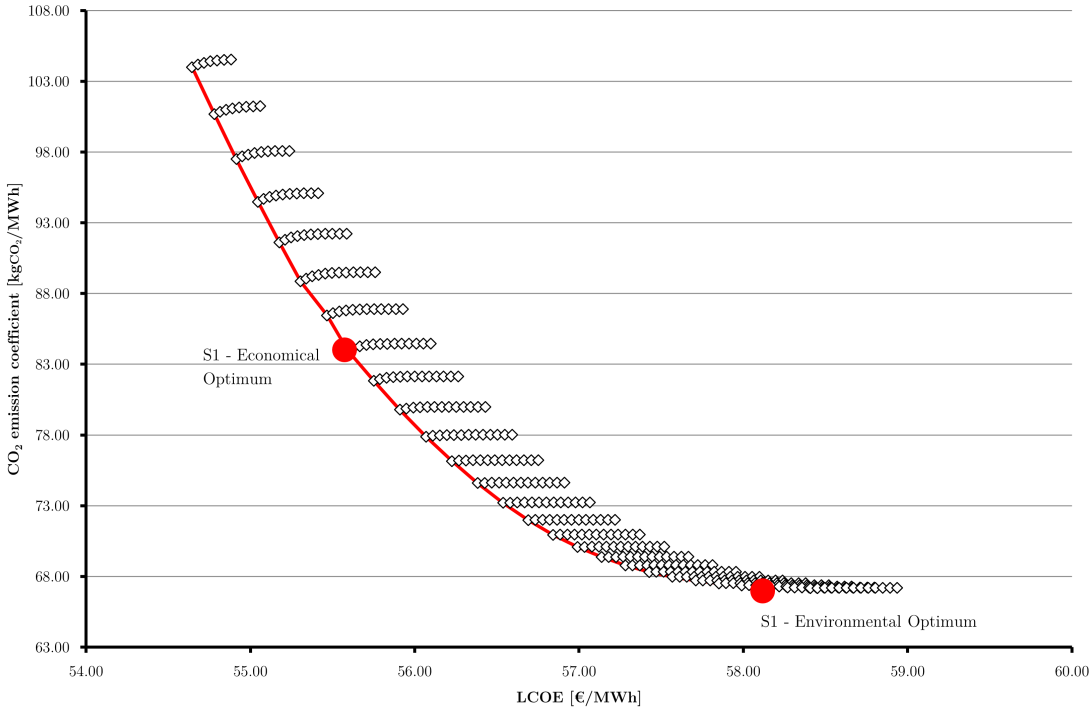

Figure 6.27: Parametric solutions from S1.

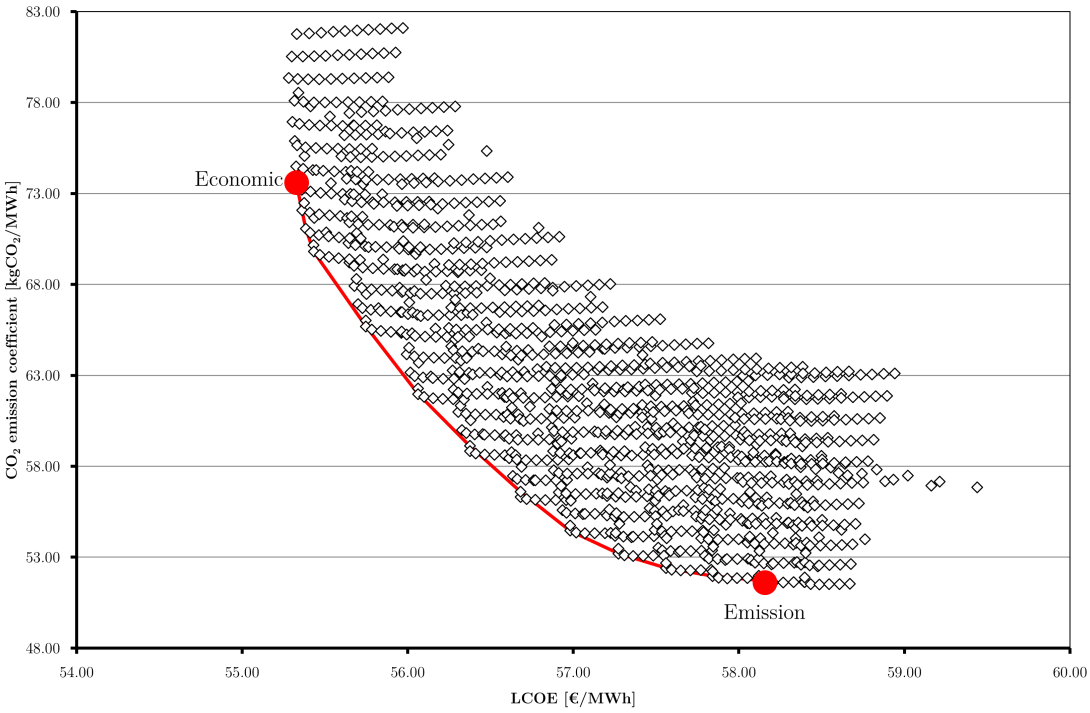

Figure 6.28: Parametric solutions from S2.

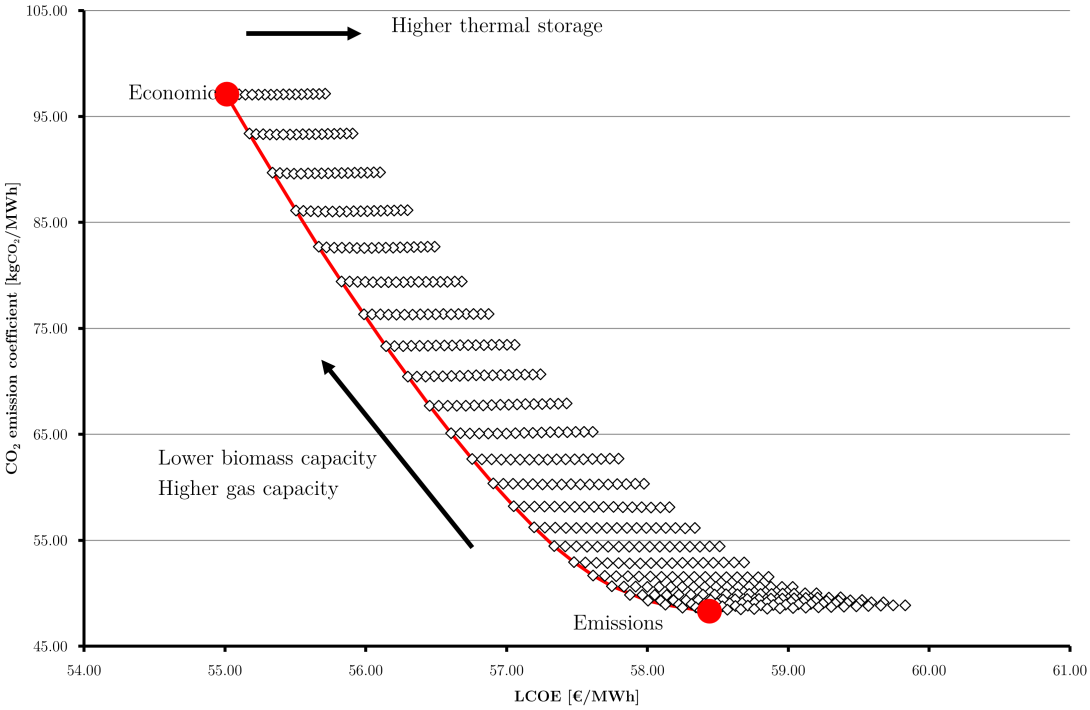

Figure 6.29: Parametric solutions from S3.

These optimum results have been summarized in Table 6.20 for better comparison.

Solution	Biomass boiler capacity [kW]	Gas boiler capacity [kW]	TES Volume [m^3]	WESSUN area [m^2]	LCOE [€/MWh]	CO_2 emission coefficient [kg/MWh]
S1-CO_2	13000	3500	0	0	58.13	67.27
S1-ECO	8750	3500	0	0	55.59	83.99
S2-CO_2	13000	3500	500	14000	58.12	51.72
S2-ECO	11000	3500	300	11000	55.33	73.39
S3-CO_2	11750	0	808	0	58.38	48.37
S3-ECO	6000	5750	412	0	55.01	97.15

Table 6.20: Mragowo Solutions optimized capacities and KPIs.

6.3 Parametric Studies

For different articles, the methodology has been used to determine optimum sizes for diverse systems. These examples aid to show the methodology's capability to help designers in the selection of proper sizes for technologies in different networks.

6.3.1 Solar Field Sizing for District Heating and Cooling

In the article "Comprehensive analysis of hot water tank sizing for a hybrid solar-biomass district heating and cooling", an optimum size of the solar field, paired with a storage tank was pursued [27]. This analysis tried to test different tank values in order to check rules of thumb used in the past (relation between tank volume and solar field area between 0.05 and 0.18 m), testing that when demand is not in line with usual domestic hot water consumption, these relations could vary.

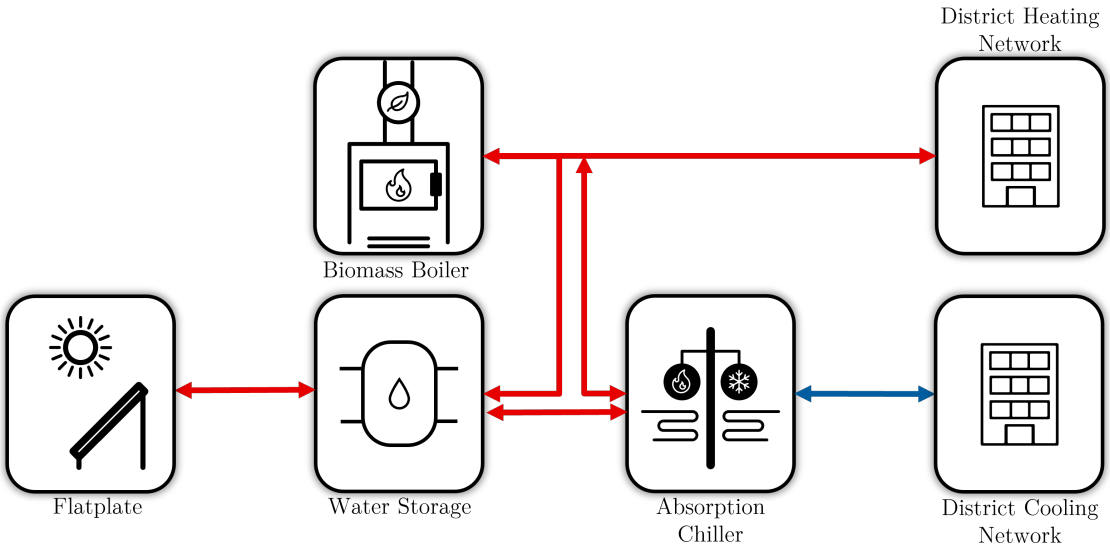

Figure 6.30: System scheme analyzed in article.

Parameter	Lower Value	Higher Value	Step
Collector Area [m2]	100	1500	100
Tank Capacity [m3]	10	100	5
Boiler Capacity [kW]	700	900	50
Abs. Chiller Cap [kW]	900	900	-

Table 6.21: Cases analyzed for study.

The system proposed was a district heating and cooling network. The heating side consisted of flat-plate collectors paired with a water tank and a biomass boiler. This heating generation also took into account the need for a heat source for an absorption chiller, which covered the cooling demand (see Figure 6.30).

For this study, 1349 cases were run to determine the different tank sizes paired with solar. Also, the possibility of biomass boiler capacity reduction was analyzed (See Table 6.21).

The result from this study can be seen in Figure 6.31. In this Figure, a final result is shown where an optimum tank size for each solar field size is marked (with red dots), considering the possible solar field sizes available for each biomass boiler size (different coloured surfaces).

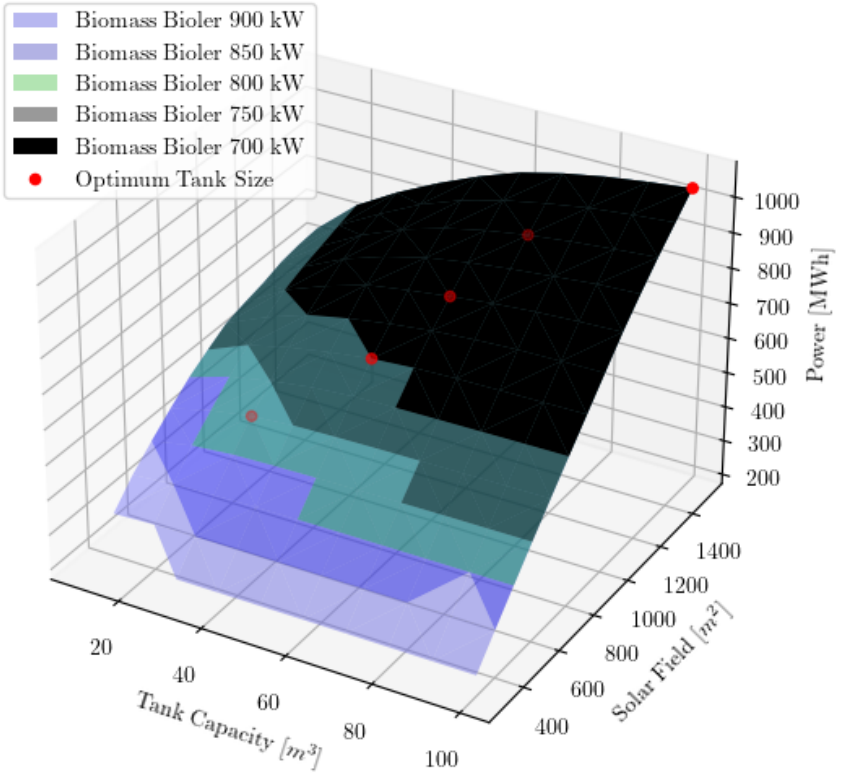

Figure 6.31: Results from system analyzed.

It was visible in these results, that the rule of thumb applies when the solar collector areas

are higher (although they tend to remain on the lower side of the range). However, when the solar collector area is limited, lower values of V/A seem technically better. For instance, smaller areas such as 600 m^2 yield values of 0.033 for this relation (<0.05), meaning that complying with the established range would make the system inefficient by losing energy to the ambient. Contrarily, larger collector areas tend to fall inside but around or below the lower limit. For example, a 1000 m^2 area yields a V/A value of 0.06 m.

6.3.2 Parametric Studies Future Works

There is a possibility to make the launcher used for parametric analysis more user-friendly and integrate the use of jEPlus in a more amicable manner not to go from one software to the other, making these studies also available for users with TRNSYS licenses.

6.4 Tool

One of the principal objectives of this thesis was to make DHC networks more accessible for new projects. With that in mind, it was decided that the best way of presenting the results of this methodology was the development of a web-based tool.

When conducting parametric studies, it is possible to store all the obtained results in ".json" format for a more organized database. This process has been automated using a Python script, and appropriate considerations have been made in the deck file to ensure that information is correctly formatted for this file to store and tabulate properly. The use of databases makes it possible to use the obtained results to tend to user requests. This concept is depicted in Figure 6.32.

Figure 6.32: Tool conceptualization.

These databases will first be done for five different established locations, which have been explained in Section 5.10.7.

Once locations were defined a combination of different systems was proposed to be able to select between different technologies, not only for district heating networks, but also for district heating and cooling networks. To size the heating and cooling demand profiles for the different locations, the methodology explained in Section 5.10.6 was used. A first batch of technological combinations was chosen. These decks were prioritized to have Wedistrict technologies used.

The first four technologies for district heating were chosen. The first combination chosen was the simplest one. In this combination, we have a biomass boiler paired with a natural gas boiler (Figure 6.33a), inside the Tool, this combination is addressed as “Biomass”. The possibility of changing existing coal-fired boilers for biomass boilers is one of the most straightforward ones, considering that there are many existing networks still using coal as fuel.

The second combination chosen was similar to the first one, but adding solar resources to the equation. In this combination, we have a biomass boiler paired with a natural gas boiler, and in this case, the solar addition is WeSSun technology (Figure 6.33b), inside the Tool, this combination is addressed as "Biomass + WeSSun". This combination starts adding solar resources to reduce the amount of boiler energy production.

The third and fourth combinations are equal to the second one, but instead of adding WeSSun technology, these combinations use PTC and Fresnel technologies for solar (see Figures figs. 6.33c and 6.33d), inside the Tool, these combinations are addressed as "Biomass + PTC" and "Biomass + Fresnel" respectively.

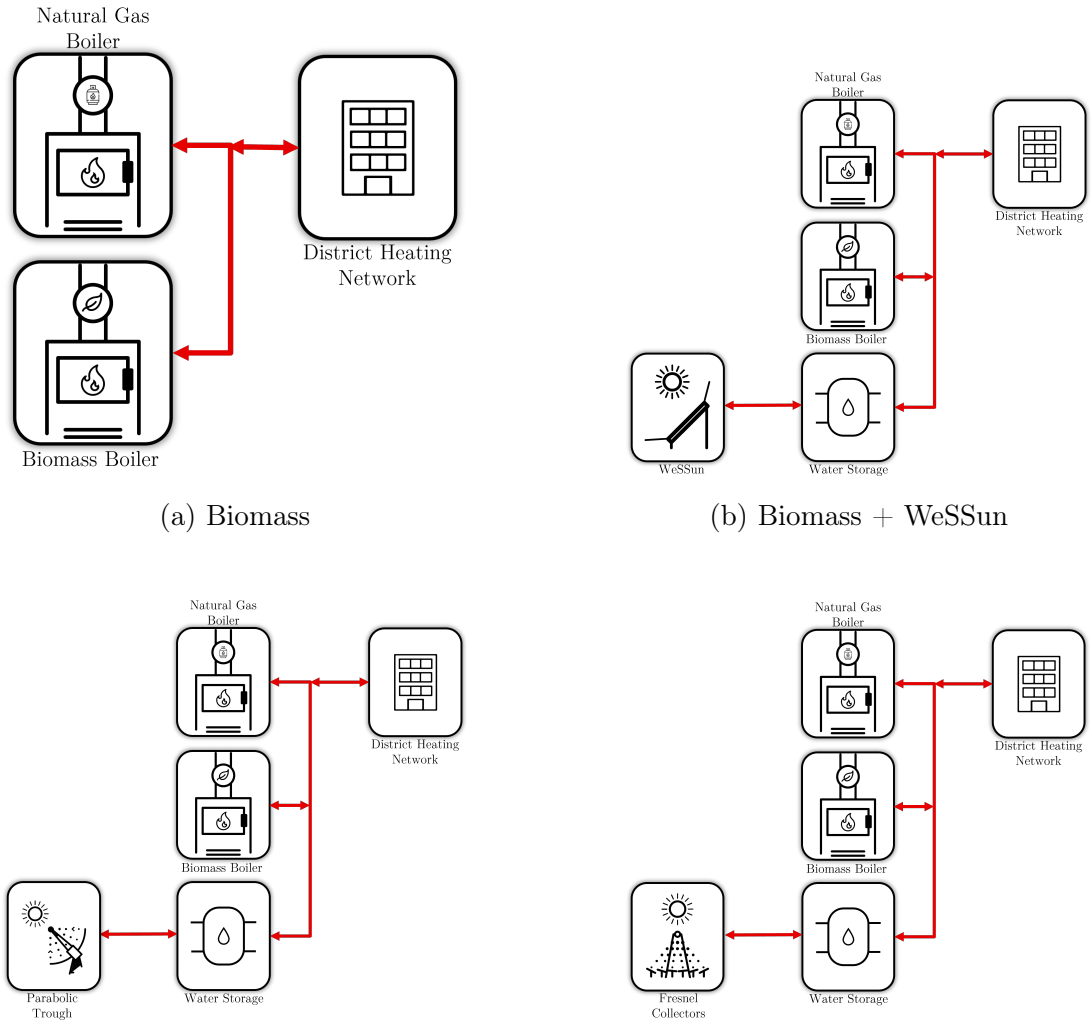

(a) Biomass

(b) Biomass + WeSSun

(c) Biomass + PTC

(d) Biomass + Fresnel

Figure 6.33: Tool combinations for district heating.

Four combinations used for district heating and cooling correspond to the ones chosen for district heating only, but adding a cooling network composed of an advanced absorption chiller and a backup compression chiller for the cooling demand peaks. These combinations would be named after the ones in district heating networks as "Biomass / Absorption Chiller",

"Biomass + WeSSun / Absorption chiller", "Biomass + PTC / Absorption chiller", and "Biomass + Fresnel / Absorption chiller" (See Figure 6.34).

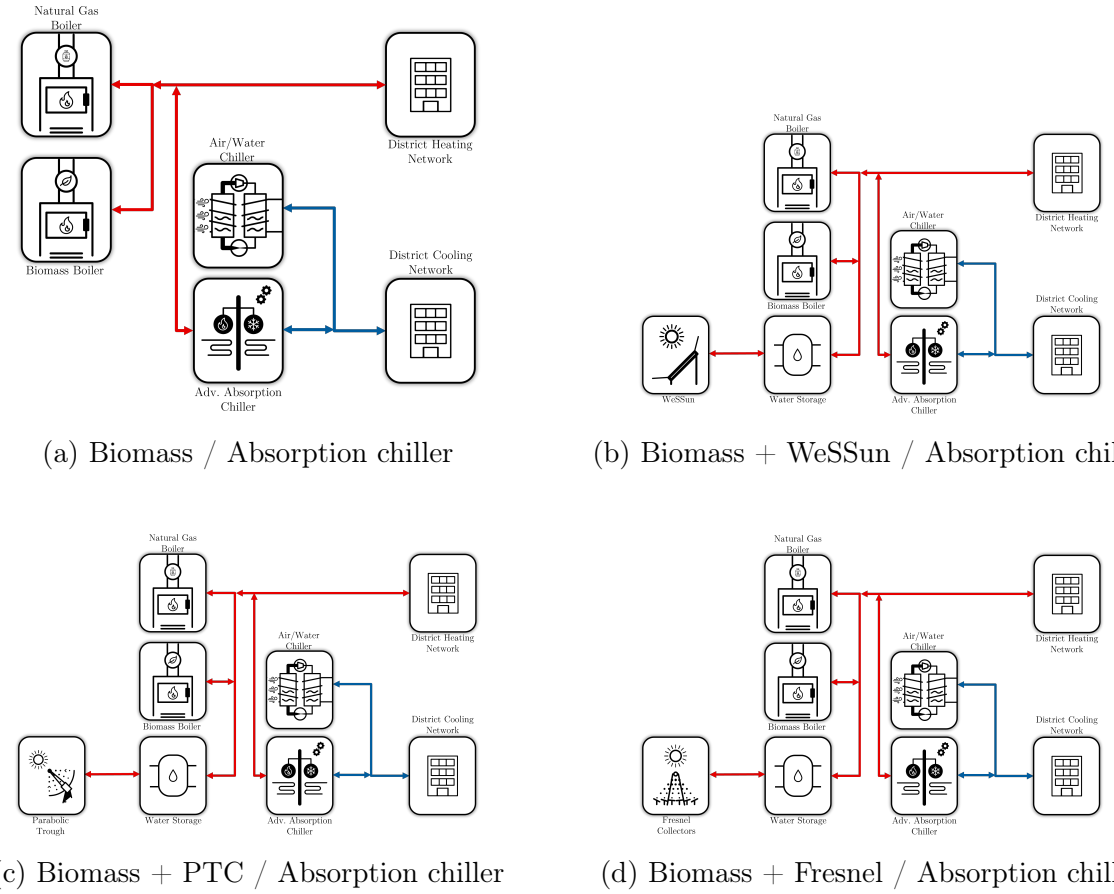

(a) Biomass / Absorption chiller

(b) Biomass + WeSSun / Absorption chiller

(c) Biomass + PTC / Absorption chiller

(d) Biomass + Fresnel / Absorption chiller

Figure 6.34: Tool combinations for district heating and cooling.

The workflow of the tool is simple. First, the user must select one of the five locations previously mentioned from the map presented in the interface. Secondly, a yearly demand is to be selected. If the user does not know the capacity needed for their area, use of Hotmaps application is advised [50]. Depending if the analyzed scenario will be district heating, or district heating and cooling, the user must select a demand ratio between these two demands. This ratio has been selected as explained in Section 5.10.7. Once demand has been covered, economic and environmental data must be covered. Default values are set for discount rate, expected lifetime of the system, costs of energy sources and emission factors of these sources, However, these values can be modified if available for the user for their specific case. After these values are set, user must choose between the combinations shown in Figures 6.33 and 6.34 (depending if the system is DH or DHC). In this screen, user can also change prices taken for the different technologies both CAPEX and OPEX values.

After this selection, the user will be presented with the results. Having the possibility of generating a report with all the KPIs and graphs available from the tool.

To use the Tool go to https://cc-suite.platform.wedistrict.eu/wTool. For more information on the Tool and its user manual, go to: https://www.wedistrict.eu/resources/.

6.4.1 Tool Future Works

In the future a wider selection of locations could be made if needed, the variability of this selection only affects the size of the database needed for the Tool. Using the methodology proposed in this thesis, other technologies or combinations could also be tested.

Chapter 7

Validation

7.1 Bucharest Demo site

One of Wedistrict's demonstration sites was planned to be in the POLITEHNICA București (UNSTPB). In this site, a series of technologies were intended to be tested and will be described in the following sections. This section will be oriented into describing the selected methodology for the validation of the technologies used in this demonstration site.

7.1.1 Technologies used

The Wedistrict project aimed to introduce a Hybrid Geothermal-PV technology at the Bucharest demonstration site, consisting of two subsystems: thermal and electrical. The thermal component will generate heat from renewable sources for heating, hot water production, and air conditioning of the Target Building (TB). Excess heat will be transferred to the local district heating network, UNSTPB DH. The main technologies included in this subsystem are as follows, signaled by numbers in Figure 7.1:

- Ground-source heat pumps (4, 5): including geothermal borehole heat exchanger (1).
- Hybrid photovoltaic thermal panels, to ensure the demand of DHW (12).
- Fan coil units, used for the distribution of thermal energy within TB (10).

The electrical subsystem mainly consists of:

- Photovoltaic panels.
- Electrical storage system controlled by an intelligent energy management system.

7.1.2 TRNSYS

Validation of models for these systems has been performed separately. As different parts of the model were validated each of them were integrated into a new, more inclusive, model.

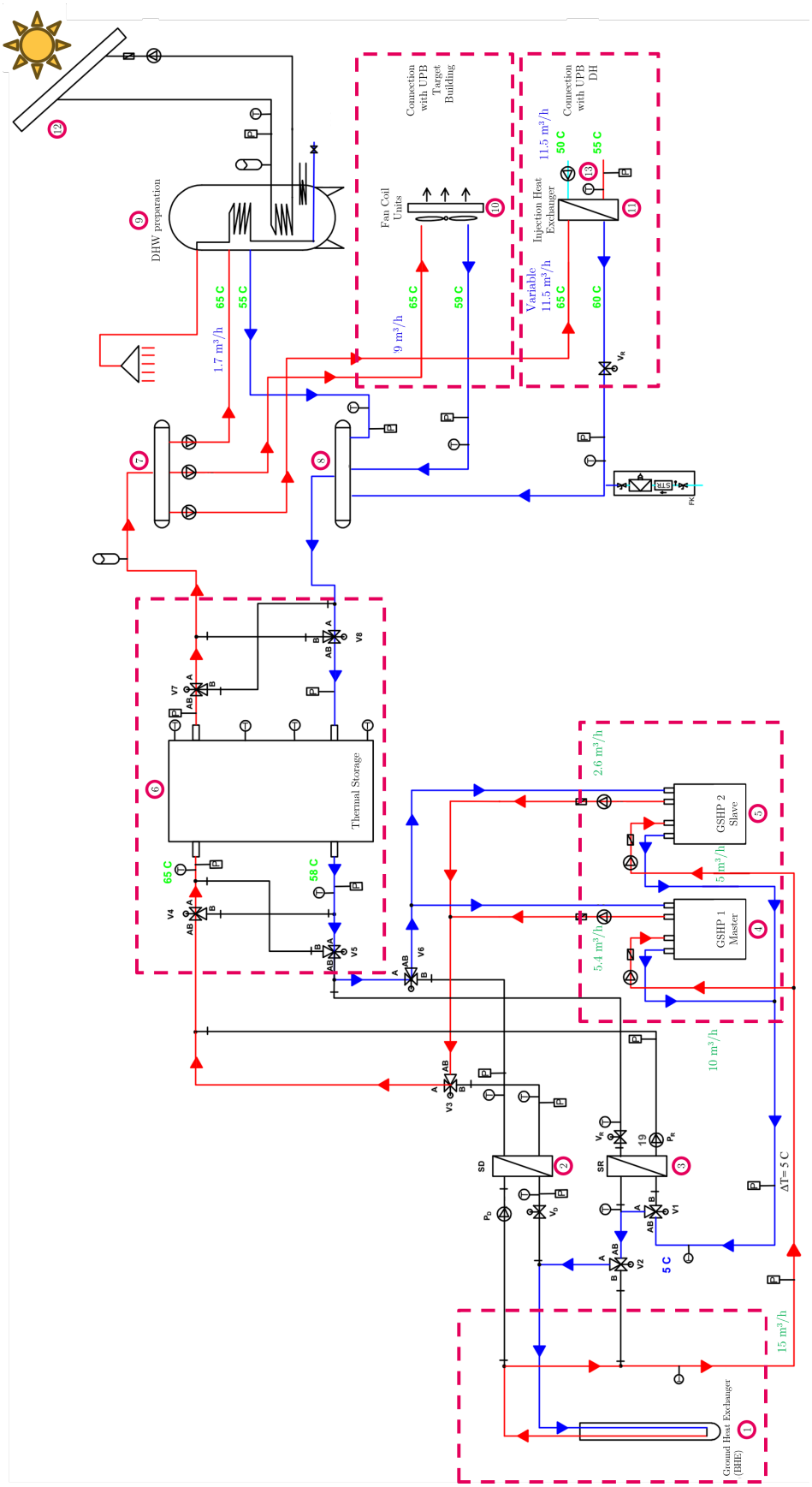

Figure 7.1: UNSTPB demonstrator Thermal Scheme from Wedistrict project modified.

Geothermal Borehole heat exchanger

For the validation of the geothermal borehole heat exchanger model (BHX), a TRNSYS deck has been developed (see Figure 7.2). In this model M0110 has been included, which is a macro intended to read the information provided by UNSTPB to feed the different validation models. In this model, a battery limit is set surrounding the M5100 macro. Different batches of information were delivered, where different operation modes and tests were being performed. The first batch of information contained data from the 1^{st} of February to the 30^{th} of April. Analyzing this information, five different periods were discovered where HPs operation differed. This segregation was based on the flow delivered to the existent DH and the flow used in the "target building" (Figure 7.3), which were the final variables to validate the complete model. For the borehole validation, the temperature inputs from the third period, which include the hours between the 4^{th} of March to the 9^{th} of April, were selected. This period proved to be the longest (36 days) with a consistent operation without changes.

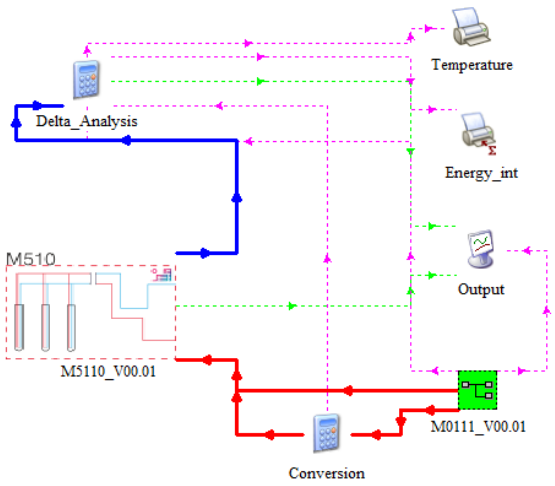

Figure 7.2: Geothermal Heat Exchanger validation model.

Water-Water Heat Pumps

Water-water heat pumps have been validated through a specific TRNSYS model, in this case, macro M0110 has also been used but supplying different information to establish a different battery limit, firstly, only the HP was considered as visible in Figure 7.4.

Once results proved to be suitable for validation, an integration of both models was proposed (BHX and HP), in which, flows were determined by supplied information to have a clear overview of the response of the model in terms of physical properties prior starting to adjust controls.

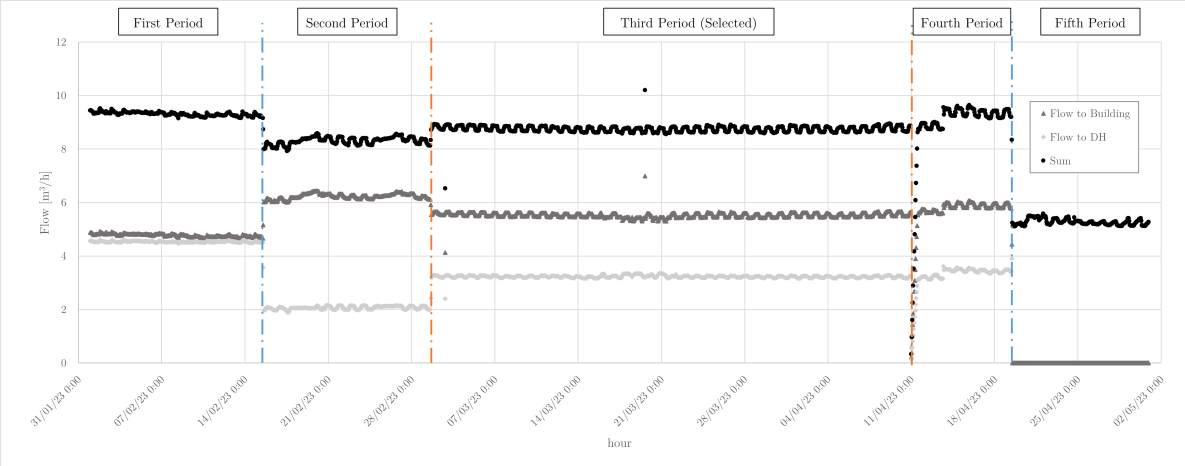

Figure 7.3: Flow data to consumers, UNSTPB first batch. Divided by operation periods.

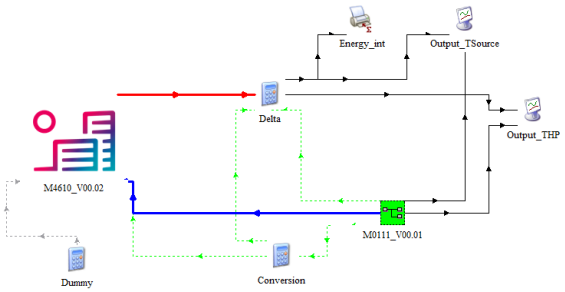

Figure 7.4: W-W HP pump validation model.

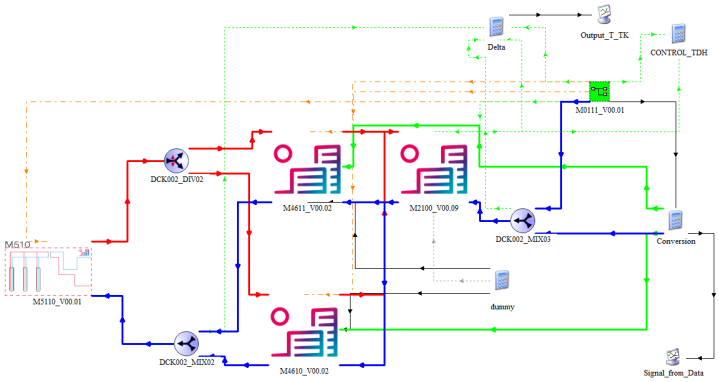

Figure 7.5: W-W HP validation model with integrated BHX.

7.1.3 Results Obatined

BHX

Results for this model have been analyzed in terms of temperature outputs, considering the deviations between the calculated temperature and the real data from the site. From this point of view, the model shows promising results, with an interesting variation when the system is in a steady state operation. Dynamic results could show improvement but this would involve further detail on the exact location of the sensors (see Figure 7.6b). Temperature difference percentual deviation has been filtered in transient cases when flow shows low values that are simulated but not consistent with reality. Those values come from extrapolating hourly information into 6-minute time steps and give temperature deviations as a result of the low flows of exchange (see Figure 7.6a). Differences around 4% in outlet temperatures (as seen for steady state in Figure 7.6b) prove to be sufficient for this kind of calculation, as it will be seen in future results, that the impact of the behavior of the source side of the HP is reduced in the more complex scheme.

HP W/W

The model described in Figure 7.4 was used for the following results. These results are taken directly from simulation taking hourly site data, filtering was needed considering values that are lower than the pump's nominal capacity as a fraction of the hour operations which produces small flows that impact the temperature results for the operation, also discussed in 7.1.3. Figure 7.7 shows a series of results for the first day in the analyzed period. Yearly results, filtered in the dynamic periods, yield a 9.8% difference between the simulation and the information from the site. For validation purposes a more thorough study was performed, which yielded the following results considering HP outlet temperature being supplied to the existing DH and the target building (T_{13}), as well as the return temperatures from both destinations (T_{15} and T_{16}). This temperature results are visible in Figure 7.8. A similar analysis was performed for the heat pump's heat output (Q_h), giving as a results the values shown in Figure 7.9.

With these results a series of statistical indicators were calculated as to evaluate the degree of accuracy achieved by the model. These indicators where:

- NMBE: Normalized Mean Bias Error. According to Equation 7.1.
- CVRMSE: Coefficient of Variance of Mean Root Square Error. According to Equation 7.2.
- Fit index: index of agreement by Willmott et al. [106].

$$NMBE = \frac{1}{\bar{m}} \cdot \frac{\sum_{i=1}^{n} (s_i - m_i)}{n - p} \tag{7.1}$$

$$CVRMSE = \frac{\left(\frac{\sum_{i=1}^{n} (s_i - m_i)^2}{(n-p)} \right)^{1/2}}{\bar{m}} \tag{7.2}$$

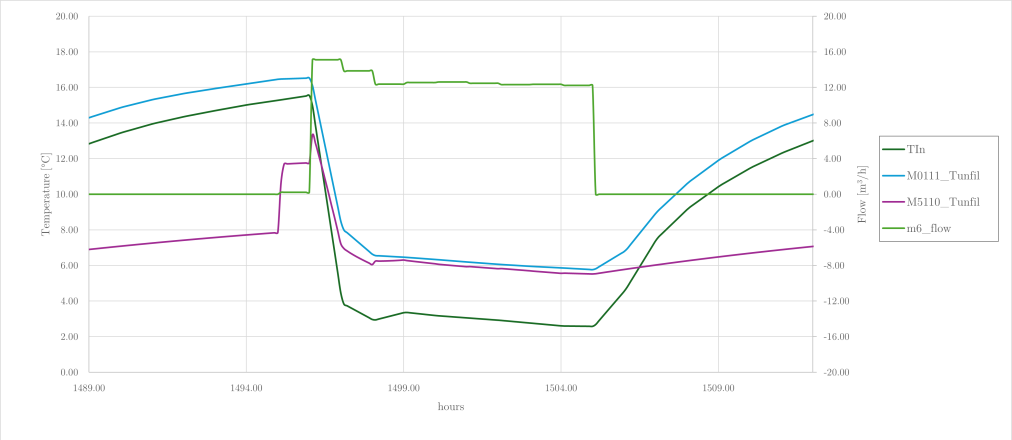

(a)

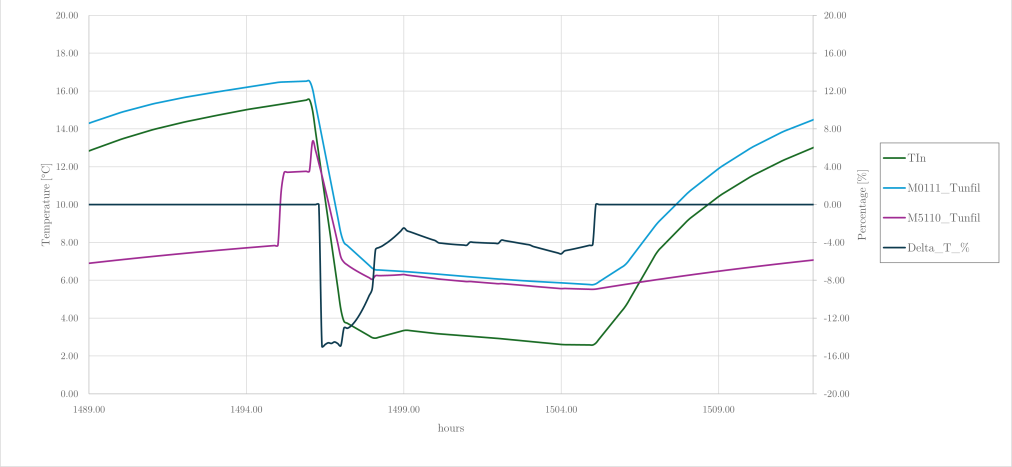

(b)

Figure 7.6: Results on the first day of the analyzed period. (a) shows results on temperatures and flows. While (b), shows the temperature percentual difference between calculated and received in experimental data.

Time step	Index	ASHRAE limits
Hourly	MBE	± 10%
	CVRMSE	30%
Monthly	MBE	± 5%
	CVRMSE	15%

Table 7.1: Index acceptance values according to [107].

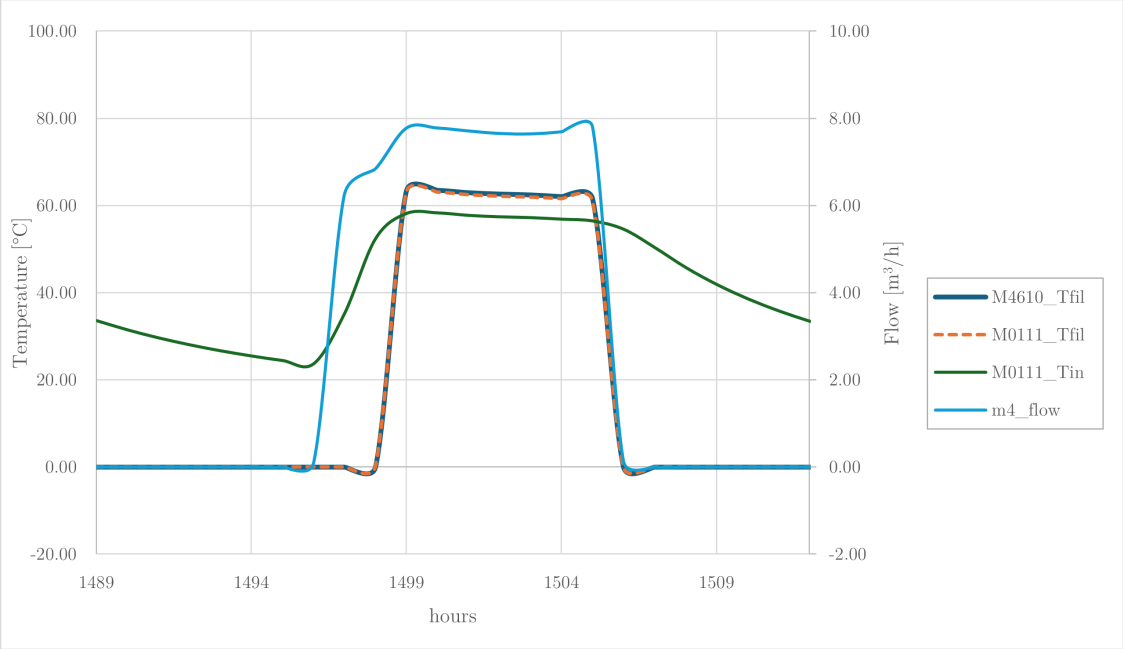

Figure 7.7: W-W HP validation model without BHX.

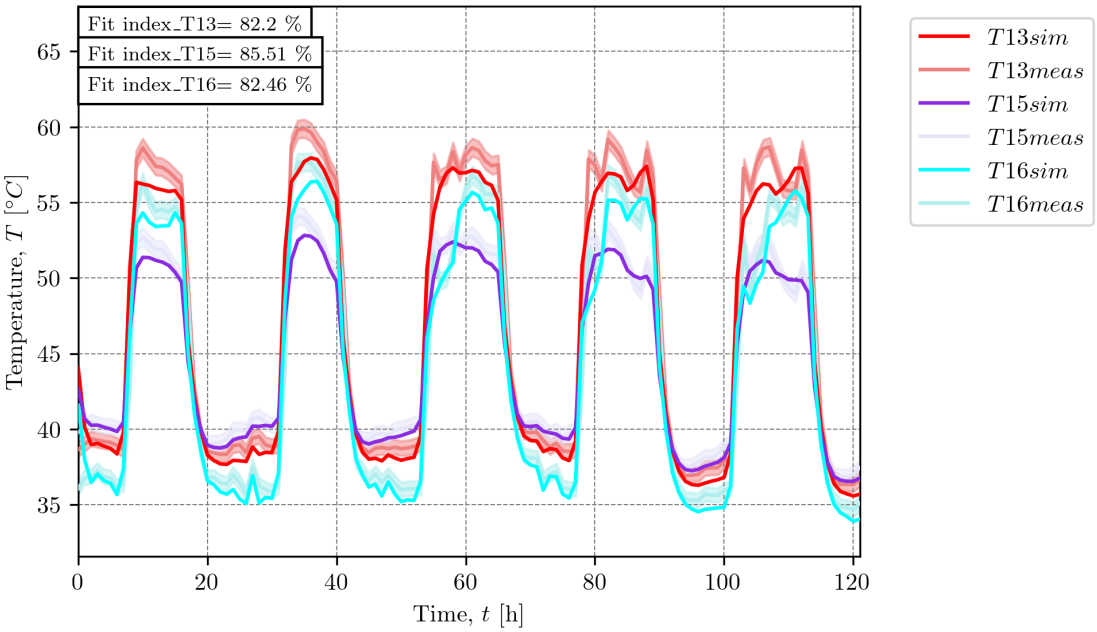

Figure 7.8: Temperature results of the system

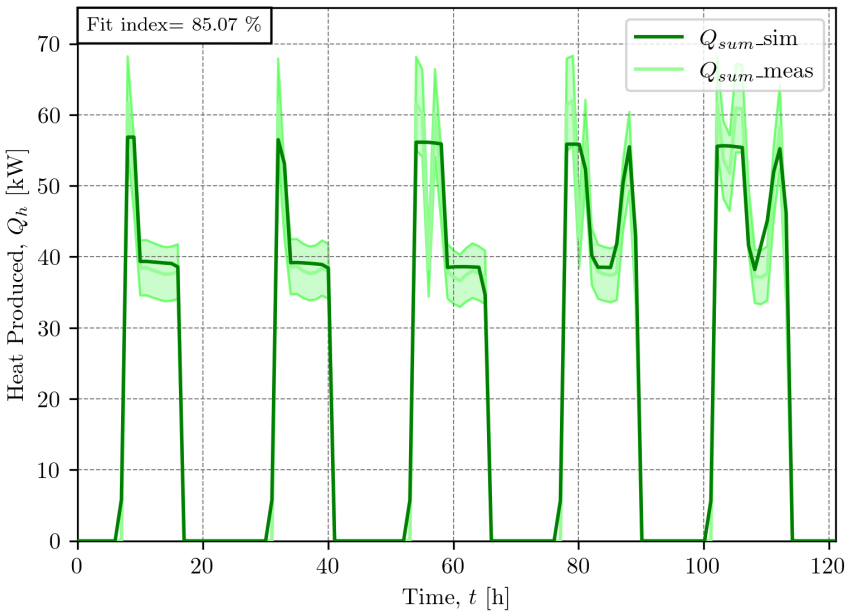

Figure 7.9: Heat delivered results of the system

Values of acceptance for these indexes are shown in Table 7.1, according to [107]. The results of the statistical indexes are shown in Table 7.2.

Variable	MBE	CVRMSE	Fit index
$Q_{h_{sum}}$	2.01%	16.76%	85.07%
T_{15}	0.92%	2.08%	85.51%
T_{16}	1.52%	3.51%	82.46%
T_{13}	1.80%	3.56%	82.20%

Table 7.2: Statistic values for POLITEHNICA

Chapter 8

Conclusion and Future Works

8.1 Thesis Conclusion

Given the current environmental context, there is an urgent need to replace fossil fuels with lower CO_2 emission options such as renewable energy. Among the potential solutions, District Heating Networks (DHNs) have been identified as a viable method to incorporate renewable energy sources to cater to heating, ventilation, and air conditioning demand (including domestic hot water). The centralization of heat generation can lead to a diversification in heat sources, apart from the implementation of renewable sources, the possibility of not depending on a sole fuel source, makes energy prices more resilient to market fluctuations. Machines used in bigger systems tend to have better efficiencies, and having only one source can lead to a reduction of installed capacity as networks are sized for maximum demand scenarios, which are not precisely the sum of all design capacities for all the nodes of the network.

Despite some exceptions, DHNs are underutilized across Europe. This presents an opportunity for many countries to adopt this technology and for others to upgrade existing networks to more environmentally friendly solutions.

A major barrier to DHN implementation is the complexity and location-dependency of the required calculations. For users who are not proficient in this area, DHN calculations can seem daunting, and obtaining results for comparison in a design stage can be particularly challenging for those unfamiliar with district heating.

There is software available for DHN simulation, but most of them tend to be difficult to use for an inexperienced user, and others, have a high demand for information to run design scenarios, which users tend not to have in the first stages of design.

To address this, the thesis presents a comprehensive methodology called the Modular Simulation Methodology (MSM). MSM aims to make DHNs more accessible to policymakers by minimizing the number of parameters required before running a simulation.

The methodology envelops from the generation of the models up to the final KPIs calculation and presentation for the user to select.

The methodology begins by creating simulation models in TRNSYS using a macro structure to compartmentalize various technologies. Once the model is established, it is parametrized holistically with a minimal number of input parameters (usually the technology 's capacity if possible). A Python script calculates different parameters such as pressure

drop for pumps, or line sizes, correlating all possible values.

Implications of the MSM are explained in Section 4. In this chapter the different concepts behind the methodology are explained:

- Nomenclature: The standard codification for the parameters used in the methodology is explained. This standardization intends to make variables recognizable at first sight.
- Parametrization: The methodology intends to correlate values for different technologies to reduce the number of values to be filled to a minimum.
- Parametric studies: The methodology 's capability to produce parametric studies using jEPlus software.

The technologies implemented in the methodology are explained in Section 5, also explaining the reasoning used behind the generation of demand files and how meteorological files are gathered. The technologies explained were:

- Solar Thermal: Including concentrating technologies and the calculation of non-concentrating using WeSSun macro.
- Conventional absorption chillers.
- Compression Chillers.
- Boilers: With different fuels.
- Water thermal storage.
- Molten salt storage tanks.
- Demand and Meteo models.

Once the model is developed and parametrized, simulations can be run using TRNSYS. jEPlus provides an efficient means for performing parametric analysis. Once the results—whether singular or parametric—are obtained, a Python script calculates key performance indicators (KPIs). The selected and calculated KPIs are:

- Cooling share (α_c).
- Renewable Energy Ratio (RER).
- Non-renewable primary energy factor (f_{nr}).
- Capital Expenditure (CAPEX).
- Opeartional Expenditure (OPEX).
- Levelized Cost of Energy (LCoE).
- Carbon Dioxide Emissions Coefficient (k_{CO_2}).

Different results obtained in the development of the methodology are shown in Chapter 6. These results include:

- Demonstration Sites: Locations to be built to demonstrate Wedistrict project technologies.
- Demonstration followers: Additional virtual demonstrators set to prove the methodology's ability to simulate new networks and test new technological combinations on existent ones.
- Parametric studies: Parametric studies done using the methodology for different articles.
- Web-based Tool: From parametric results databases from different locations a tool was developed.

This last result (Developing a web-based tool), was deemed the best approach to provide broad access across Europe.

The thesis also includes a validation section (Section 7), where specific models, such as water-water heat pumps and geothermal heat exchangers, were validated against real values. The results indicated promising accuracy, with some deviations explained by dynamic operational factors and sensor placement.

To summarize, the MSM standardizes the generation of Macros in TRNSYS, facilitating easier connections between technologies for district heating and cooling network simulations. The methodology also includes generating results with selected KPIs commonly used in projects to compare network value and technical performance against other software calculations and technological solutions. This capability of developing results and adding other technologies to the combinations makes its versatility one of the strong points of this work. Technologies tend to improve continuously, and new applications are developed every year. This makes the MSM capability of standardization a powerful characteristic.

Combinations developed outside the Tool add up to 54 different networks between heating, cooling, and heating and cooling (17, 8, and 29 respectively). These numbers are aligned with the existing situation, having more heating than cooling networks. However, these combinations show a great amount of DHC networks, which is not what could be considered usual. This number is due to the amount of combinations possible in DHC networks, as more technologies are available, combinations grow. Nevertheless, existent networks nowadays are mostly heating only. This amount of DHC networks serves as a desire statement, looking forward to reducing the growing amount of individual cooling installations in existing cities.

The main conclusions of this thesis are:

1. There is currently a wide variety of district network simulation tools available, mostly focused on simulating fixed topologies. However, incorporating new technology can be challenging with these tools as they are based on models that require a large number of parameters, making them difficult to use for non-experts.
2. In this sense, the MSM methodology presents a:

- Flexible both in terms of models and KPIs: models can be generated using the methodology, and a wide variety of KPIs are available, from economical to environmental.
- User-friendly, simulations can be carried out with just a few parameters: if not known values are defined by standard to have a first approach to the simulation.
- Scalable: as technologies can be added to models, these models can increment the complexity of the network and the size of the demand.
- This methodology can be used for different studies:
  - Perform models that represent the operation of an existing or future network.
  - Perform optimization studies of a new network or upgrade of an existing network.
  - Perform databases with different simulations.

8.2 Future Works

In future work, it would be interesting to incorporate models of additional technologies such as seasonal storage, organic Rankine cycle, and heat recovery. Improving the models used in cogeneration and adapting the methodology for simulating fifth-generation district networks (or Neutral Temperature Networks) would also be an intriguing direction. Simulation of third and fourth-generation networks could only signify a reduction in temperature, but fourth-generation networks also implement prosumers or waste heat recovery to the equation. This from a simulation standpoint in TRNSYS could be challenging. A similar situation appears with NTN. This type of network would need a different approach from a simulation standpoint as a distributed heat source and sink would be simulated (both being the same element), an option that would assume a big change simulating in TRNSYS given that the possibility of having dual sense lines is impossible, meaning that duplication of variables would be needed in various points.

In addition, it would be interesting to incorporate algorithms that, starting from a model developed according to MSM, would allow the determination of the parameters that automatically optimize the DHN according to different objective functions. Currently, the actual version of MSM allows optimization studies to be carried out employing parametric analysis. These studies are based on the use of the jEPlus tool. This software is based on code that executes in parallel the same TRSNYS model with different parameters. Using this approach as a starting point, a program would be developed that would perform the optimization process automatically using the different existing algorithms (such as linear programming or gradient descent) without the need to simulate all possible combinations. This would improve the current performance of MSM by obtaining a more accurate result and reducing simulation times.

From the tool's perspective further development can always be done, primarily to automatize the reading of databases to acquire updated economical data. Also generation of meta-models through wide spectrum of results to make the use of computational resources more efficient and thus faster.

Further efforts will be made to disseminate the Tool, with the expectation that, with knowledge of costs and emissions of district networks, their capability, and versatility in reducing the amount of non-renewable fuels, further implementation will arrive in countries such as Spain, to improve the share of renewable fuels in future constructions.

References

[1] Conference of the Parties, "THE PARIS AGREEMENT," United Nations, Paris, Tech. Rep., Nov. 2016. [Online]. Available: https://treaties.un.org/Pages/ViewDetails.aspx?src=TREATY&mtdsg_no=XXVII-7-.

[2] Eurostat, "Disaggregated final energy consumption in households - quantities [dataset]," Tech. Rep.

[3] Euroheat & Power, "DHC Market Outlook Insights & Trends," Tech. Rep., 2023.

[4] IEA, " Tracking Clean Energy Progress 2023," IEA, Tech. Rep., Jul. 2023. [Online]. Available: https://www.iea.org/reports/tracking-clean-energy-progress-2023.

[5] Interantional Enegy Agency, "Global Energy and Climate Model Documentation 2023," Tech. Rep., 2023. [Online]. Available: www.iea.org.

[6] J. F. Collins, "The history of district heating," *District Heating*, vol. 44, no. 4, pp. 154–161, 1959.

[7] P. Woods and J. Overgaard, "1 - Historical development of district heating and characteristics of a modern district heating system," in *Advanced District Heating and Cooling (DHC) Systems*, R. Wiltshire, Ed., Oxford: Woodhead Publishing, 2016, pp. 3–15, ISBN: 978-1-78242-374-4. DOI: https://doi.org/10.1016/B978-1-78242-374-4.00001-X. [Online]. Available: https://www.sciencedirect.com/science/article/pii/B978178242374400001X.

[8] H. Lund, S. Werner, R. Wiltshire, S. Svendsen, J. E. Thorsen, F. Hvelplund, and B. V. Mathiesen, "4th Generation District Heating (4GDH): Integrating smart thermal grids into future sustainable energy systems," *Energy*, vol. 68, pp. 1–11, 2014, ISSN: 0360-5442. DOI: https://doi.org/10.1016/j.energy.2014.02.089. [Online]. Available: https://www.sciencedirect.com/science/article/pii/S0360544214002369.

[9] H. Lund, P. A. Østergaard, T. B. Nielsen, S. Werner, J. E. Thorsen, O. Gudmundsson, A. Arabkoohsar, and B. V. Mathiesen, "Perspectives on fourth and fifth generation district heating," *Energy*, vol. 227, Jul. 2021, ISSN: 03605442. DOI: 10.1016/j.energy.2021.120520.

[10] N. Perez-Mora, F. Bava, M. Andersen, C. Bales, G. Lennermo, C. Nielsen, S. Furbo, and V. Martínez-Moll, *Solar district heating and cooling: A review*, Mar. 2018. DOI: 10.1002/er.3888.

[11] S. Werner, *International review of district heating and cooling*, Oct. 2017. DOI: 10.1016/j.energy.2017.04.045.

[12] J. Huang, J. Fan, S. Furbo, D. Chen, Y. Dai, and W. Kong, "Economic analysis and optimization of combined solar district heating technologies and systems," *Energy*, vol. 186, Nov. 2019, ISSN: 03605442. DOI: 10.1016/j.energy.2019.115886.

[13] H. Dorotić, T. Pukšec, D. R. Schneider, and N. Duić, "Evaluation of district heating with regard to individual systems – Importance of carbon and cost allocation in cogeneration units," *Energy*, vol. 221, Apr. 2021, ISSN: 03605442. DOI: 10.1016/j.energy.2021.119905.

[14] B. Doračić, T. Novosel, T. Pukšec, and N. Duić, "Evaluation of excess heat utilization in district heating systems by implementing levelized cost of excess heat," *Energies*, vol. 11, no. 3, Feb. 2018, ISSN: 19961073. DOI: 10.3390/en11030575.

[15] M. Münster, P. E. Morthorst, H. V. Larsen, L. Bregnbæk, J. Werling, H. H. Lindboe, and H. Ravn, "The role of district heating in the future Danish energy system," *Energy*, vol. 48, no. 1, pp. 47–55, 2012, ISSN: 03605442. DOI: 10.1016/j.energy.2012.06.011.

[16] U. Persson, E. Wiechers, B. Möller, and S. Werner, "Heat Roadmap Europe: Heat distribution costs," *Energy*, vol. 176, pp. 604–622, Jun. 2019, ISSN: 03605442. DOI: 10.1016/j.energy.2019.03.189.

[17] S. Calixto, M. Cozzini, and G. Manzolini, "Modelling of an existing neutral temperature district heating network: Detailed and approximate approaches," *Energies*, vol. 14, no. 2, Jan. 2021, ISSN: 19961073. DOI: 10.3390/en14020379.

[18] P. A. Østergaard, S. Werner, A. Dyrelund, H. Lund, A. Arabkoohsar, P. Sorknæs, O. Gudmundsson, J. E. Thorsen, and B. V. Mathiesen, "The four generations of district cooling - A categorization of the development in district cooling from origin to future prospect," *Energy*, vol. 253, Aug. 2022, ISSN: 03605442. DOI: 10.1016/j.energy.2022.124098.

[19] United Nations Environment Programme (UNEP) Ozone Secretariat, "1987 Montreal Protocol on Substances that Deplete the Ozone Layer," Tech. Rep.

[20] J. Pelda, S. Holler, and U. Persson, "District heating atlas - Analysis of the German district heating sector," *Energy*, vol. 233, Oct. 2021, ISSN: 03605442. DOI: 10.1016/j.energy.2021.121018.

[21] GeoDH Project, *Geo_DH*. [Online]. Available: https://map.mbfsz.gov.hu/geo_DH/.

[22] J. g. S. P. U. Pelda, *District Heating Atlas*. [Online]. Available: https://fernwaerme-atlas.hawk.de/.

[23] Via Sèva, *Cartographie des réseaux de chaleur & de froid*. [Online]. Available: https://carte.reseauxdechaleur2030.fr/main.php.

[24] European Commission, "Overview of District Heating and Cooling Markets and Regulatory Frameworks under the Revised Renewable Energy Directive Main Report Final version," Tech. Rep., Oct. 2021.

[25] T. Bossmann Pierre Attard Gaspard Peña Verrier Laurent Fournié, "METIS Studies Study S9 Cost-efficient district heating development 2 Prepared by," Tech. Rep., 2018. [Online]. Available: http://europa.eu.

[26] A. Abánades, J. Rodríguez-Martín, J. J. Roncal, A. Caraballo, and F. Galindo, "Proposal of a thermocline molten salt storage tank for district heating and cooling," *Applied Thermal Engineering*, vol. 218, Jan. 2023, ISSN: 13594311. DOI: 10.1016/j.applthermaleng.2022.119309.

[27] J. J. Roncal-Casano, J. Rodriguez-Martín, A. Abánades, J. Muñoz-Antón, I. Gurruchaga, and D. González Castellví, "Comprehensive analysis of hot water tank sizing for a hybrid solar-biomass district heating and cooling," *Results in Engineering*, vol. 18, p. 101 160, Jun. 2023, ISSN: 2590-1230. DOI: 10.1016/J.RINENG.2023.101160.

[28] B. Talebi, P. A. Mirzaei, A. Bastani, and F. Haghighat, *A review of district heating systems: Modeling and optimization*, Oct. 2016. DOI: 10.3389/fbuil.2016.00022.

[29] D. Connolly, H. Lund, B. V. Mathiesen, S. Werner, B. Möller, U. Persson, T. Boermans, D. Trier, P. A. Østergaard, and S. Nielsen, "Heat roadmap Europe: Combining district heating with heat savings to decarbonise the EU energy system," *Energy Policy*, vol. 65, pp. 475–489, Feb. 2014, ISSN: 03014215. DOI: 10.1016/j.enpol.2013.10.035.

[30] I. Beausoleil-Morrison, F. Macdonald, M. Kummert, T. McDowell, and R. Jost, "Co-simulation between ESP-r and TRNSYS," *Journal of Building Performance Simulation*, vol. 7, no. 2, pp. 133–151, Mar. 2014, ISSN: 19401493. DOI: 10.1080/19401493.2013.794864.

[31] S. Klein and et all, *TRNSYS 18: A Transient System Simulation Program*, 2017. [Online]. Available: http://sel.me.wisc.edu/trnsys..

[32] P. A. Ostergaard, A. N. Andersen, and P. Sorknæs, "The business-economic energy system modelling tool energyPRO," *Energy*, vol. 257, Oct. 2022, ISSN: 03605442. DOI: 10.1016/j.energy.2022.124792.

[33] D. B. Crawley, L. K. Lawrie, C. O. Pedersen, and F. C. Winkelmann, "Energy plus: energy simulation program," *ASHRAE journal*, vol. 42, no. 4, pp. 49–56, 2000.

[34] A. Chiodi, J. P. Deane, M. Gargiulo, and B. P. Ó. Gallachóir, "Modelling Electricity Generation-Comparing Results: From a Power Systems Model and an Energy Systems Model," Tech. Rep., 2011. [Online]. Available: https://www.researchgate.net/publication/228822212.

[35] A. Witzig, M. Pfeiffer, S. Geisshüsler, P. Kistler, and R. Bornatico, "Polysun Inside: A Universal Platform for Commercial Software and Research Applications," International Solar Energy Society (ISES), Apr. 2016, pp. 1–8. DOI: 10.18086/eurosun.2010.04.18.

[36] H. Lund, J. Z. Thellufsen, P. A. Østergaard, P. Sorknæs, I. R. Skov, and B. V. Mathiesen, "EnergyPLAN – Advanced analysis of smart energy systems," *Smart Energy*, vol. 1, Feb. 2021, ISSN: 26669552. DOI: 10.1016/j.segy.2021.100007.

[37] A. Brown, A. Foley, D. Laverty, S. McLoone, and P. Keatley, "Heating and cooling networks: A comprehensive review of modelling approaches to map future directions," *Energy*, vol. 261, Dec. 2022, ISSN: 03605442. DOI: 10.1016/j.energy.2022.125060.

[38] Y. Shimoda, T. Fujii, T. Morikawa, and M. Mizuno, "Residential end-use energy simulation at city scale," *Building and Environment*, vol. 39, no. 8, pp. 959–967, Aug. 2004, ISSN: 0360-1323. DOI: 10.1016/J.BUILDENV.2004.01.020.

[39] P. Sehrawat and K. Kensek, "Urban Energy Modeling: GIS as an Alternative to BIM," *Proceedings of ASHRAE/IBPSA-USA Building Simulation Conference*, vol. 6, pp. 235–242, 2014.

[40] S. Heiple and D. J. Sailor, "Using building energy simulation and geospatial modeling techniques to determine high resolution building sector energy consumption profiles," *Energy and Buildings*, vol. 40, no. 8, pp. 1426–1436, 2008, ISSN: 03787788. DOI: 10.1016/j.enbuild.2008.01.005.

[41] I. Theodoridou, A. M. Papadopoulos, and M. Hegger, "A typological classification of the Greek residential building stock," *Energy and Buildings*, vol. 43, no. 10, pp. 2779–2787, Oct. 2011, ISSN: 0378-7788. DOI: 10.1016/J.ENBUILD.2011.06.036.

[42] G. Dall'O', A. Galante, and M. Torri, "A methodology for the energy performance classification of residential building stock on an urban scale," *Energy and Buildings*, vol. 48, pp. 211–219, 2012, ISSN: 0378-7788. DOI: https://doi.org/10.1016/j.enbuild.2012.01.034. [Online]. Available: https://www.sciencedirect.com/science/article/pii/S0378778812000515.

[43] R. Nouvel, C. Schulte, U. Eicker, D. Pietruschka, and V. Coors, "Citygml-based 3d City Model For Energy Diagnostics And Urban Energy Policy Support," Aug. 2013. DOI: 10.26868/25222708.2013.989. [Online]. Available: https://publications.ibpsa.org/conference/paper/?id=bs2013_989.

[44] P. Caputo, G. Costa, and S. Ferrari, "A supporting method for defining energy strategies in the building sector at urban scale," *Energy Policy*, vol. 55, pp. 261–270, 2013, ISSN: 0301-4215. DOI: https://doi.org/10.1016/j.enpol.2012.12.006. [Online]. Available: https://www.sciencedirect.com/science/article/pii/S0301421512010518.

[45] L. Filogamo, G. Peri, G. Rizzo, and A. Giaccone, "On the classification of large residential buildings stocks by sample typologies for energy planning purposes," *Applied Energy*, vol. 135, pp. 825–835, 2014, ISSN: 0306-2619. DOI: https://doi.org/10.1016/j.apenergy.2014.04.002. [Online]. Available: https://www.sciencedirect.com/science/article/pii/S0306261914003353.

[46] F. Koene, L. Bakker, D. Lanceta, and S. Narmsara, "Simplified Building Model of Districts," in *Proceedings of BauSim Conference 2014: 5th Conference of IBPSA-Germany and Austria*, ser. BauSim Conference, IBPSA-Germany and Austria, vol. 5, Dresden, Germany: IBPSA-Germany and Austria, Sep. 2014, pp. 152–159, ISBN: 978-3-00-047160-5. [Online]. Available: https://publications.ibpsa.org/conference/paper/?id=bausim2014_1128.

[47] J. A. Fonseca and A. Schlueter, "Integrated model for characterization of spatiotemporal building energy consumption patterns in neighborhoods and city districts," *Applied Energy*, vol. 142, pp. 247–265, Mar. 2015, ISSN: 0306-2619. DOI: 10.1016/J.APENERGY.2014.12.068.

[48] K. Orehounig, G. Mavromatidis, R. Evins, V. Dorer, and J. Carmeliet, "Predicting energy consumption of a neighbourhood using building performance simulations," *Proceedings of BSO14*, p. 72, 2014. [Online]. Available: https://www.research-collection.ethz.ch:443/handle/20.500.11850/200137.

[49] L. Frayssinet, L. Merlier, F. Kuznik, J.-L. Hubert, M. Milliez, and J.-J. Roux, "Modeling the heating and cooling energy demand of urban buildings at city scale," 2017. DOI: 10.1016/j.rser.2017.06.040. [Online]. Available: http://dx.doi.org/10.1016/j.rser.2017.06.040.

[50] Hotmaps Team, *Hotmaps Toolbox*, Sep. 2020. [Online]. Available: https://www.hotmaps.eu/map.

[51] D. Connolly, "Creating Hourly Profiles to Model both Demand and Supply Work Package 2 Background Report 2 The STRATEGO project (Multi-level actions for enhanced Heating &," Tech. Rep., 2015.

[52] Association for the Advancement of Cost Engineering (AACE), "COST ENGINEERING TERMINOLOGY," Tech. Rep., 2024.

[53] S. Bozorgmehr Nia, M. Taheri, and R. Jamalpour, "Achieving Realistic Cost Estimates in Building Construction Projects: A Reliability Assessment of Pre-Construction Stage Cost Estimates," *International Journal of Construction Engineering and Management*, vol. 12, no. 3, pp. 81–90, Aug. 2023, ISSN: 2326-1102. DOI: 10.5923/j.ijcem.20231203.02.

[54] M. Wirtz, "nPro: A web-based planning tool for designing district energy systems and thermal networks," *Energy*, vol. 268, Apr. 2023, ISSN: 03605442. DOI: 10.1016/j.energy.2022.126575.

[55] M. Wirtz, *nPro Tool*, 2024. [Online]. Available: https://app.npro.energy/en.

[56] S. A. Kalogirou, *Solar Energy Engineering : Processes and Systems*. Saint Louis, UNITED STATES: Elsevier Science & Technology, 2014, ISBN: 9780123972569. [Online]. Available: http://ebookcentral.proquest.com/lib/upmes/detail.action?docID=1517436.

[57] J. A. Duffie and W. A. Beckman, *Solar Engineering of Thermal Processes*. Somerset, UNITED STATES: John Wiley & Sons, Incorporated, 2013, ISBN: 9781118418123. [Online]. Available: http://ebookcentral.proquest.com/lib/upmes/detail.action?docID=1162079.

[58] S. A. Kalogirou, *Solar thermal collectors and applications*, 2004. DOI: 10.1016/j.pecs.2004.02.001.

[59] K. Vignarooban, X. Xu, A. Arvay, K. Hsu, and A. M. Kannan, *Heat transfer fluids for concentrating solar power systems - A review*, May 2015. DOI: 10.1016/j.apenergy.2015.01.125.

[60] ANSI/ASHRAE, "ANSI/ASHRAE Standard 93-2010 (R2014): Methods Of Testing To Determine The Thermal Performance Of Solar Collectors," ANSI, Tech. Rep., 2010.

[61] International Organization for Standardization, "Solar energy - Solar thermal collectors - Test methods (ISO 9806:2017)," Tech. Rep., 2017.

[62] J. Twidell and T. Weir, *Renewable energy resources*, p. 784, ISBN: 9780415584388.

[63] K. Rayaprolu, *Boilers: A Practical Reference* (CRC Mechanical Engineering Series). Taylor & Francis, 2012, ISBN: 9781466500532. [Online]. Available: https://books.google.es/books?id=ELgp4ctCzXkC.

[64] F. J. Gutiérrez Ortiz, "Modeling of fire-tube boilers," *Applied Thermal Engineering*, vol. 31, no. 16, pp. 3463–3478, Nov. 2011, ISSN: 13594311. DOI: 10.1016/j.applthermaleng.2011.07.001.

[65] E. U. Schlünder, I. C. f. H. Transfer, and Mass, *Heat Exchanger Design Handbook* (Heat Exchanger Design Handbook v. 1;v. 2,pts. 1-2;v. 3,pts. 1-2;v. 4;v. 5,pts. 1-2). Hemisphere Publishing Corporation, 1983, ISBN: 9780891161257. [Online]. Available: https://books.google.es/books?id=kOBSAAAAMAAJ.

[66] P. Mckendry, "Energy production from biomass (part 1): overview of biomass," Tech. Rep.

[67] S. Frederiksen and S. Werner, *District Heating and Cooling*. Professional Publishing Svc., 2013, ISBN: 9789144085302. [Online]. Available: https://books.google.es/books?id=vH5zngEACAAJ.

[68] L. D. D. Harvey, *A Handbook on Low-Energy Buildings and District-Energy Systems: Fundamentals, Techniques and Examples*. CRC Press, 2012, ISBN: 9781136573026. [Online]. Available: https://books.google.es/books?id=Mx_wy9VmargC.

[69] M. Panagiotidou, L. Aye, and B. Rismanchi, "Alternative Heating and Cooling Systems for the Retrofit of Medium-Rise Residential Buildings in Greece," *Energy Technology*, vol. 9, no. 11, Nov. 2021, ISSN: 21944296. DOI: 10.1002/ente.202100377.

[70] L. D. Harvey, *Reducing energy use in the buildings sector: Measures, costs, and examples*, 2009. DOI: 10.1007/s12053-009-9041-2.

[71] YASAKI, *YASAKI-WFC Sales Brochure*.

[72] X. Wang and H. T. Chua, "Absorption Cooling: A Review of Lithium Bromide-Water Chiller Technologies," *Recent Patents on Mechanical Engineering*, vol. 2, no. 3, pp. 193–213, Jan. 2010, ISSN: 1874477X. DOI: 10.2174/1874477x10902030193.

[73] S. C. Kaushik and A. Arora, "Energy and exergy analysis of single effect and series flow double effect water-lithium bromide absorption refrigeration systems," *International Journal of Refrigeration*, vol. 32, no. 6, pp. 1247–1258, Sep. 2009, ISSN: 01407007. DOI: 10.1016/j.ijrefrig.2009.01.017.

[74] H. Tahaineh, M. H. Frihat, and M. Al-Rashdan, "Exergy Analysis of a Single-Effect Water-Lithium Bromide Absorption Chiller Powered by Waste Energy Source for Different Cooling Capacities," Tech. Rep., 2020. [Online]. Available: https://www.researchgate.net/publication/342335726.

[75] G. Alva, Y. Lin, and G. Fang, *An overview of thermal energy storage systems*, Feb. 2018. DOI: 10.1016/j.energy.2017.12.037.

[76] E. Guelpa and V. Verda, *Thermal energy storage in district heating and cooling systems: A review*, Oct. 2019. DOI: 10.1016/j.apenergy.2019.113474.

[77] L. F. Cabeza, "Components | Thermal Energy Storage," *Comprehensive Renewable Energy*, pp. 246–293, Jan. 2022. DOI: 10.1016/B978-0-12-819727-1.00033-9.

[78] M. Gong and S. Werner, "Exergy analysis of network temperature levels in Swedish and Danish district heating systems," *Renewable Energy*, vol. 84, pp. 106–113, Feb. 2015, ISSN: 09601481. DOI: 10.1016/j.renene.2015.06.001.

[79] I. Dinçer and M. A. Rosen, *Thermal Energy Storage: Systems and Applications*. 2011, ISBN: 978-0-470-74706-3.

[80] J. Sunku Prasad, P. Muthukumar, F. Desai, D. N. Basu, and M. M. Rahman, *A critical review of high-temperature reversible thermochemical energy storage systems*, Nov. 2019. DOI: 10.1016/j.apenergy.2019.113733.

[81] Irene Tzinis, *Technology Readiness Level*, Oct. 2012.

[82] Australian Renewable Energy Agency (ARENA), "Commercial Readiness Index for Renewable Energy Sectors," Tech. Rep., 2014. [Online]. Available: https://arena.gov.au/assets/2014/02/Commercial-Readiness-Index.pdf.

[83] J. Twitchell, K. DeSomber, and D. Bhatnagar, *Defining long duration energy storage*, Apr. 2023. DOI: 10.1016/j.est.2022.105787.

[84] P. Fleuchaus, B. Godschalk, I. Stober, and P. Blum, "Worldwide application of aquifer thermal energy storage – A review," *Renewable and Sustainable Energy Reviews*, vol. 94, pp. 861–876, Oct. 2018, ISSN: 18790690. DOI: 10.1016/j.rser.2018.06.057.

[85] Thermal Energy System Specialists, "Storage Tank Library Mathematical Reference," Tech. Rep., 2021. [Online]. Available: http://www.trnsys.com.

[86] University of Wisconsin-Madison, "TRNSYS 18. Volume 1. Getting started.," Tech. Rep., 2018. [Online]. Available: http://sel.me.wisc.edu/trnsyshttp://software.cstb.frhttp://www.tess-inc.com.

[87] A. Ivančić, J. Romaní, J. Salom, and M. V. Cambronero, "Performance assessment of district energy systems with common elements for heating and cooling," *Energies*, vol. 14, no. 8, Apr. 2021, ISSN: 19961073. DOI: 10.3390/en14082334.

[88] D. Brundage, C. Melissa Goren, M. Lane, *et al.*, "ASHRAE Standard Project Committee 90.1 Cognizant TC: 7.6 Systems Energy Utilization SPLS Liaison: Charles Barnaby ASHRAE Staff Liaisons: Emily Toto IES Liaison: Mark Lien," ISSN: 2021-2022.

[89] Y. Zhang, *Use jEPlus as an Efficient Building Design Optimisation Tool*, 2012. [Online]. Available: https://www.researchgate.net/publication/304404398.

[90] International Organization for Standardization, "Energy performance of buildings Overarching EPB assessment Part 1: General framework and procedures (ISO 52000-1:2017)," Tech. Rep., 2019. [Online]. Available: www.une.org.

[91] Ecoheat4cities, "Guidelines for technical assessment of District Heating systems," Tech. Rep., 2012. [Online]. Available: www.ecoheat4cities.eu.

[92] University of Winsconsin-Madison, *TRNSYS 17. Volume 4. Mathematical Reference.* 2009. [Online]. Available: http://web.mit.edu/parmstr/Public/TRNSYS/04-MathematicalReference.pdf.

[93] I. J. Hall and Sandia Laboratories, *Generation of a typical meteorological year*, Sandia Laboratories, Ed. 1978.

[94] AENOR, "Hygrothermal performance of buildings Calculation and presentation of climatic data Part 4: Hourly data for assessing the annual energy use for heating and cooling (ISO 15927-4:2005)," Tech. Rep., 2011. [Online]. Available: www.aenor.es.

[95] T. Huld, E. Paietta, P. Zangheri, and I. P. Pascua, "Assembling typical meteorological year data sets for building energy performance using reanalysis and satellite-based data," *Atmosphere*, vol. 9, no. 2, Feb. 2018, ISSN: 20734433. DOI: 10.3390/atmos9020053.

[96] *JRC Photovoltaic Geographical Information System (PVGIS) - European Commission.* [Online]. Available: https://re.jrc.ec.europa.eu/pvg_tools/en/.

[97] L. F. Cabeza, "3.07 - Thermal Energy Storage," in *Comprehensive Renewable Energy*, Elsevier, Jan. 2012, pp. 211–253, ISBN: 9780080878737. DOI: 10.1016/B978-0-08-087872-0.00307-3.

[98] S. Pezzutto, S. Zambotti, S. Croce, *et al.*, "D2.3 WP2 Report-Open Data Set for the EU28," Tech. Rep. [Online]. Available: www.eeg.tuwien.ac.at.

[99] J. E. Caskex and H. C. S. Thom, "Monthly Weather Review The Rational Relationship Between Heating Degree Days and Temperature," Tech. Rep., Jan. 1954. DOI: https://doi.org/10.1175/1520-0493(1954)082{\%}3C0001:TRRBHD{\%}3E2.0.CO;2.

[100] CIBSE, *Degree-Days - Theory and Application - TM41 : 2006.* CIBSE, 2006, ISBN: 1903287766.

[101] eurostat, *File:Share of final energy consumption in the residential sector by type of end-use, 2020 (%) v5.png - Statistics Explained.* [Online]. Available: https://ec.europa.eu/eurostat/statistics-explained/index.php?title=File:Share_of_final_energy_consumption_in_the_residential_sector_by_type_of_end-use,_2020_(%25)_v5.png.

[102] Danish Energy Agency, "Technology Data - Energy transport," Tech. Rep., 2017.

[103] B. Möller and S. Werner, "Quantifying the Potential for District Heating and Cooling in EU Member States The STRATEGO project (Multi-level actions for enhanced Heating &," Tech. Rep., 2016.

[104] Wedistrict, "D5.7 Simulation models for WEDISTRICT demo-sites," Tech. Rep., Dec. 2021.

[105] Wedistrict and Christophe Saint-sardos, "D5.8 Virtual demo designs," Tech. Rep., 2022. [Online]. Available: https://www.wedistrict.eu/wp-content/uploads/2023/06/Virtual-demo-designs-for-WEDISTRICT.pdf.

[106] C. Willmott, S. Robeson, and K. Matsuura, "A refined index of model performance," *International Journal of Climatology*, vol. 32, Jul. 2012. DOI: 10.1002/joc.2419.

[107] A. Novel, F. Allard, and P. Joubert, "Metamodeling of building energy consumption focused on climate, operation, space use and users related factors; Metamodeling of building energy consumption focused on climate, operation, space use and users related factors," 2019. DOI: 10.1051/e3sconf/2019111040. [Online]. Available: https://doi.org/10.1051/e3sconf/2019111040.